BERICHTE
aus dem Fachbereich Geowissenschaften
der Universität Bremen

Nr. 207

Rakic, S.

UNTERSUCHUNGEN ZUR POLYMORPHIE UND KRISTALLCHEMIE VON SILIKATEN DER ZUSAMMENSETZUNG $Me_2Si_2O_5$ (Me:Na, K)

Berichte, Fachbereich Geowissenschaften, Universität Bremen, Nr. 207,
139 Seiten, Bremen 2003

ISSN 0931-0800

Die "Berichte aus dem Fachbereich Geowissenschaften" werden in unregelmäßigen Abständen vom Fachbereich 5, Universität Bremen, herausgegeben.

Sie dienen der Veröffentlichung von Forschungsarbeiten, Doktorarbeiten und wissenschaftlichen Beiträgen, die im Fachbereich angefertigt wurden.

Die Berichte können bei:

Frau Monika Bachur

Forschungszentrum Ozeanränder, RCOM

Universität Bremen

Postfach 330 440

D 28334 BREMEN

Telefon: (49) 421 218-8960

Fax: (49) 421 218-7429

e-mail: MBachur@uni-bremen.de

angefordert werden.

Zitat:

Rakic, S.

Untersuchungen zur Polymorphie und Kristallchemie von Silikaten der Zusammensetzung $Me_2Si_2O_5$ (Me:Na, K).

Berichte, Fachbereich Geowissenschaften, Universität Bremen, Nr. 207, 139 Seiten, Bremen, 2003.

ISSN 0931-0800

Untersuchungen zur Polymorphie und Kristallchemie von Silikaten der Zusammensetzung $Me_2Si_2O_5$ (Me: Na, K)

Dissertation

zur Erlangung des

Doktorgrades der Naturwissenschaften

am Fachbereich 5 – Geowissenschaften

der Universität Bremen

vorgelegt von

Srdjan Rakic

Bremen 2003

Tag des Kolloquiums: 18.03.2003.

Gutachter:

1. Prof.Dr. V. Kahlenberg

2. Prof.Dr. R.X. Fischer

Prüfer:

1. Prof. Dr. O. Brockamp

2. Prof. Dr. M. Olesch

Vorwort

Die vorliegende Arbeit entstand im Rahmen des von der Deutschen Forschungsgemeinschaft geförderten Projekts Ka1342/1 mit dem Titel *Untersuchungen zur Polymorphie und Kristallchemie von Phyllosilikaten der Zusammensetzung $Me_2Si_2O_5$ (Me : Na, K).* In die Promotionsschrift wurden die folgenden sechs Manuskripte aufgenommen:

Abschnitt 7. *The crystal structure of a mixed alkali phyllosilicate with composition $Na_{1.55}K_{0.45}Si_2O_5$.*

Diese im Band 13 (2001) des *European Journal of Mineralogy* publizierte Arbeit wurde von mir mit Prof. Dr. Volker Kahlenberg als Co - Autor verfaßt. Die Kristallsynthese, sowie die strukturelle Charakterisierung sind von mir eigenständig durchgeführt worden.

Abschnitt 8. *Single crystal structure investigation of twinned $NaKSi_2O_5$ - a novel single layer silicate.*

Dieses in der Zeitschrift *Solid State Sciences* (Band 3, 2001) veröffentlichte Manuskript ist von mir zusammen mit Prof. Dr. Volker Kahlenberg als Co - Autor verfaßt worden. Die präparativen Arbeiten und die Strukturrechnungen wurden ausschließlich im Rahmen dieser Dissertation von mir ausgeführt.

Abschnitt 9. *Structural characterization of high pressure C - $Na_2Si_2O_5$ by single crystal diffraction and ^{29}Si MAS NMR.*

Die Ergebnisse dieser in *Physics and Chemistry of Minerals* (Band 29, 2002) abgedruckten Arbeit sind von mir zusammen mit Prof. Dr. Volker Kahlenberg, Dr. Claudia Weidenthaler und Dr. Bodo Zibrowius erarbeitet worden. Die thermischen Untersuchungen wurden von Frau Dr. Weidenthaler durchgeführt, die Festkörper-NMR Messungen, sowie deren Auswertung stammen von Herrn Dr. Zibrowius. Die Einkristallstrukturanalysen und die kristallchemische Diskussion stellen meinen Beitrag an dieser gemeinsamen Arbeit dar.

Abschnitt 10. *Hydrothermal synthesis and structural characterization of κ-$Na_2Si_2O_5$ and $Na_{1.84}K_{0.16}Si_2O_5$.*

Dieses inzwischen bei der Zeitschrift *Solid State Sciences* im Druck befindliche Manuskript ist von mir zusammen mit Prof. Dr. Volker Kahlenberg und Dr. Burkhard Schmidt als Co-Autoren verfaßt worden. Herr Dr. Schmidt hat die von mir am Bayerischen Geoinstitut

durchgeführten Hochdruckexperimente betreut und die chemische Zusammensetzung des Mischkristalls bestimmt. Alle strukturellen Aspekte sind von mir erarbeitet worden.

Abschnitt 11. *High pressure mixed alkali disilicates in the system $Na_{2-x}K_xSi_2O_5$: hydrothermal synthesis and crystal structures of $NaKSi_2O_5$-II and $Na_{0.67}K_{1.33}Si_2O_5$.*

Diese Arbeit wurde von mir zusammen mit Prof. Dr. Volker Kahlenberg und Dr. Burkhard Schmidt als Co-Autoren verfaßt. Die Synthesen wurden in Kooperation mit Herrn Dr. Schmidt in Bayreuth durchgeführt. Die Einkristallbeugungsexperimente und deren Auswertung stammen von mir. Das Manuskript zu dieser Arbeit ist in der *Zeitschrift für Kristallographie* zur Veröffentlichung akzeptiert worden.

Abschnitt 12. *Room - and high - temperature single crystal diffraction studies on γ-$Na_2Si_2O_5$: an interrupted framework with exclusively Q^3-units.*

Dieses bei der *Zeitschrift für Kristallographie* im Druck befindliche Manuskript wurde von Prof. Dr. Volker Kahlenberg verfaßt. Teile des Textes, die Beugungsuntersuchungen bei Raumtemperatur und bei höheren Temperaturen, sowie die Synthesen stammen von mir. Frau Dr. Weidenthaler hat den Phasenübergang thermoanalytisch charakterisiert.

Danksagung

Zunächst einmal möchte ich mich bei meinem Betreuer, Herrn Prof. Dr. Volker Kahlenberg, für die Themenstellung, die Diskussionen und die Unterstützung bei der praktischen Durchführung dieser Arbeit bedanken.

Auch Herrn Prof. Dr. Reinhard X. Fischer und allen Mitgliedern des Arbeitskreises Kristallographie sei an dieser Stelle für die Anregungen und die schöne Zeit in Bremen ausdrücklich gedankt.

Die Dissertation entstand mit einer finanziellen Förderung durch die Deutsche Forschungsgemeinschaft (DFG).

Ein besonderer Dank gilt weiterhin:

Frau Dr. Claudia Weidenthaler und Herrn Dr. Bodo Zibrowius (Max Planck Institut für Kohlenforschung, Mülheim an der Ruhr) für die TG-DTA-DSC-Messungen, die Pulverbeugungsuntersuchungen bei höheren Temperaturen und die ^{29}Si-MAS-NMR Analysen.

Herrn Dr. Burkhard Schmidt (Bayerisches Geoinstitut, Bayreuth) für die Hilfestellung bei den Hydrothermalsynthesen.

Inhaltsverzeichnis

1. Einleitung und kurzer Überblick der bisherigen Untersuchungen an Na - K -Disilikaten

Seit den ersten Arbeiten von Morey & Bowen [1] bzw. Kracek [2] im System Na_2O - SiO_2 sind die Natriumsilikate wiederholt Gegenstand von phasenanalytischen Untersuchungen gewesen. Im Bereich der experimentellen Petrologie wurde die Existenz kristalliner Natriumsilikat-Hochdruckphasen in den letzten 10 Jahren eingehender untersucht [3-5]. Gläser und Schmelzen der Zusammensetzung $Na_2Si_2O_5$ wiederum dienen in den Geowissenschaften als vergleichsweise einfache Modellsysteme zum Verständnis der Vorgänge in den wesentlich komplexeren natürlichen Schmelzen [6]. Aber auch aus materialwissenschaftlicher Sicht kommt den Natriumdisilikaten eine besondere Bedeutung zu. So findet man sie z.B. als kristalline Verunreinigung der technologisch wichtigen Kalk-Natron-Gläser [7]. Großtechnisch werden sie insbesondere als Ionentauscher in Waschmitteln eingesetzt [8]. Ferner sind sie auch hinsichtlich der Eignung als Na-Ionenleiter untersucht worden [9]. Ein weiterer interessanter Aspekt liegt in der ausgeprägten Neigung zur Bildung verschiedener stabiler und metastabiler polymorpher Formen als Funktion der Synthesebedingungen.

Nach den Untersuchungen von Willgallis & Range [10] bzw. Williamson & Glasser [11] kann man durch Temperung von $Na_2Si_2O_5$-Gläsern bei Normaldruck drei verschiedene Modifikationen erhalten. Bei Leuterungstemperaturen zwischen 500°C und 580°C entsteht zunächst das sogenannte γ - $Na_2Si_2O_5$, zwischen 580°C und 670°C kristallisiert die β-Phase, und oberhalb 670°C bildet sich schließlich die α-Modifikation. Nach Williamson & Glasser verlaufen die Umwandlungen $\gamma \rightarrow \beta \rightarrow \alpha$ irreversibel. Die bei Raumtemperatur stabile Phase des α-$Na_2Si_2O_5$ wurde erstmals von Liebau [12] bzw. Pant & Cruickshank [13] strukturell untersucht. Die Struktur des β-Natriumdisilikats wurde von Pant [14] gelöst. In beiden Fällen handelt es sich um Einfachschichtsilikate.

Für α - und γ-$Na_2Si_2O_5$ werden nach thermischen Messungen in der Literatur verschiedene Hochtemperatur-Modifikationen unterschieden, die als Zusatz römische Ziffern tragen (vgl. Tabelle 1.1). Die Transformationstemperaturen liegen für die *HT*-Formen des α-$Na_2Si_2O_5$ bei T_{III}? T_{II} = 676°C, bzw. T_{II}? T_I = 706°C [11]. Für γ-$Na_2Si_2O_5$ wurden unterhalb der Umwandlung in die β-Phase insgesamt drei thermische Ereignisse bei etwa 555°C, 574°C und 595°C beobachtet. Die γ_{IV}-Phase soll dabei nach Hoffmann & Scheel [15] im Beugungsbild die Merkmale einer inkommensurabel modulierten Struktur aufweisen.

Die Existenz einer weiteren metastabilen Disilikatvariante des sogenannten δ-$Na_2Si_2O_5$ wurde ebenfalls von Hoffmann & Scheel nachgewiesen. Diese Phase kann durch die Temperung von amorphem Wasserglas auf Trägertabletten aus gesinterten Oxiden erhalten werden. Ein Strukturmodell der δ-Phase wurde von Kahlenberg et al. [16] bestimmt.

Tabelle 1.1 Gitterkonstanten und Raumgruppen der $Na_2Si_2O_5$ - Modifikationen, die sich bei Normaldruck herstellen lassen.

Phase	Raumgruppe	*a* [Å]	*b* [Å]	*c* [Å]	Mon.Winkel [°]	Literatur
α_{III}	*Pcnb*	6.409	15.422	4.896		[13]
α_{II}	mon.	6.64	7.72	4.94	91	[11]
α_{I}	orthor.	6.64	7.72	4.98		[11]
β	$P112_1/b$	8.133	12.329	4.848	104.2	[14]
γ_{IV}	orthor.	11.732	11.673	7.087		[15]
δ	$P12_1/n1$	8.393	12.083	4.843	90.37	[16]

Durch Anwendung von Druck als zusätzlichem Syntheseparameter sind aus der Literatur zwei weitere Disilikatmodifikationen bekannt. Die sogenannte C - Phase bildet sich schon bei vergleichsweise niedrigen Drucken oberhalb circa 100 bar [11]. Bei sehr hohen Drucken (70 kbar) wurde die Existenz des ε-$Na_2Si_2O_5$ von Fleet & Henderson [3] nachgewiesen und strukturell charakterisiert. Kanzaki et al. [5] berichteten über eine ζ-$Na_2Si_2O_5$ Phase. Spätere Arbeiten [4] zeigten jedoch, daß es sich bei dieser Verbindung um ein Natriumheptasilikat der Zusammensetzung $Na_8Si_7O_{18}$ handelt.

Tabelle 1.2 Gitterkonstanten und Raumgruppen der bisher bekannten $Na_2Si_2O_5$ - Hochdruck-modifikationen.

Phase	Raumgruppe	*a* [Å]	*b* [Å]	*c* [Å]	Mon.Winkel [°]	Literatur
C	mon.	8.12	23.70	4.85	90	[11]
ε	$P2_1ca$	8.356	5.580	9.441		[3]

Im Gegensatz zum Natriumdisilikat ist das Kaliumdisilikat und seine Polymorphie deutlich weniger gut untersucht worden. Durch Temperung stöchiometrisch zusammengesetzter Gläser konnten Schweinsberg & Liebau [17] eine wahrscheinlich monokline Phase (α - $K_2Si_2O_5$) herstellen.

Diese zeigt nach Sheybany [18] zwischen 240°C-250°C bzw. bei 560°C zwei thermische Effekte, die auf die Existenz von Hochtemperaturmodifikationen hindeuten. Ferner wurde kürzlich von de Jong et al. [19] eine weitere, wahrscheinlich metastabile Form des Kaliumdisilikats publiziert (β - $K_2Si_2O_5$), bei der es sich im Gegensatz zu allen anderen bislang bekannten Na- und K- Disilikaten nicht um ein Schichtsilikat, sondern um ein unterbrochenes Tetraedergerüst handelt.

Tabelle 1.3 Gitterkonstanten und Raumgruppen der bekannten $K_2Si_2O_5$ - Modifikationen.

Phase	Raumgruppe	*a* [Å]	*b* [Å]	*c* [Å]	Mon.Winkel [°]	Literatur
α	mon.	9.72	25.26	14.24	90	[17]
β	*C*1*c*1	16.322	11.243	9.919	115.97	[19]

Geht man schließlich von den Endgliedern des Systems $Na_{2-x}K_xSi_2O_5$ zu den kristallinen Na-K-Mischphasen über, fehlten bislang jegliche strukturelle Informationen. Dies ist um so erstaunlicher, da die entsprechenden Gläser gleicher Zusammensetzung schon wiederholt Gegenstand spektroskopischer Untersuchungen waren [20-22]. Von den kristallinen $(Na,K)_2Si_2O_5$-Phasen war nur ein indiziertes Pulverbeugungsdiagramm für eine Mischphase der Zusammensetzung $Na_{1.30}K_{0.70}Si_2O_5$ bekannt (Sakaguchi et al. [23]). Die Ähnlichkeit des Beugungsbildes deutete auf eine mögliche Verwandtschaft mit δ-$Na_2Si_2O_5$ hin. Zusammenfassend läßt sich also sagen, daß es immer noch gravierende Lücken bezüglich kristallchemischer Basisdaten sowohl bei den Endgliedern, als auch bei den Mischphasen des Systems $Na_2Si_2O_5$ - $K_2Si_2O_5$ gibt. Die vorliegende Arbeit soll ein Beitrag dazu sein, diese Lücken möglichst zu schließen.

2. Strukturelle Hochtemperaturuntersuchungen an α-$Na_2Si_2O_5$

2.1 Stand der Forschung

Die Kristallstruktur des α - Natriumdisilikates bei Raumtemperatur ist von Liebau [12] bzw. Pant & Cruickshank [13] eingehend untersucht worden. Die Struktur kristallisiert in der orthorhombischen Raumgruppe *Pcnb* und gehört zur Gruppe der Einfachschichtsilikate (vgl. Abbildung 2.1). Jeder SiO_4 - Tetraeder besitzt ein freies und drei verbrückende Sauerstoffatome. Durch die Verknüpfung der Tetraeder über eine 2_1- Schraubenachse entstehen zunächst *Zweier*-Einfachketten, die parallel zu [001] verlaufen. Durch die Verknüpfung der Ketten in *a* - Richtung über gemeinsame Ecken entstehen schließlich Schichten, die Sechserringe aus Tetraedern in *UDUDUD* Konformation enthalten und senkrecht zur *b* - Achse liegen. Die Schichten sind nicht etwa planar, sondern weisen eine ausgeprägte Faltung auf, die innerhalb der Schichten zu kanalartigen Strukturen führt, vor deren Öffnungen die Na - Ionen liegen. Jedes Natriumatom ist von fünf Sauerstoffliganden in Form einer verzerrten trigonalen Bipyramide umgeben.

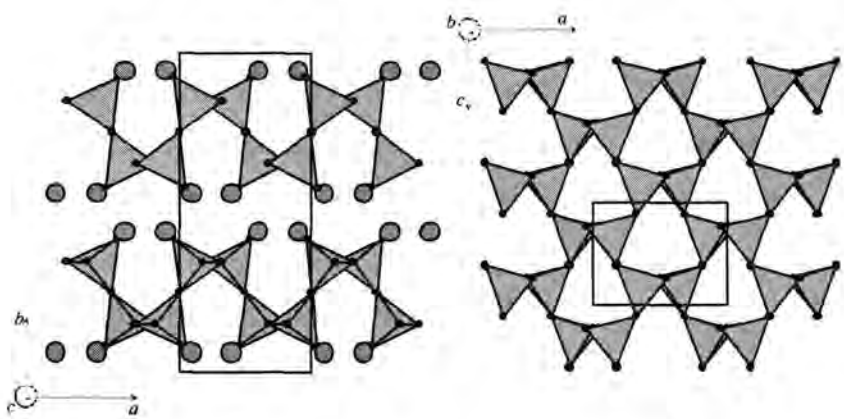

(a) (b)

Abb. 2.1: (a) Projektion der Struktur des α-$Na_2Si_2O_5$ längs [001] (b) Projektion einer Einzelschicht längs [010]

Erste Untersuchungen über die thermisch induzierten Umwandlungen der Phasen im System Na_2O-SiO_2 stammen von Morey & Bowen [1] bzw. Kracek [2]. Diese wurden durch spätere Arbeiten von Willgallis & Range [10] sowie von Williamson & Glasser [11] ergänzt. Im Fall des α-$Na_2Si_2O_5$ wurden beim Aufheizen zwei schwache endotherme Effekte bei etwa 676°C und 706°C beobachtet, die bei der Abkühlung als exotherme Ereignisse mit einer geringen Temperaturverschiebung ebenfalls beobachtbar sind. Dieses Resultat führte zu der Hypothese, daß beim α-$Na_2Si_2O_5$ insgesamt drei Sub-Modifikationen unterschieden werden müssen, die sich reversibel ineinander umwandeln :

$$\alpha_{III} - Na_2Si_2O_5 \xleftrightarrow{676^0C} \alpha_{II} - Na_2Si_2O_5 \xleftrightarrow{706^0C} \alpha_I - Na_2Si_2O_5$$

Gemäß den von Williamson & Glasser durchgeführten Pulverbeugungsmessungen sind die Umwandlungen mit sehr kleinen Änderungen im Beugungsdiagramm verknüpft. Die Autoren geben dabei die folgenden Gitterparameter an :

α_{III} (bei RT): a = 6.409 Å, b = 15.422 Å, c = 4.896 Å, orthorhombische Symmetrie

α_{II} (bei 695°C): a = 6.64 Å, b = 4.94 Å, c = 7.72 Å , β=91°, monokline Symmetrie

α_I (bei 765°C): a = 6.64 Å, b = 7.72 Å, c = 4.98 Å , orthorhombische Symmetrie

Neuere thermische und röntgenographische Untersuchungen stammen von Jacobsen [24] bzw. Remmert [25]. Die DTA Messungen bestätigen prinzipiell die früheren Ergebnisse zur Existenz zweier reversibler Effekte. Die pulverdiffraktometrischen Messungen führten allerdings zu unterschiedlichen Ergebnissen. Die von Williamson & Glasser für die α_{II} - Phase postulierte monokline Zelle mit $\beta = 91°$ hätte zu einer Vielzahl von Reflexaufspaltungen führen müssen, die jedoch von den beiden oben genannten Autoren nicht nachvollzogen werden konnten.

2.2 Synthesen

Die Herstellung von einkristallinem Material des α- $Na_2Si_2O_5$ erfolgte durch Rekristallisation eines Glases. Dazu wurden 5g einer Mischung aus Na_2CO_3 (Fluka, 99%) und SiO_2 (Quarz-Feinmehl) im molaren Verhältnis 1:2 eingewogen und im Achatmörser homogenisiert. Anschließend wurden die Reaktanden in einen offenen Platintiegel gegeben, in einem Widerstandsofen bei 1100°C für 1 Stunde aufgeschmolzen und danach an Luft abgeschreckt. Zur Verbesserung der Homogenität des resultierenden Natriumdisilikatglases wurde die Probe aufgemahlen und der Vorgang insgesamt dreimal wiederholt. Die Kristallisation des Glases erfolgte durch Temperung bei 800°C innerhalb von 24h. Eine Kontrolle des Syntheseprodukts unter dem Polarisationsmikroskop zeigte nur noch geringe Glasanteile neben einer großen Zahl optisch zweiachsiger Kristalle (bis zu 0.3 mm Durchmesser), die eine scharfe Auslöschung aufwiesen. Um Hochtemperatur - Einkristallstrukturanalysen durchzuführen, wurden insgesamt vier Kristalle ausgewählt und in Kapillaren aus Quarzglas (Durchmesser 0.2 mm) eingebracht. Die Größe der Kristalle wurde so gewählt, daß diese durch einfaches Einklemmen in den Kapillaren fixiert werden konnten. Die verbleibende Menge der Probe wurde gemahlen und für die thermische Analyse, sowie Hochtemperatur- Pulveraufnahmen vorbereitet.

2.3 Thermische Untersuchungen

Die thermisch induzierten Umwandlungen wurden mittels einer simultanen TG-DTA-DSC Thermoanalyse der Firma SETARAM (Typ SETSYS TG DTA 12) untersucht. Eine Menge von 85.63 mg der gemahlenen Disilikatprobe wurde an Luft mit einer Heizrate von je 10 K/min zunächst aufgeheizt und anschließend abgekühlt. Die Ergebnisse der Messungen sind in den folgenden Abbildungen 2.2 und 2.3 dargestellt

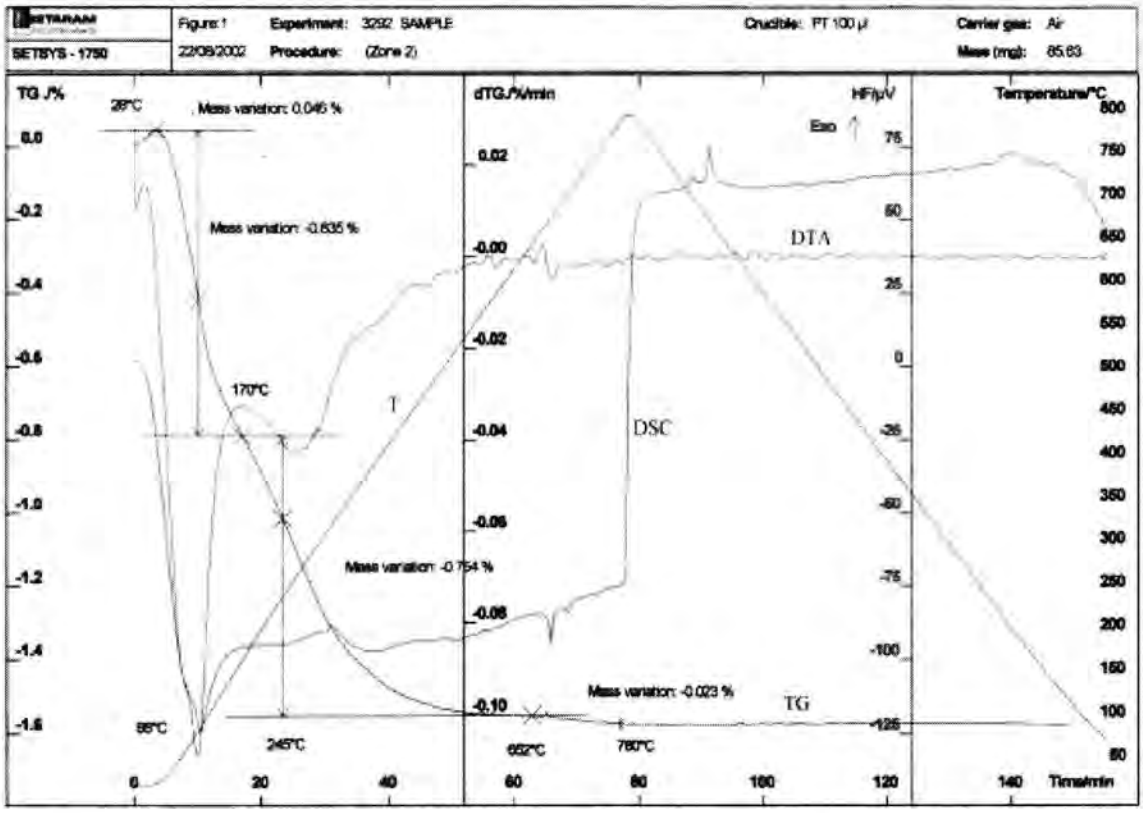

Abb. 2.2: TG(%)-, DTG(%)-, T(°C)- und Wärmefluß Kurven (DSC) als Zeitfunktion (min.)

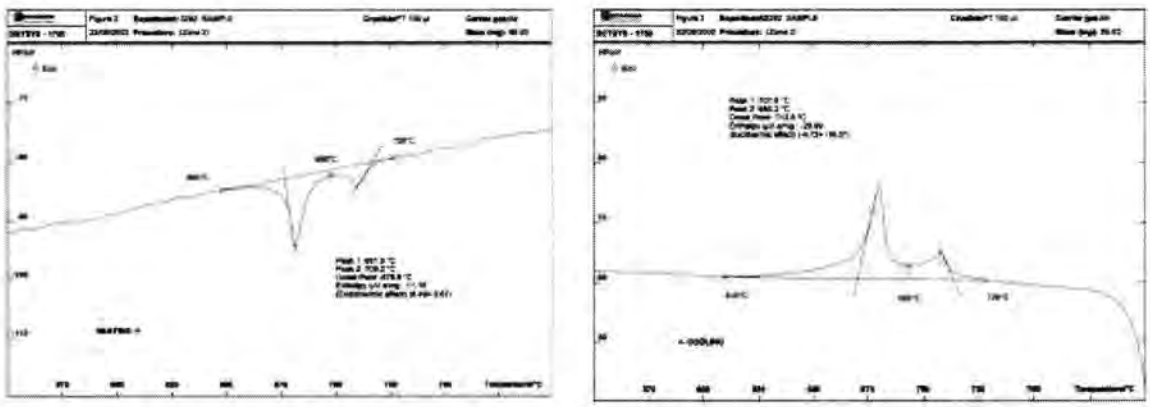

(a) (b)

Abb. 2.3: Die DSC Kurve als Temperaturfunktion während (a) Aufheizung und (b) Abkühlung

Die thermogravimetrische Kurve (TG, vgl. Abbildung 2.2) zeigt innerhalb des gemessenen Bereiches während des Aufheizens einen Massenverlust von etwa 1.7 Gew.%, der der Abgabe von adsorptiv gebundenem Wasser zugeordnet wird. In der DSC Kurve (vgl. Abbildung 2.3) sind im Temperaturintervall zwischen 650°C und 726°C zwei endotherme thermische Ereignisse erkennbar. Der erste Effekt zwischen 650°C und 698°C erreicht sein Maximum bei 681.5°C, während der zweite (zwischen 698°C und 726°C) ein $T_{max.}$ = 709.2°C aufweist. Die Signale sind relativ breit und überlappen teilweise (die DSC Kurve zwischen den Peaks kehrt nicht zur Nullinie zurück). Beide Effekte sind reversibel, jedoch kommt es zu einer kleineren Hysterese ($T_{max.}$= 707.8°C bzw. 680.2°C). Zusammenfassend läßt sich aussagen, daß die eigenen thermoanalytischen Messungen die Resultate der älteren Arbeiten bestätigen.

2.4 Hochtemperatur - Pulverdiffraktometrie mittels Neutronenbeugung

Die Beobachtung, daß die Phasenübergänge im α - $Na_2Si_2O_5$ nahezu keine thermische Hysterese zeigen und kleine Umwandlungsenthalpien aufweisen, macht es wahrscheinlich, daß die Transformationen nur mit kleinen strukturellen Änderungen verknüpft sind. Da die früheren röntgenographischen *HT*-Beugungsuntersuchungen an Pulverproben zu widersprüchlichen Ergebnissen führten, wurden im Rahmen dieser Arbeit ergänzende Experimente unter Verwendung von Neutronenstrahlung in Kooperation mit dem Hahn-Meitner-Institut in Berlin durchgeführt. Die temperaturabhängigen Messungen erfolgten dabei am sogenannten "flat cone" E2 Diffraktometer, das mit einem gebogenen ortsempfindlichen BF_3 Detektor ausgerüstet ist und einen Bereich von 90° 2θ erfaßt. Etwa 2g der Probe wurden in einen Probenbehälter aus Vanadium (Durchmesser etwa 8 mm) eingebracht, der dann in einen Ofen montiert und auf dem Diffraktometer justiert wurde. Insgesamt wurden sechs Datensätze bei Raumtemperatur (1); 670°C (2); 690°C (3); 700°C (4); 720°C (5); 750°C (6) aufgenommen. Die Wellenlänge betrug 1.2194 Å. Die Abbildung 2.4 zeigt je einen Ausschnitt dieser Beugungsdiagramme im Bereich zwischen 10° und 54° 2θ als Funktion der Temperatur. Zusätzlich markiert sind Reflexe, die durch Streustrahlung an den Niobschilden der Probenheizung verursacht wurden. Für die Reflexgruppe (101), (111) und (040) sollte es nach den Ergebnissen von Williamson & Glasser und den von uns gewählten Meßbedingungen zu einer deutlich erkennbaren Aufspaltung kommen, die jedoch nicht beobachtet werden konnte. Somit konnte die von Williamson & Glasser postulierte Umwandlungsabfolge der orthorhombischen α_{III}-Phase in eine monokline α_{II}-Phase und anschließend wieder in die orthorhombische α_I-Phase nicht nachvollzogen werden.

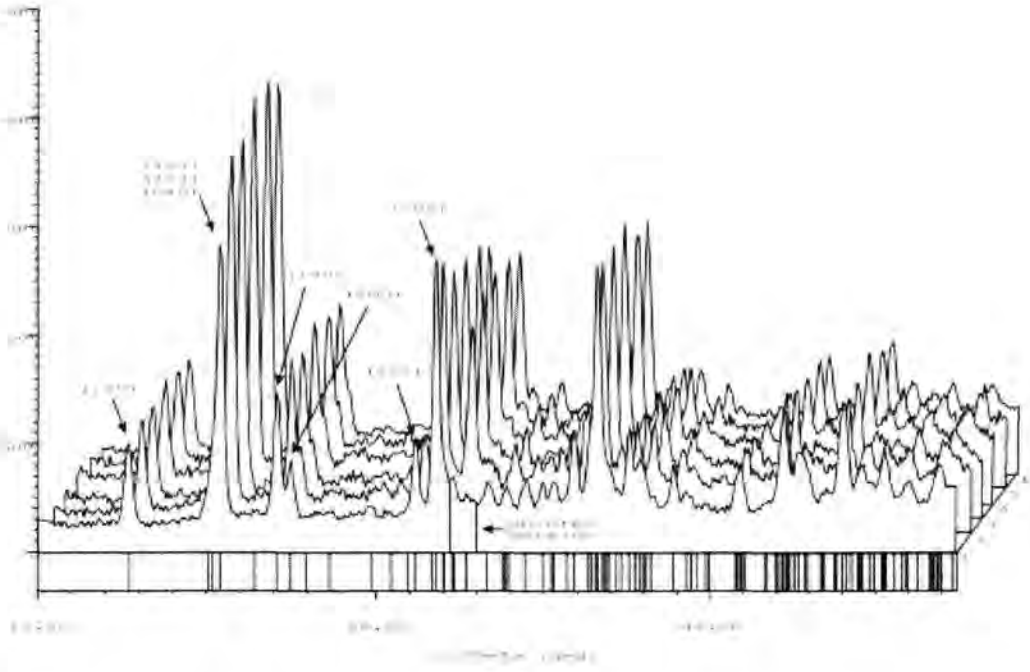

Abb. 2.4: Neutronen-Pulverbeugungsaufnahme von α - $Na_2Si_2O_5$ bei verschiedenen Temperaturen : (1) Raumtemperatur; (2) 670°C; (3) 690°C; (4) 700°C; (5) 720°C; (6) 750°C

2.5 Hochtemperatur - Einkristalldiffraktometrie

Die Hochtemperaturmessungen an Einkristallen wurden an einem STOE IPDS-Diffraktometer durchgeführt. Das Gerät enthält als Zusatz einen Blaseofen, der Messungen bis etwa 1000°C ermöglicht. Details zur Konstruktion des Ofens finden sich z.B. in der Arbeit von Scheufler [26]. Die Aufheizung der Probe erfolgte im heißen Stickstoffgasstrom bei einem Gasdurchfluß von circa 50 l/h. Nach jeder Temperaturerhöhung wurde jeweils zur Einstellung des thermischen Gleichgewichts am Probenort eine Haltezeit von 30 min eingelegt. Nach Ende der Messung erfolgte die übliche Datenreduktion. Für die strukturellen Rechnungen wurde das Programm SHELXL-93 [27] verwendet. Eine Zusammenstellung der Meßbedingungen und der Ergebnisse der Strukturuntersuchungen zeigt die folgende Tabelle :

Tabelle 2.1: Zusammenstellung der strukturellen Rechungen.

Datensammlung	
Kristallgestalt	Platte (0.08 x 0.23 x 0.15 mm^3)
Diffraktometer	Stoe - IPDS
Monochromator	Graphit
Röntgenstrahlung	MoK_α, $\lambda = 0.71073$ Å
Generatoreinstellungen	50 kV, 40 mA
Abstand zwischen Detektor und Probe	70 mm
Schrittweite in ϕ (°)	2.0

Anzahl der gesammelten Bilder			100					
Belichtungszeit / Bild (min.)			3.0					
θ - Bereich (°)			3.3° - 52.1°					
Temperaturen (°C)	20	215	411	650	684	690	694	720
Reflexbereiche	h_{min}, h_{max}		-7, 7				-6, 6	-8, 7
	k_{min}, k_{max}		-19, 19				0, 18	-18, 18
	l_{min}, l_{max}		-6, 6				0, 7	-5, 5
Anzahl der gemessenen Reflexe	3783	3797	3834	3864	3904	3778	1929	1957
Anzahl der unabhängigen Reflexe in *mmm*	454	454	461	466	464	465	460	460
R_{int} in *mmm* (%)	3.45	3.51	3.44	7.30	8.38	9.36	2.84	3.66
Anzahl der beobachteten Reflexe ($I > 2\,\sigma(I)$)	2837	2708	2620	2382	2022	1988	1466	1316
Verfeinerung der Strukturen								
Temperatur (°C)	20	215	411	650	684	690	694	720
Anzahl der verfeinerten Parameter					42			
R1 ($F_o > 4\,\sigma(F_o)$)	2.92	3.13	4.22	8.26	14.67	11.57	7.96	9.22
wR2 ($F_o > 4\,\sigma(F_o)$) (%)	7.72	6.86	10.94	18.20	30.17	21.85	19.81	20.55
Wichtungsparameter a ($\times 10^{-4}$)	483	472	494	770	996	621	1340	1497
Goodness of Fit	1.220	1.048	1.496	1.075	1.022	1.088	1.136	1.094
Finale $\Delta\rho_{min}$ (e / Å^3)	-0.25	-0.29	-0.27	-0.35	-1.21	-0.50	-0.53	-0.49
Finale $\Delta\rho_{max}$ (e / Å^3)	0.35	0.33	0.38	0.84	1.28	1.35	0.73	0.95
$R1 = \Sigma \, \|\|F_o\| - \|F_c\|\| \, / \, \Sigma \, \|F_o\|$			$wR2 = (\Sigma(w(F_o^2 - F_c^2)^2) / \Sigma(w(F_o^2)^2))^{1/2}$					
$w = 1 / (\sigma^2 (F_o^2) + (aP)^2)$			$P = (2F_c^2 + \max(F_o^2, 0)) / 3$					

Der Verlauf der Gitterkonstanten als Funktion der Temperatur ist in der Abbildung 2.5 wiedergegeben. Abweichungen von der durch die thermische Ausdehnung bedingten normalen Entwicklung sind im Bereich der Phasenübergänge insbesondere für die Abhängigkeit der *b* - Achse (Abbildung 2.5(b)) in Form einer Diskontinuität zu erkennen.

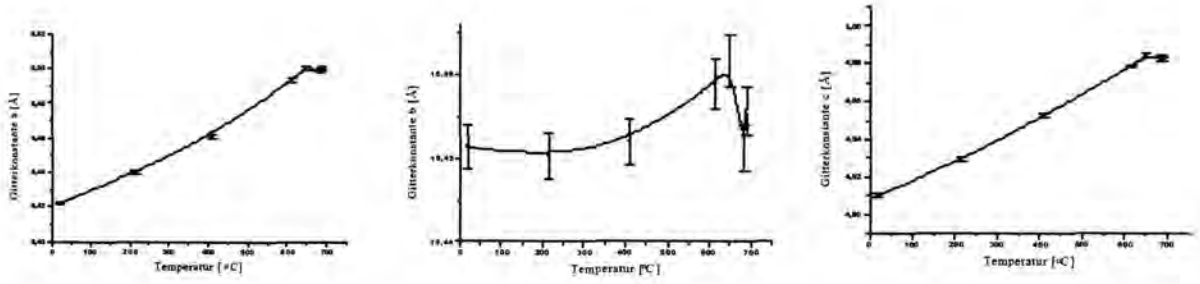

(a) (b) (c)

Abb. 2.5: Temperaturabhängigkeit von Gitterkonstanten (a) *a* ; (b) *b* ; (c) *c*

Betrachtet man die Intensitäten der Datensätze, so ist zwischen 690°C und 694°C eine deutliche Änderung zu beobachten. Während bei 690°C noch eine orthorhombische primitive Zelle vorliegt, zeigt der bei 694°C aufgenommene Datensatz eine integrale Auslöschung, die für die Existenz einer A - Zentrierung spricht. Die Untersuchung aller systematischen Auslöschungen ergab für die *HT*-Phase die Raumgruppe *Aba*2 mit der folgenden Metrik : a = 6.5050(12) Å, b = 15.437(3) Å, c = 4.9938(15) Å, V = 501.49 Å^3. Die Kristallstrukturanalyse der *HT*-Phase wurde an dem bei 720°C aufgenommen Datensatz vorgenommen und bestätigte die Hypothese einer engen Verwandtschaft zwischen den beiden Phasen (vgl. Abbildung 2.6).

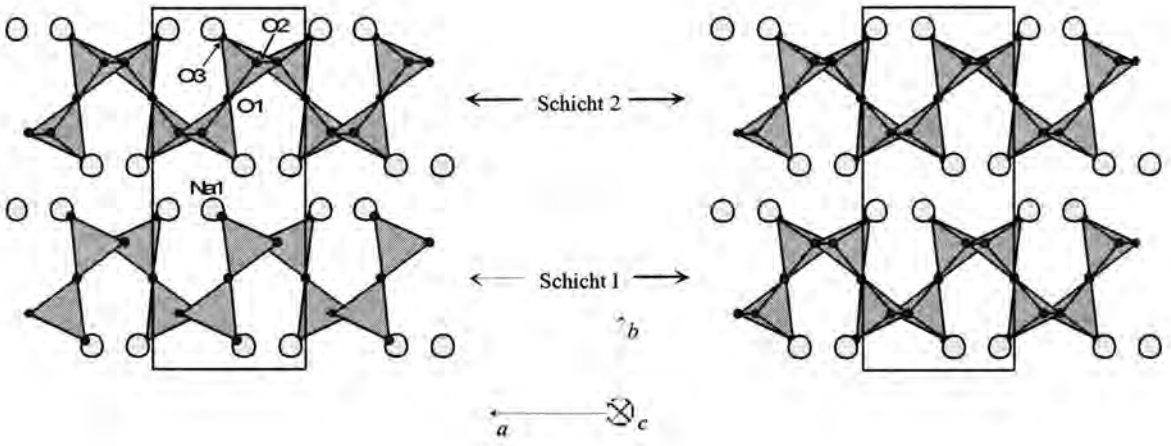

(a) (b)

Abb. 2.6: Projektionen der Strukturen (a) der α_{III}-Phase (20°C) und (b) der *HT*-Phase (720°C)

Auch in der *HT*-Modifikation enthalten die Schichten Sechseringe aus [SiO_4] - Tetraedern in der *UDUDUD* Konformation. Die Kanäle in Richtung der c-Achse sind ebenfalls von Na^+ Ionen besetzt, die je fünffach in Form einer verzerrten trigonalen Bipyramide von O-Atomen koordiniert sind. Die wesentliche strukturelle Änderung vollzieht sich innerhalb der sogenannten *Schicht 1*, während die *Schicht 2* nahezu unverändert bleibt (vgl. Abbildung 2.7 bzw. 2.8). Sie kann auf eine Bewegung der Sauerstoffatome O2 zurückgeführt werden, die sich in der a - c - Ebene abspielt. Die Verschiebung führt zu einer Änderung der Orientierung der ditrigonalen Sechseringe, zum Verlust der Symmetriezentren zwischen benachbarten Schichtpaketen und letztendlich zur Symmetrieänderung von *Pcnb* nach *Aba*2.

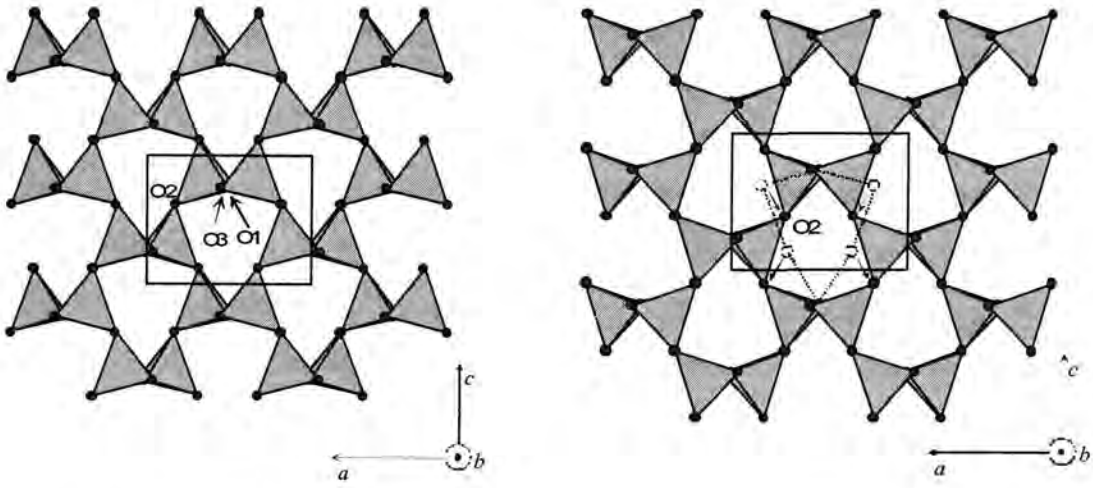

(a) (b)

Abb. 2.7: Projektion der Schicht 1 auf die a-c Ebene: (a) α_{III}-Phase (20°C) und (b) *HT*-Phase (720°C)

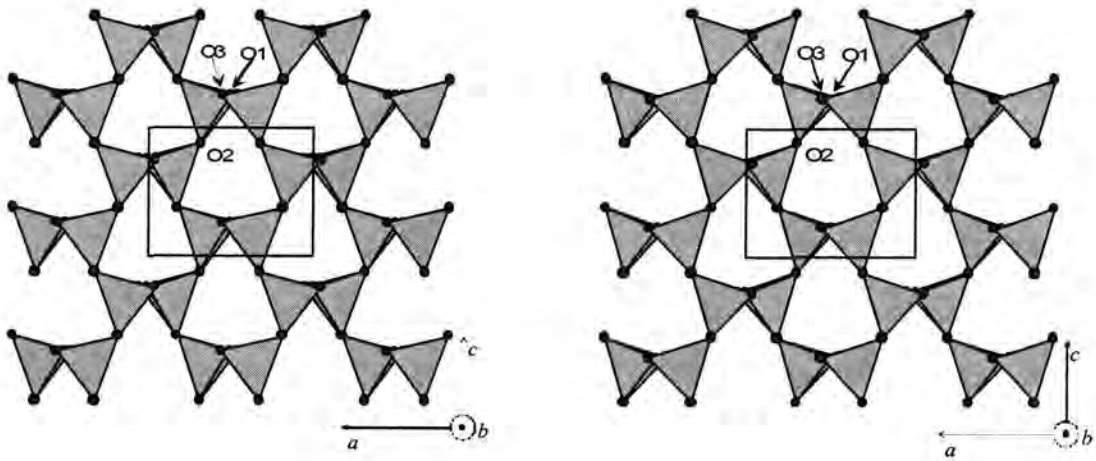

(a) (b)

Abb. 2.8: Projektion der Schicht 2 auf die a-c Ebene : (a) α_{III}-Phase (20°C) und (b) *HT*-Phase (720°C)

Zusammenfassend läßt sich aussagen, daß die Ergebnisse der Einkristallstruktur-untersuchungen momentan nur auf die Existenz eines Phasenübergangs hinweisen. Dieser Befund steht im Widerspruch zu den Resultaten der thermischen Messungen. Eine mögliche Erklärung hierfür könnte in der mangelnden thermischen Langzeitstabilität der Heizung am Diffraktometer liegen, die eine Auflösung der dicht benachbarten Effekte stark erschwert und die sichere Temperaturzuordnung beeinträchtigt. Es läßt sich nicht ausschließen, daß es während der Messungen innerhalb des kritischen T-Intervalls von etwa 30°C zu einer "Verschmierung" der Umwandlungen kommt und die intermediäre Phase daher nicht erfaßt werden konnte.

3. Strukturelle Untersuchungen an Kaliumdisilikat ($K_2Si_2O_5$)

3.1 Stand der Forschung

Im Vergleich zum Natriumdisilikat lagen zur entsprechenden kaliumhaltigen Verbindung bislang nur wenige Informationen vor. Eine kristalline Phase der Zusammensetzung $K_2Si_2O_5$ wurde erstmals von Kracek et al. [28] erwähnt. Diese soll bei 594°±5°C eine reversible Umwandlung durchlaufen. Aus den Ergebnissen einer späteren Arbeit zur Temperaturabhängigkeit des Brechungsindex im $K_2Si_2O_5$ schloß Sheybany [18] auf die Existenz von zwei Phasenübergängen im Temperaturbereich zwischen 200°C und 600°C und postulierte die folgende Phasenabfolge:

$$K_2Si_2O_5 - I \xleftarrow{240^\circ - 250^\circ C} K_2Si_2O_5 - II \xleftarrow{\approx 560^\circ C} K_2Si_2O_5 - III$$

Aus röntgenographischen Untersuchungen bei Raumtemperatur konnten bisher zwei verschiedene Varianten unterschieden werden. DeJong et al. [19] beschrieben eine $K_2Si_2O_5$ - Phase, die in einer für ein Si : O Verhältnis von 1 : 2.5 recht ungewöhnlichen unterbrochenen Tetraedergerüststruktur kristallisiert (Raumgruppe *Cc* mit a = 16.322(2) Å, b = 11.243(2) Å, c = 9.919(1) Å, β = 115.97(1)°, Z = 12). Es liegen dabei ausschließlich ternäre (Q^3) Tetraeder vor. Die Struktur kann im Prinzip aus der Cristobalitstruktur abgeleitet werden und enthält Schichten aus einfachen Sechserringen von Tetraedern (S6R) in der sogenannten „chair"-Konformation. Die Synthese erfolgte durch die Decarbonatisierung der Reaktionsmischung (K_2CO_3 und Quarz im Verhältnis 1:2) bei 750°C, die dann zunächst bei 1300°C aufgeschmolzen und schließlich mit 30°C/h bis auf 785°C abgekühlt wurde. Das resultierende Glas wurde dann für insgesamt 78 Stunden auf dieser Endtemperatur gehalten und abgeschreckt. Es sei an dieser Stelle darauf hingewiesen, daß nach De Jong et al. genau ein(!) Kristall dieser Phase in der gesamten Probe gefunden wurde. Über die anderen kristallinen Phasen finden sich leider keine weiteren Angaben.

Eine zweite Modifikation ist schon seit längerer Zeit bekannt und von Schweinsberg & Liebau [17] untersucht worden. Die ebenfalls durch die Kristallisation von Gläsern erhaltene Verbindung zeigte in Einkristallbeugungsaufnahmen eine orthorhombische Zelle mit Gitterkonstanten von a = 9.72(6) Å, b = 25.26(10) Å, c = 14.24(11) Å. Die systematischen Auslöschungen ließen sich allerdings mit keiner orthorhombischen Raumgruppe vereinbaren. Ferner zeigte die Intensitätsverteilung im reziproken Raum die typischen Merkmale einer Überstruktur: Reflexe mit k = 3n waren deutlich intensitätsstärker.

Eine detaillierte Strukturanalyse scheiterte an der intensiven polysynthetischen Verzwillingung, die in ausnahmslos allen untersuchten Kristallen auftrat.

3.2 Synthese

Die eigenen Synthesen orientierten sich an der in [17] angegebenen Vorschrift. Kaliumcarbonat wurde mit Quarz gemäß der Gleichung

$$2SiO_2 + K_2CO_3 \rightarrow K_2Si_2O_5 + CO_2$$

umgesetzt. Je 2g einer Reaktionsmischung (K_2CO_3 Riedel deHaën 99% und SiO_2 Feinmehl) wurden im offenen Platintiegel decarbonatisiert, bei 1100°C für 2h aufgeschmolzen und auf Raumtemperatur abgeschreckt. Nach erneutem Aufmahlen, Homogenisieren und Aufschmelzen erfolgte die Kristallisation des glasigen Produktes schließlich bei 800°C. Da sich die Edukte an Luft innerhalb von 1 - 2 Stunden zersetzten, wurden die Proben sofort in einen Trockenschrank bei 200°C eingebracht. Die Präparationsvorgänge für die Pulverröntgenaufnahmen, die NMR-Messungen und thermischen Analysen wurden in einer Glovebox unter Argonatmosphäre durchgeführt. Die Vorauswahl von einkristallinem Material für die Beugungsexperimente erfolgte unter dem Polarisationsmikroskop, wobei die Probe zum Schutz gegen Hydratisieren in Immersionsöl eingebettet wurde. Die Kristallite zeigten einen plattigen Habitus und die schon in [17] erwähnte ausgeprägte Neigung zur Zwillingsbildung.

3.3 Thermische Untersuchungen

Die thermoanalytische Charakterisierung wurde an einer NETZSCH STA 449C - Anlage durchgeführt. Eine Pulverprobe von 48.87 mg wurde in einer Argonatmosphäre zwischen Raumtemperatur und 800°C in Korundtiegeln untersucht. Für Aufheizung und Abkühlung wurde jeweils eine Rate von 10°C/min. gewählt. Die Ergebnisse sind in den folgenden Abbildungen 3.1 und 3.2 dargestellt.

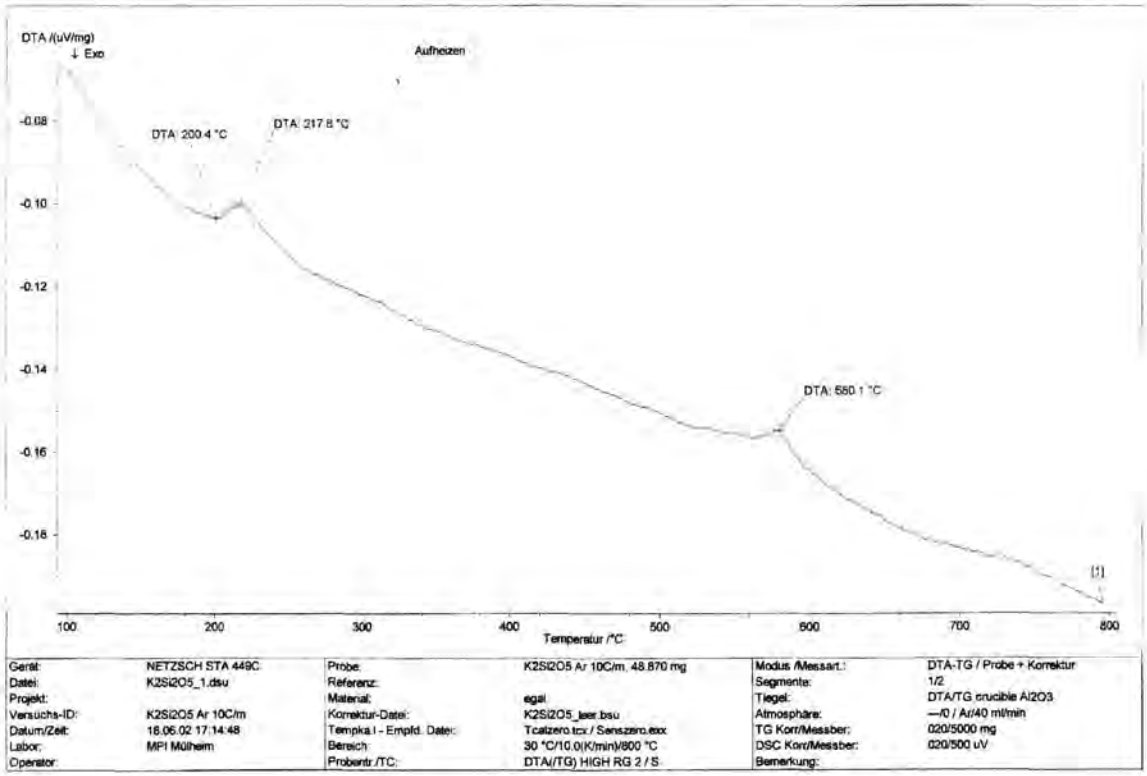

Abb. 3.1: DTA-Kurve von Kaliumdisilikat ($K_2Si_2O_5$) bei der Aufheizung

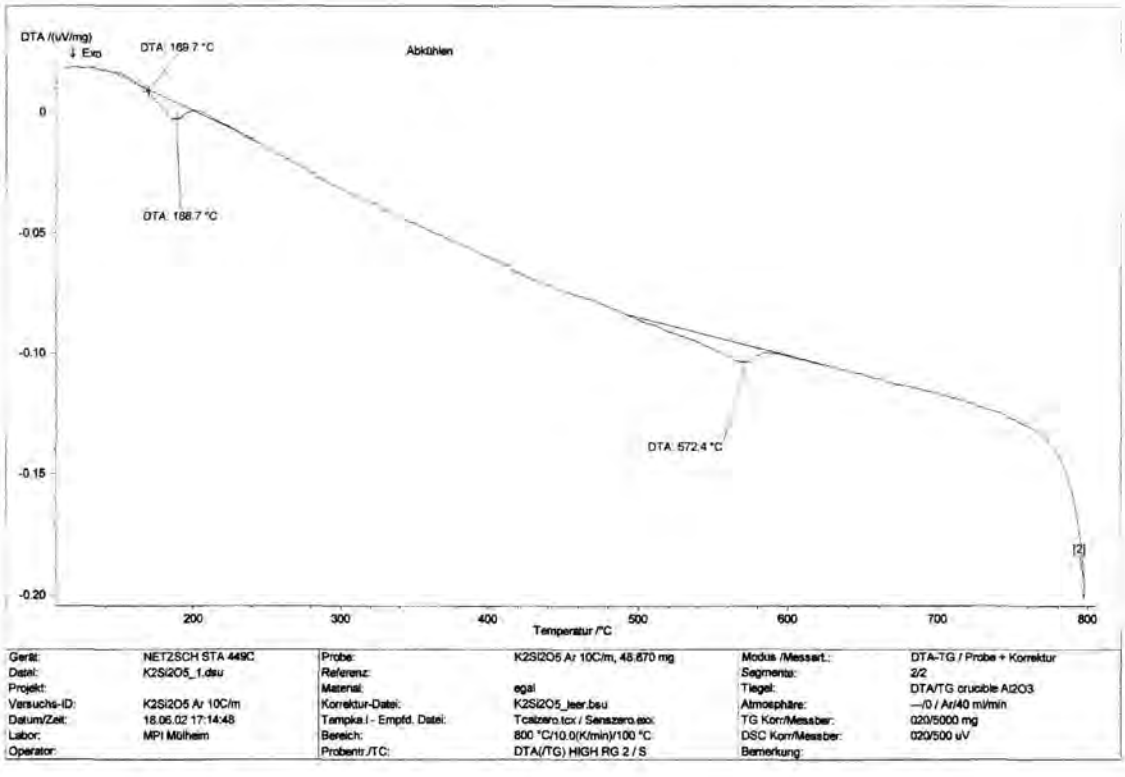

Abb. 3.2: DTA-Kurve von Kaliumdisilikat ($K_2Si_2O_5$) bei der Abkühlung

Während der Aufheizung finden im Temperaturbereich zwischen 200°C und 600°C zwei endotherme Ereignisse bei 217.8°C und 580.1°C statt.

Beide Effekte sind vergleichsweise breit und mit niedrigen Wärmetönungen verknüpft. Die Umwandlungen verlaufen reversibel, zeigen jedoch bei der Abkühlung eine deutliche Hysterese ($T_{max.}$ = 572.4°C bzw. 188.7°C). Die Gewichtsverluste während der Messung waren zu vernachlässigen.

3.4 Röntgenstrukturanalyse

Um die Gefahr der Zersetzung der luftempfindlichen Kristalle während der Datensammlung zu reduzieren, wurde die Messung am IPDS Einkristalldiffraktometer bei einer Temperatur von -100°C durchgeführt. Dazu wurde ein verzwillingter Kristall mit einem Durchmesser von circa 0.1 mm mittels eines Glasfadens aus dem Immersionsöl aufgenommen und sofort in den kalten Stickstoffgasstrom des Tieftemperaturzusatzes (Oxford Cryosystems – 600 Series Cryostream) gebracht. Das Öl wird bei dieser niedrigen Temperatur fest, fixiert den Kristall und umhüllt ihn gleichzeitig mit einer luftundurchlässigen Schutzhaut. Eine Zusammenstellung der Meßbedingungen ist in der folgenden Tabelle wiedergegeben.

Tabelle 3.1: Zusammenstellung der Meßparameter für $K_2Si_2O_5$.

Kristallgestalt	Platte
Diffraktometer	Stoe - IPDS
Monochromator	Graphit
Strahlung	MoK_α, λ = 0.71073 Å
Generatorleistung	50 kV, 40 mA
Abstand Detektor-Probe	70 mm
Schrittweite in ϕ (°)	2.0
Anzahl der gesammelten Bilder	100
Belichtungszeit / Bild (min.)	3.0
2θ - Bereich (°)	3.3- 52.1
Temperatur (°C)	-100
Anzahl der gemessenen Reflexe	36698
Anzahl der beobachteten Reflexe ($I > 2\sigma(I)$)	6724

Die resultierende primitive Zellmetrik (a = 9.7477(10) Å, b = 14.2330(32) Å, c = 24.8812(26) Å, V = 3452.0(15) Å^3) zeigt, daß es sich bei den Kristallen um die gleiche Phase handelt, die auch schon von Schweinsberg beschrieben wurde [17]. Die Mittelung der Daten in der Lauegruppe *mmm* ergab einen vergleichsweise schlechten inneren R-Wert von 0.19. Im nächsten Schritt wurden die Intensitäten nun in den drei monoklinen Untergruppen $m11$, $1m1$

bzw. 11*m* gemittelt. Während die inneren R-Werte in den ersten beiden Fällen nahezu unverändert schlecht blieben, resultierte für die Lauesymmetrie 11*m* eine deutliche Verbesserung ($R_{int.}$ = 0.11). Die Verbindung gehört also offenbar dem monoklinen Kristallsystem an, wobei die symmetrietragende Richtung in der oben gewählten Aufstellung längs *c* verläuft. Versuche, die Struktur dieser Phase zu lösen, schlugen bislang fehl. Eine mögliche Erklärung hierfür liegt in der stark ungleichen Intensitätsverteilung der Reflexe im reziproken Raum. Neben wenigen starken Hauptreflexen gibt es eine große Zahl sehr schwacher Überstrukturreflexe (vgl. Abb. 3.3).

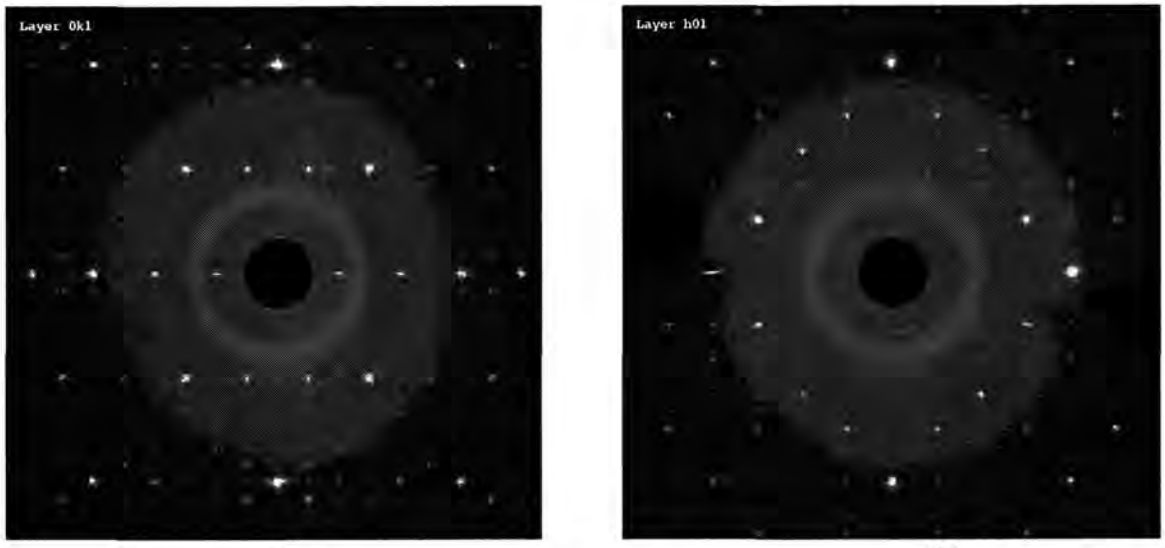

(a) (b)

Abb. 3.3: Schichten 0kl (a) und h0l (b) im reziproken Raum.

Reflexe (*hkl*) mit *l* = 3·n sind überdurchschnittlich stark. Die Kristallstruktur des Kaliumdisilikats kann somit im Prinzip durch die kommensurable Modulation einer gemittelten Struktur erklärt werden, deren Gitterkonstante in Richtung [001] nur etwa 8.3 ? (= *c*/3) beträgt. Um zumindest eine Aussage über diese gemittelte Struktur treffen zu können, wurde der Datensatz auf die Hauptreflexe mit *l* = 3n reduziert und eine Transformation von der *ersten* in die *zweite* monokline Aufstellung vorgenommen. Diese Untermenge von Reflexen zeigte integrale und serielle Auslöschungen, deren Systematik auf die möglichen Raumgruppen *Cc* bzw. *C*2/*c* hindeuteten.

Die Anwendung direkter Methoden [29] führte im Fall der Raumgruppe *C2/c* zu einem kristallchemisch plausiblen Strukturmodell, wobei allerdings bei der Beurteilung in Betracht gezogen werden muß, daß es sich um eine Projektion von insgesamt drei leicht verschiedenen Subzellen in einer gemeinsamen Zelle handelt. Die gefundene Strukturlösung wurde mittels des Programms SHELXL-93 [27] mit isotropen Temperaturfaktoren verfeinert.

Tabelle 3.2: Zusammenfassung der Struktur- und Verfeinerungsparameter der gemittelten Struktur des $K_2Si_2O_5$.

(A)	**Kristallographische Basisdaten**	
	a (Å)	9.7477(10)
	b (Å)	8.2937(9)
	c (Å)	14.2330(32)
	β (°)	90.14(1)
	V ($Å^3$)	1150.7(5)
	Raumgruppe	*C*2/*c*
	Z	8
	Chemische Zusammensetzung	$K_2Si_2O_5$
	D_{calc} ($g\ cm^{-3}$)	2.475
	μ (mm^{-1})	2.00
	Indexbereich	$\|h\| \leq 8 ; 0 \leq k \leq 10 ; 0 \leq l \leq 14$
	Anzahl der unabhängigen Reflexe im 2/m	1073
	R_{int} in 2/m	0.079
(B)	**Strukturverfeinerung**	
	Anzahl der verfeinerten Parameter	50
	R1 ($F_o > 4\ \sigma(F_o)$)	0.087
	wR2 ($F_o > 4\ \sigma(F_o)$)	0.228
	Wichtungsfaktor a	0.0994
	Goodness of Fit	1.026
	Final $\Delta\rho_{min}$ (e / $Å^3$)	-0.91
	Final $\Delta\rho_{max}$ (e / $Å^3$)	1.41
	$R1 = \Sigma \|\|F_o\| - \|F_c\|\| / \Sigma \|F_o\|$	$wR2 = (\Sigma(w(F_o^2 - F_c^2)^2) / \Sigma(w(F_o^2)^2))^{1/2}$
	$w = 1 / (\sigma^2 (F_o^2) + (aP)^2)$	$P = (2F_c^2 + \max(F_o^2, 0)) / 3$

Die gemittelte Struktur gehört zur Gruppe der Einfach-Schichtsilikate, zu der auch andere kaliumhaltige Disilikate, wie z.B. $KLiSi_2O_5$ [30] oder mehrere der im Rahmen dieser Arbeit charakterisierten Na-K-Disilikate zählen. Die Schichten laufen senkrecht zur *c*-Achse und bestehen ausschließlich aus Vierer- und Achterringen (Abbildung 3.4). Dieses Ergebnis unterscheidet das Kaliumdisilikat allerdings deutlich von den Na-haltigen Schichtsilikaten mit Disilikatchemismus, in denen immer auch Sechserringe vorkommen. Die Verfeinerung zeigte, daß alle verbrückenden Sauerstoffatomen (O2-O3, O4-O8, O6 und O7) Splitpositionen

besetzen. Dies ist nicht unbedingt verwunderlich, da die es sich um eine Projektionstruktur handelt. Die mittleren Si-O Abstände der zwei unabhängigen Si-Atome betragen 1.628Å bzw. 1.634Å. Diese Werte sind signifikant größer als der von Baur [31] für Schichtsilikate angegebene Mittelwert von 1.617Å. Die mittleren O-Si-O Winkel nehmen Werte von 110.1° bzw. 108.95° an.

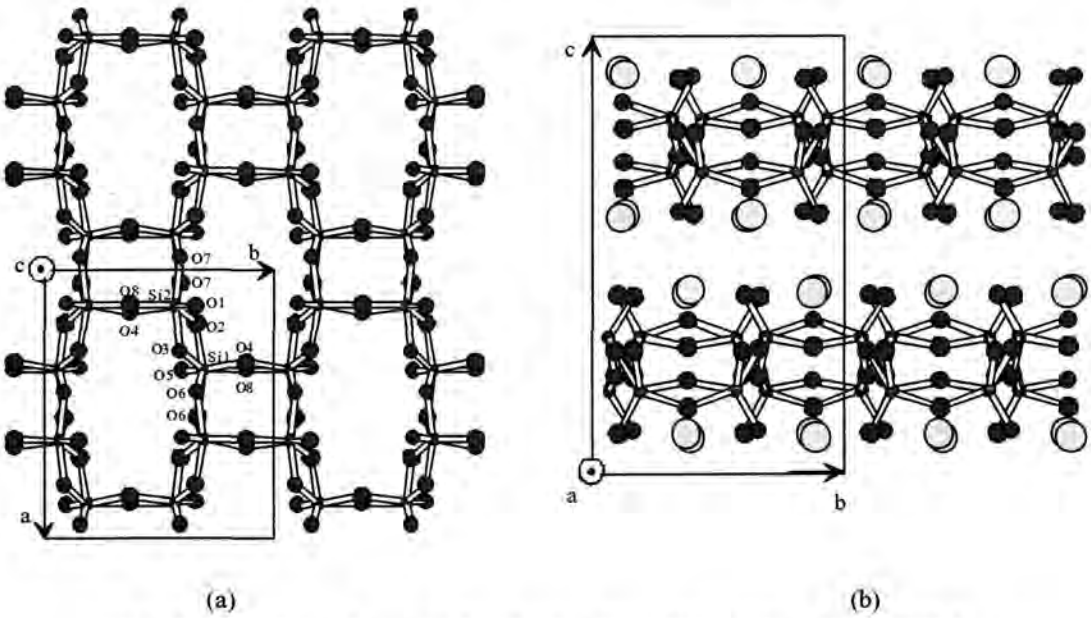

(a) (b)

Abb. 3.4: Projektion der gemittelten Struktur längs [001] (a) bzw. längs [100] (b).

In den Hohlräumen zwischen den Schichten liegen die hellgrau eingezeichneten Kaliumatome. Sie sind von jeweils mindestens fünf Sauerstoffatomen koordiniert. Auf eine detaillierte Auflistung der Atomkoordinaten und der interatomaren Abstände und Winkel sei an dieser Stelle verzichtet, da es sich bei der Lösung der gemittelten Struktur lediglich um ein vorläufiges Ergebnis handelt.

3.5 Pulverdiffraktometrische Messungen

Pulverdiffraktometrische Untersuchungen an polykristallinem Kaliumdisilikat wurden bei Raumtemperatur und bei erhöhten Temperaturen an einem Transmissionsgerät der Firma STOE mit linearem PSD Detektor durchgeführt. Als Probenbehälter wurden Quarzglaskapillaren (Durchmesser ca. 0.5 mm) verwendet. Die Messungen erfolgten in einer Schutzgasatmosphäre (Argon) im Winkelbereich zwischen 10.03° und 99.99° 2θ mit Schrittweiten von 0.01°. Die Abbildungen 3.5 und 3.6 zeigen die Ergebnisse zweier strukturunabhängiger Profilanpassungen bei Raumtemperatur nach der Le-Bail Methode, die mit dem Programm FULLPROF vorgenommen wurden [32]. Für den in Abbildung 3.5

wiedergegeben Fit wurde die kleine C-zentrierte Zelle der gemittelten Struktur verwendet. Das in Abbildung 3.6 gezeigte Ergebnis basiert dagegen auf der großen orthorhombischen Zelle mit verdreifachter *c*-Gitterkonstante.

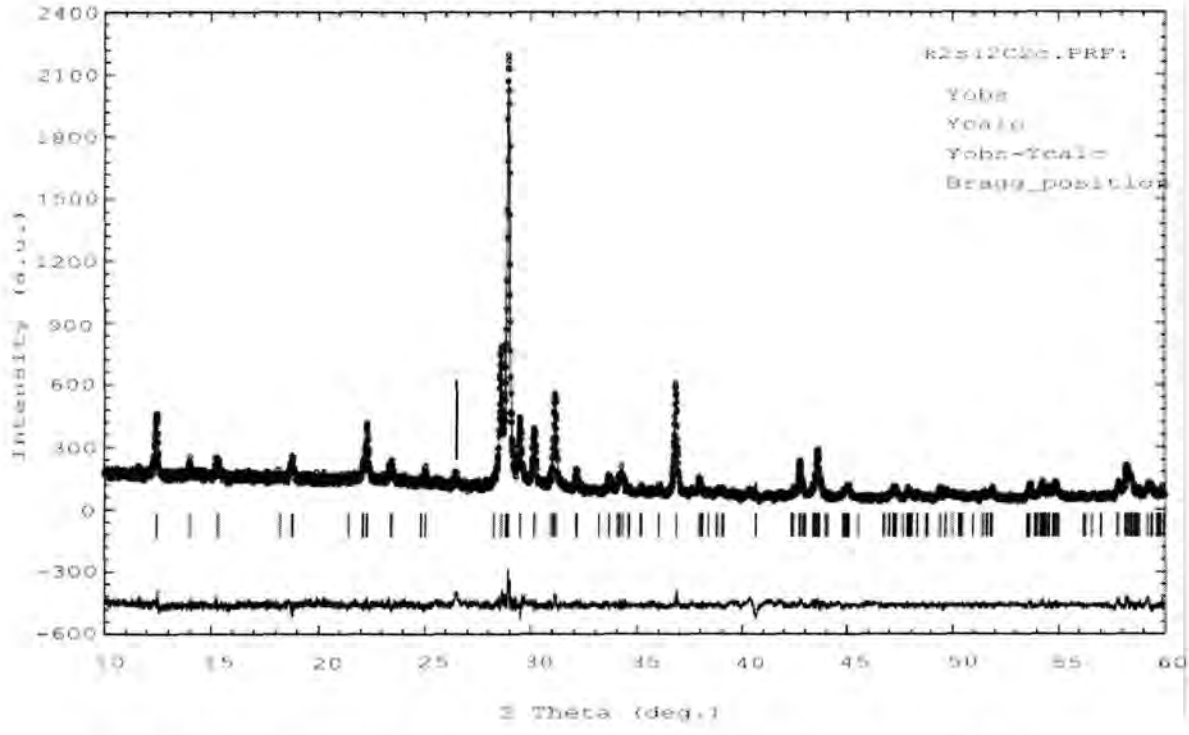

Abb. 3.5: Profilanpassung mit a = 9.751 Å, b = 8.296 Å, c = 14.213 Å, β = 90.1° R.G. C 2/c

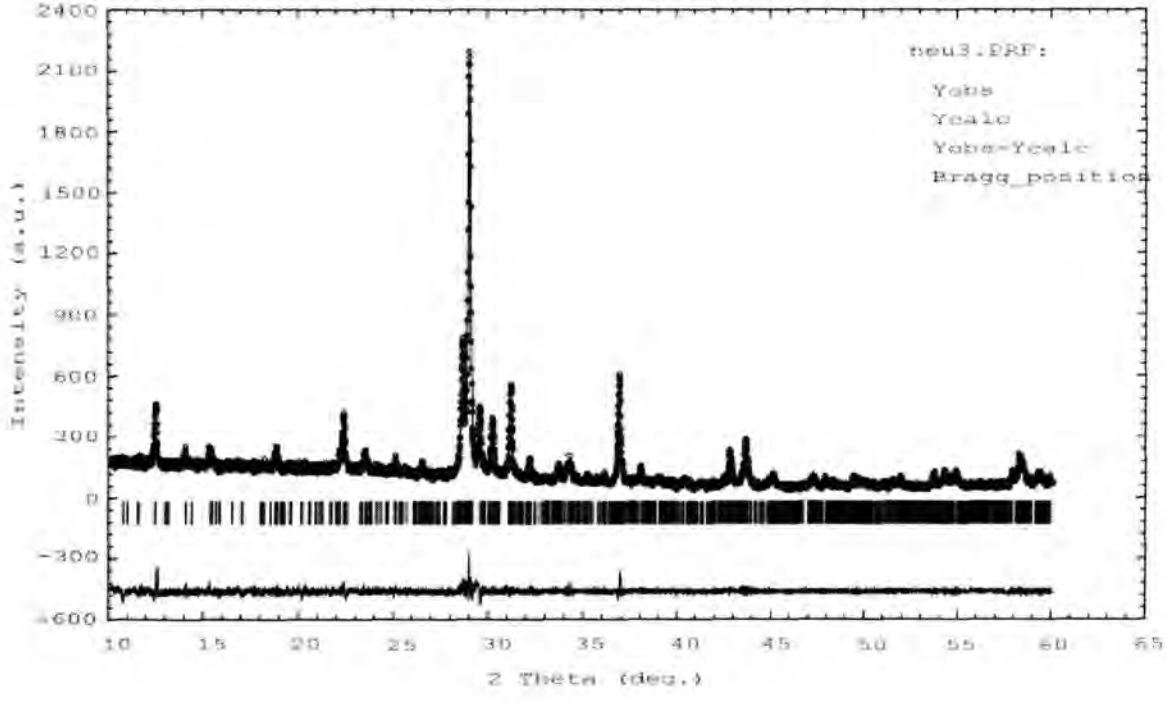

Abb. 3.6: Profilanpassung mit a = 9.733 Å, b = 24.586 Å, c = 14.136 Å, β = 90.29° R.G. P 2/m

Der Fit unter Verwendung der Metrik der gemittelten Struktur ergibt eine signifikant schlechtere Anpassung. So läßt sich z.B. der im Abb. 3.5 mit einem Pfeil markierte Reflex bei etwa 26.3° 2θ nicht mit der dieser Zelle erklären. Da es bei einer Pulveraufnahme im Gegensatz zu einem Einkristallbeugungsexperiment auf Grund der Mittelung über viele Kristallitorientierungen zu keiner Vortäuschung zu großer Zellen als Folge einer pseudomeroedrischen Verzwillingung kommen kann, muß die Gesamtstruktur tatsächlich in einer großen Zelle mit einer *c*-Gitterkonstante von knapp 25 Å beschrieben werden.

Ergänzt wurden die pulverdiffraktometrischen Untersuchungen durch HT-Messungen bei 300°C bzw. 650°C. Eventuelle strukturelle Änderungen der beiden in den thermischen Analysen beobachteten Effekte sollten damit nachweisbar sein. Die Abbildung 3.7 zeigt die entsprechenden Beugungsdiagramme, ergänzt durch zwei Messungen bei Raumtemperatur, die jeweils vor bzw. nach der Aufheizung erfolgten. Aufgrund des durch die Probenumgebung bedingten relativ hohen Untergrunds war eine weitergehende Analyse der Auswirkungen auf die Pulverdiagramme, insbesondere bei den schwachen Reflexen, nicht gegeben. Die zwei auffälligsten Bereiche in denen sich Änderungen in den Beugungsaufnahmen vollziehen, sind markiert.

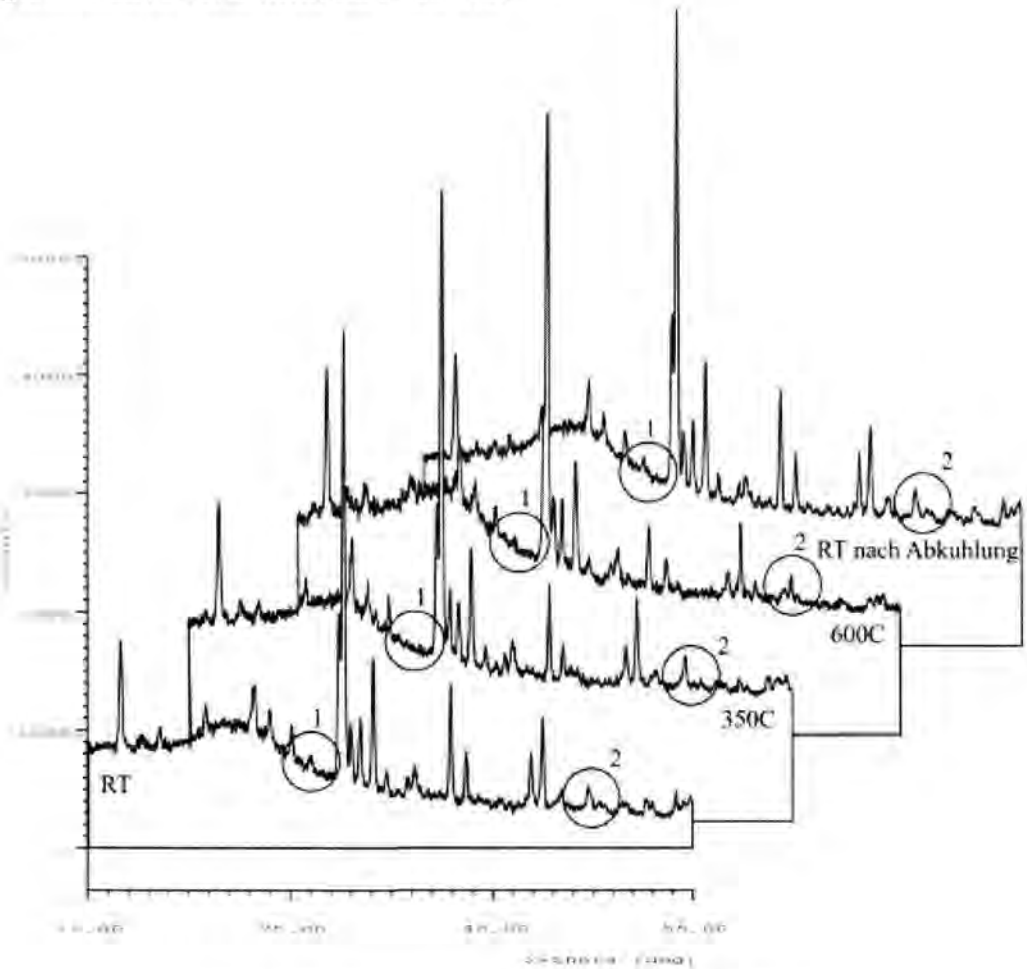

Abb. 3.7: Hochtemperatur-Pulveraufnahmen von $K_2Si_2O_5$

3.6 ^{29}Si MAS NMR-Untersuchungen an $K_2Si_2O_5$

Im Rahmen dieser Arbeit wurde versucht, mittels ^{29}Si-MAS-NMR-Spektroskopie zusätzliche Informationen über die Si-Lagen innerhalb der Elementarzelle zu gewinnen. Diese Methode ist in unserem Fall eine empfindliche Sonde zur Untersuchung der Si-Umgebung. Das Isotop ^{29}Si hat den Kernspin I=1/2 und kann mit einer natürlichen Häufigkeit von ca. 5% bei NMR-Untersuchungen als sogenannter *isolierter* Kern betrachtet werden, was die Analyse und den Messvorgang sehr vereinfacht. Die Messung selbst erfolgte an einem BRUKER Avance 500WB Spektrometer. Die Stärke des Magnetfeldes war 11T , die MAS-Frequenz betrug 20.83 kHz. Die Resonanzfrequenz liegt bei 99.4 MHz. Die Abbildung 3.8 zeigt das gemessene ^{29}Si-MAS-NMR Spektrum des $K_2Si_2O_5$.

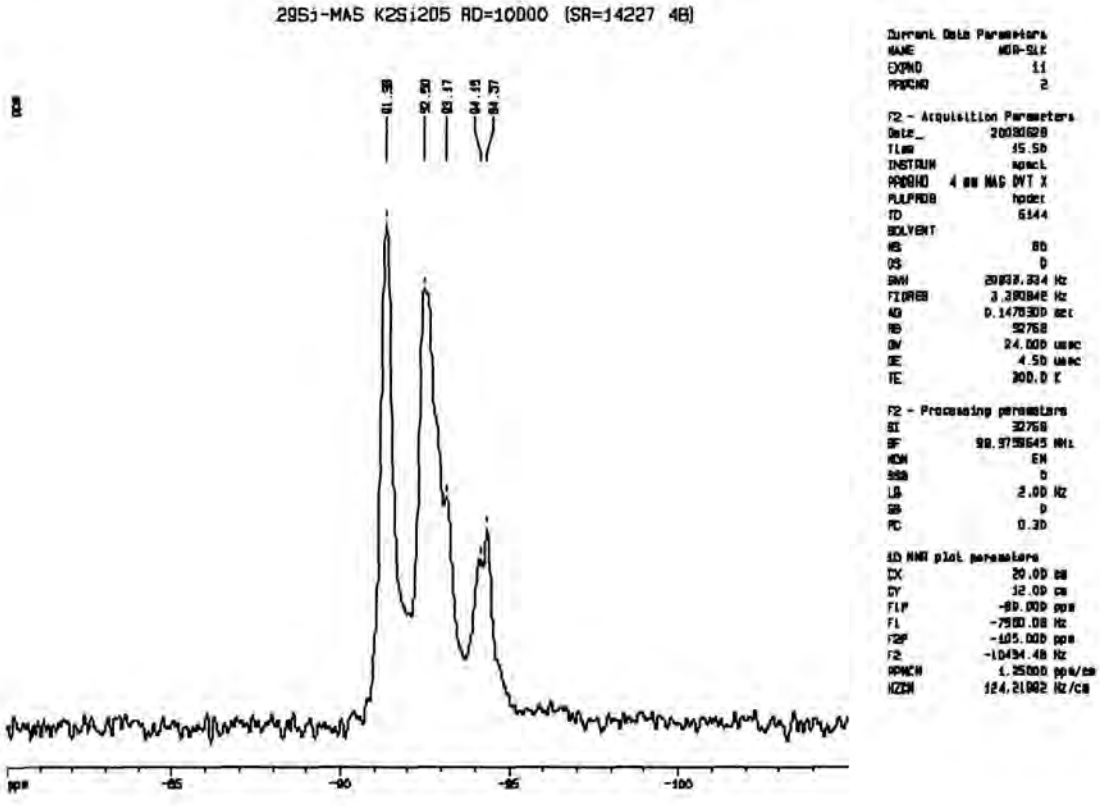

Abb 3.8: ^{29}Si-MAS-NMR Spektrum des $K_2Si_2O_5$

Das Spektrum zeigt einen scharfen Peak bei –91.38 ppm und noch zwei zusätzliche breite Signale, in denen sich mindestens vier zusätzliche Peaks bei –92.50 ppm, –93.17 ppm, –94.15 ppm und –94.37 ppm verbergen. Dies deutet darauf hin, daß in der wahren Zelle der Kaliumdisilikatstruktur von mindestens fünf symmetrisch unabhängigen Si-Atomlagen auszugehen ist. Die angegebenen chemischen Verschiebungen liegen zwischen den beim δ-$Na_2Si_2O_5$ gemessenen Werten (–90 ppm) und denen des α-$Na_2Si_2O_5$ (–94 ppm).

4. Hydrothermalsynthesen und röntgenographische Untersuchungen an den Mischphasen $Na_{2-x}K_xSi_2O_5$

4.1 Stand der Forschung

Erste Untersuchungen im System $Na_2Si_2O_5$ bei Drucken bis 400 bar wurden von Williamson & Glasser [11] vorgenommen. Die Autoren bestimmten die Existenzbereiche von insgesamt drei Modifikationen: α-$Na_2Si_2O_5$, β-$Na_2Si_2O_5$ und das sogenannte C-$Na_2Si_2O_5$. Während die α- und β- Phase sich auch bei Normaldruck bilden, handelt es sich bei der C-Variante um eine reine Hochdruckphase, die allerdings abgeschreckt werden kann. Der Tripelpunkt der drei Phasen liegt etwa bei einer Temperatur von 715°C und einem Druck von 90 bar. Diese Ergebnisse wurden prinzipiell in einer späteren Arbeit von Jacobsen [24] bestätigt. Im Bereich höherer Drucke ist die Existenz der oben erwähnten G-Phase bis mindestens 25 kbar (bei 900°C) gesichert (Kanzaki et al. [5]). Oberhalb 50 bis 60 kbar schließlich taucht dann eine neue Phase, das sogenannte ε-$Na_2Si_2O_5$ auf (Fleet & Henderson [3]). Über die Bildung von Hochdruckphasen der Zusammensetzungen $Na_{2-x}K_xSi_2O_5$ lagen bislang keine Informationen vor. Entsprechende Synthesen waren erstmals Gegenstand dieser Arbeit.

4.2 Synthesen und Ergebnisse

Als Startsubstanzen zur Synthese dienten Natriumcarbonat Na_2CO_3 (Fluka 99%), Kaliumcarbonat $K_2Si_2O_5$ (Riedel deHaen 99%) und Quarz-Feinmehl. Nach der Homogenisierung im Achatmörser wurden die Reaktionsgemische (je 1g der Ausgangsprodukte) im Pt-Tiegel decarbonatisiert, bei 1000°C innerhalb 20 Minuten aufgeschmolzen und danach an Luft abgeschreckt. Die resultierenden Gläser wurden insgesamt dreimal aufgemahlen und der Schmelzvorgang wiederholt, um eine bessere Homogenität zu erreichen. Zwischen 0.20 und 0.25g der Glasproben wurden anschließend zusammen mit 1 Gew.% Wasser in Goldkapseln (5 mm Innendurchmesser, 0.2 mm Wanddicke, Länge 22-25 mm) gefüllt und zugeschweißt. Vor jeder Hydrothermalsynthese erfolgte ein Test, ob die Kapseln auch dicht verschlossen waren. Die Proben wurden in der Hydrothermalanlage des Bayerischen Geoinstituts in Bayreuth zunächst bei Raumtemperatur auf den jeweiligen Enddruck gebracht. Danach erfolgte die isobare Erwärmung auf die gewünschte Synthesetemperatur, die für jeweils 24h gehalten wurde. Anschließend wurden die Kapseln auf Raumbedingungen abgeschreckt. Als druckübertragendes Medium wurde Wasser verwendet. Die Synthesebedingungen, sowie die Produkte sind in der Tabelle 4.1 zusammengefaßt. Die kristallinen Phasen sind mit (1), (2), (3) und (4) bezeichnet.

Die strukturellen Charakterisierungen sind in den Manuskripten des Anhangs enthalten. Die einzelnen Nummern stehen dabei für die folgenden Phasen :

Typ 1 – $Na_{0.67}K_{1.33}Si_2O_5$ (Siehe Seite 92 - 110)

Typ 2 – $NaKSi_2O_5$-II (Siehe Seite 92 - 110)

Typ 3 – $Na_{1.84}K_{0.16}Si_2O_5$ (Siehe Seite 75 - 91)

Typ 4 – κ-$Na_2Si_2O_5$ (Siehe Seite 75 - 91)

Tabelle 4.1: Zusammenstellung der Ergebnisse der Hydrothermalsynthesen an Mischphasen der Zusammensetzung $Na_{2-x}K_xSi_2O_5$

Zusammensetzung des Glases	t [°C]	p [kbar]	Zeit [h]	Produkte
$K_2Si_2O_5$	500	1	je	
	500	3	24	Glas + polykristallines $K_2Si_2O_5$,
	700	1		sehr luftempfindlich
	700	3		
$Na_{0.5}K_{1.5}Si_2O_5$	500	1	je	Glas + Typ1 (polykrist. / größere Krist.)
	500	3	24	Glas + größere Kristalle des Typ1
	700	1		Glas
	700	3		Glas
$NaKSi_2O_5$	500	1	je	Glas + größere Kristalle des Typ 2
	500	3	24	Glas
	700	1		Glas
	700	3		Glas
$Na_{1.5}K_{0.5}Si_2O_5$	500	1		Glas
	500	3	24	Glas
	600	1		Glas + Typ3 (polykrist. / größere Krist.)
	600	3		Glas
	700	1		Glas
	700	3		Glas
$Na_2Si_2O_5$	500	1		Glas + β-$Na_2Si_2O_5$
	500	3	24	Glas + β-$Na_2Si_2O_5$ + Quarz
	700	1		Glas + C-$Na_2Si_2O_5$
	700	3		Glas + größere Kristalle des Typ 4

5. Synthesen bei Normaldruck und röntgenographische Untersuchungen an den Mischphasen $Na_{2-x}K_xSi_2O_5$

5.1 Stand der Forschung

Wie schon in der Einleitung dieser Arbeit erwähnt, lagen bislang nur wenige kristallchemische Informationen über die kristallinen Phasen im System $Na_{2-x}K_xSi_2O_5$ vor. Lediglich von Sakaguchi et al. [23] ist eine Arbeit bekannt, in der durch Fällungsreaktionen Phasen der Zusammenstzung $Na_{2-x}K_xSi_2O_5$ mit x~0.6-0.9 hergestellt werden konnten. Das Pulverbeugungsdiagramm einer Probe mit der Zusammensetzung $Na_{1.3}K_{0.7}Si_2O_5$ konnte in einer monoklinen Zelle mit $a = 4.84$ Å, $b = 8.69$ Å, $c = 11.97$ Å, $\beta = 90.37°$ indiziert werden. Als mögliche Raumgruppe wurde $P2_1/c$ in Betracht gezogen, eine Strukturlösung allerdings nicht durchgeführt.

5.2 Synthesen und Ergebnisse

Die eigenen Synthesen im Bereich $0 = x = 1$ basierten auf der Kristallisation von Gläsern. Als Edukte dienten Natriumcarbonat Na_2CO_3 (Fluka 99%), Kaliumcarbonat $K_2Si_2O_5$ (Riedel deHaën 99%) und Quarz-Feinmehl. Die Herstellung der Ausgangsgläser erfolgte analog zu den entsprechenden Synthesen für die Hydrothermalexperimente. Diese wurden dann jeweils bei verschiedenen Temperaturen und über verschiedene Zeitintervalle getempert (vgl. Tabelle 5.1).

Tabelle 5.1: Zusammenstellung der Synthesebedingungen.

Zusammensetzung der Ausgangsgläser	Temperatur [°C]	Temperzeiten [Tagen]
$Na_{1.9}K_{0.1}Si_2O_5$	700	7
$Na_{1.8}K_{0.2}Si_2O_5$	700	7
$Na_{1.7}K_{0.3}Si_2O_5$	700	7
$Na_{1.6}K_{0.4}Si_2O_5$	700	25
$Na_{1.5}K_{0.5}Si_2O_5$	700	25
$Na_{1.4}K_{0.6}Si_2O_5$	700	25
$Na_{1.3}K_{0.7}Si_2O_5$	700	40
$Na_{1.2}K_{0.8}Si_2O_5$	700	40
$Na_{1.1}K_{0.9}Si_2O_5$	700	40
$NaKSi_2O_5$	750	25

Die Produkte wurden polarisationsmikroskopisch und röntgenographisch untersucht. Die Quantifizierung der kristallinen Phasen erfolgte, soweit möglich, nach der Rietveldmethode. Die Ergebnisse sind in der folgenden Tabelle 5.2 zusammengefaßt. Mit Typ A, B und C sollen dabei die folgenden Strukturtypen bezeichnet werden, die in den Manuskripten im Detail behandelt werden :

Typ A – Strukturtyp des $Na_{1.55}K_{0.45}Si_2O_5$ (Siehe Seite 30 - 42)

Typ B – Strukturtyp des $Na_{1.84}K_{0.16}Si_2O_5$ (Siehe Seite 75 - 91)

Typ C – Strukturtyp des $NaKSi_2O_5$-I (Siehe Seite 43 - 56)

Tabelle 5.2: Phasenanalytische Untersuchungen der rekristallisierten Gläser bei Normaldruck.

Zusammensetzung der Gläser	Produkt(e) und deren Anteile in Gew.%		Gitterkonstanten (a [Å], b[Å], c[Å], β) und Raumgruppe
$Na_{1.9}K_{0.1}Si_2O_5$	α-$Na_2Si_2O_5$	47.6%	6.431 ; 15.426 ; 4.902 ; Pcnb
	Typ A	52.4%	4.844 ; 8.422 ; 12.034 ; 90.38° ; $P2_1/c$
$Na_{1.8}K_{0.2}Si_2O_5$	α-$Na_2Si_2O_5$	88.7%	6.440 ; 15.426 ; 4.841 ; Pcnb
	Typ A	11.3%	4.955 ; 8.431 ; 11.993 ; 91.09° ; $P2_1/c$
$Na_{1.7}K_{0.3}Si_2O_5$	α-$Na_2Si_2O_5$	3%	6.421 ; 15.417 ; 4.878 ; Pcnb
	Typ A	97%	4.825 ; 8.428 ; 11.978 ; 90.66° ; $P2_1/c$
$Na_{1.6}K_{0.4}Si_2O_5$	α-$Na_2Si_2O_5$	40.6%	6.419 ; 15.423 ; 4.901 ; Pcnb
	Typ A	59.4%	4.835 ; 8.416 ; 12.080 ; 90.41° ; $P2_1/c$
$Na_{1.5}K_{0.5}Si_2O_5$	Typ A		4.840 ; 8.169 ; 12.087 ; 90.36° ; $P2_1/c$
$Na_{1.4}K_{0.6}Si_2O_5$	Typ A		4.813 ; 8.302 ; 11.996 ; 90.43° ; $P2_1/c$
	Glas		
$Na_{1.3}K_{0.7}Si_2O_5$	Typ A	89.2%	4.845 ; 8.703 ; 11.970 ; 90.36° ; $P2_1/c$
	Typ B	10.8%	8.701 ; 4.902 ; 12.072 ; $Pn2_1a$
$Na_{1.2}K_{0.8}Si_2O_5$	Typ A	75.8%	4.829 ; 8.675 ; 11.927 ; 90.38° ; $P2_1/c$
	Typ B	24.2%	8.189 ; 4.843 ; 12.040 ; $Pn2_1a$
$Na_{1.1}K_{0.9}Si_2O_5$	Typ A		4.846 ; 8.681 ; 11.962 ; 90.32° ; $P2_1/c$
	Typ B		8.202 ; 4.877 ; 12.090 ; $Pn2_1a$
	unbekannte Phase		
$NaKSi_2O_5$	Typ C		7.3005 ; 17.389 ; 12.353 ; 91.14 ; $P2_1/n$
	unbekannte Phase		

Im Allgemeinen wurden mehrphasige Produkte erhalten. Vertreter des Strukturtyps A tauchten über einen weiten Bereich von x = 0.1 bis x = 0.9 auf. Interessant ist in diesem Zusammenhang, daß in den Synthesen auch offensichtlich Kristalle des Typs B auftreten, die auch in den Hydrothermalsynthesen in Form von Einkristallen nachgewiesen wurden. Für x = 1.0 kommt es zu einer drastischen Änderung des Phasenbestands. Neben Kristallen des Typs C liegt polykristallines Material vor, daß sich bislang nicht identifizieren ließ ("unbekannte Phase").

6. Literaturverzeichnis

[1] Morey, G.W. & Bowen, N.L.: The binary system sodium metasilica – silica. *J. Phys. Chem.* **28** (1924) 1167 – 1179.

[2] Kracek, F.C.: The system sodium oxide – silica. *J. Phys. Chem.* **34** (1930) 1583 – 1598.

[3] Fleet, M.E. & Henderson, G.S.: Epsilon Sodium Disilicate: A high pressure layer structure [$Na_2Si_2O_5$]. *J. Sol. State Chem.* **119** (1995) 400 – 404.

[4] Fleet, M.E.: Sodium heptasilicate: A high-pressure silicate with six-membered rings of tetrahedra interconnected by SiO_6 octahedra: ($Na_8Si[Si_6O_{18}]$). *Am. Mineral.* **83** (1998) 618 – 624.

[5] Kanzaki, M., Xue, X. & Stebbins, J.F.: Phase relations in Na_2O – SiO_2 and $K_2Si_4O_9$ systems up to 14 Gpa and ^{29}Si NMR study of the new high – pressure phases: implications to the structure of high – pressure silicate glasses. *Phys. Earth Planet Int.* **107** (1998) 9 – 21.

[6] Maekawa, H. & Yokokawa, T.: Effects of temperature on silicate melt structure: A high temperature ^{29}Si NMR study of $Na_2Si_2O_5$. *Geochim. Cosmochim. Acta* **61** (1997) 2569 – 2575.

[7] Scott, W.D. & Pask, A.: Nucleation and growth of sodium disilicate crystals in sodium disilicate glass. *J. Amer. Ceram. Soc.* **44** (1961) 181 – 187.

[8] Wilkens, J.: Structure – property relationships of sodium disilicates. *Tenside Surf. Det.* **32** (1995) 476 – 482.

[9] Heinemann, I.: Natriumtransport in glasigem und kristallinen $Na_2Si_2O_5$. Dissertation TU Clausthal (1987).

[10] Willgallis, A. & Range, K.J.: Zur Polymorphie des $Na_2Si_2O_5$. *Glastechn. Ber.* **37** (1963) 194 – 200.

[11] Williamson, J. & Glasser, F.P.: The crystallisation of $Na_2O{\cdot}SiO_2$ – SiO_2 glasses. *Phys. Chem. Glasses* **7** (1966) 127 –138.

[12] Liebau, F.: Untersuchungen an Schichtsilikaten des Formeltyps $A_m(Si_2O_5)_n$. II. Über die Kristallstruktur des α - $Na_2Si_2O_5$. *Acta Cryst.* **14** (1961) 395 – 398.

[13] Pant, A.K. & Cruickshank, D.W.J.: The Crystal Structure of α - $Na_2Si_2O_5$. *Acta Cryst.* **B 24** (1968) 13 – 19.

[14] Pant, A.K.: A Reconsideration of the Crystal Structure of β - $Na_2Si_2O_5$. *Acta Cryst.* **B 24** (1968) 1077 – 1083.

[15] Hoffmann, W. & Scheel, H.J.: Über die γ - und δ - Modifikationen des Natriumdisilikates, $Na_2Si_2O_5$. *Z. Kristallogr.* **129** (1969) 396 – 404.

[16] Kahlenberg, V., Dörsam, G., Wendschuh-Josties, M. & Fischer, R.X.: The crystal structure of δ - $Na_2Si_2O_5$. *J. Sol. State Chem.* **146** (1999) 380 – 386.

[17] Schweinsberg, H. & Liebau, F.: Darstellung und kristallograpische Daten von $K_2Si_2O_5$, $KHSi_2O_5$-I und $K_2Si_4O_9$. *Z. Anorg. Allg. Chem.* **387** (1972) 241 – 251.

[18] Sheybany, H.A.: De la structure des verres alcalino-silicatés mixtes. *Verres et Réfract.* **3** (1949) 27 – 39.

[19] de Jong, B.H.W., Supèr, H.T.J., Spek, A.L., Veldman, N., Nachtegaal, G. & Fischer, J.C.: Mixed alkali systems: Structure and ^{29}Si MASNMR of $Li_2Si_2O_5$ and $K_2Si_2O_5$. *Acta Cryst.* **B 54** (1998) 568 – 577.

[20] Florian, P., Vermillion, K.E., Grandinetti, P.J., Farnan, I. & Stebbins, J.F.: Cation distribution in mixed alkali disilicate glasses. *J. Am. Chem. Soc.* **118** (1996) 3493 – 3497.

[21] Greaves, G.N.: Structural studies of the mixed alkali effect in disilicate glasses. *Solid State Ionics* **105** (1998) 243 – 248.

[22] Brawer, S.A. & White, W.B.: Raman spectroscopic investigations of the structure of silicate glasses. I. The binary alkali silicates. *J. Chem. Phys.* **63** (1975) 2421 – 2432.

[23] Sakaguchi, M., Sakamoto, I., Akagi, R. & Toraya, H.: Powder data for potassium sodium silicate $Na_{1.3}K_{0.7}Si_2O_5$. *Powder Diffr.* **10** (1995) 290 – 292.

[24] Jacobsen, H.: Neue Untersuchungen an Natriumdisilikat ($Na_2Si_2O_5$). Diplomarbeit Universität Hannover (1991).

[25] Remmert, P.: Phasenbeziehungen der α-, β- und δ-Modifikation von Natriumdisilicat unter besonderer Berücksichtigung der Darstellung aus Sprühprodukten. Dissertation Universität Giessen (1999).

[26] Scheufler, C.: Aufbau, Kalibrierung und Test einer Gasstromheizung für ein automatisches Röntgen - Einkristall - Diffraktometer (Siemens P3 / PC). Diplomarbeit Universität Würzburg.

[27] Sheldrick, G.M., SHELXL-93. A program for the refinement of crystal structures. Universität Göttingen, Germany, 1993.

[28] Kracek, F.C., Bowen, N.L. & Morey, G.W.: The Systems Potassium-Metasilicate-Silica. *J. Phys. Chem.* **33** (1929) 1857.

[29] Altomare, A., Cascarano, G., Giacovazzo, C., Guargliardi, A., Burla, M.C., Polidori, G. & Camalli, M.: SIR92 – a program for automatic solution of structures by direct methods. *J.Appl.Cryst.* **27** (1992) 435.

[30] de Jong, B.H.W.S., Super, H.T., Spek, A.L., Veldman, N., van Wezel, W. & van der Mee, V.: Structure of $KLiSi_2O_5$ and the Hygroscopicity of Glassy Mixed Alkali Disilicates. *Acta Cryst.* **B52** (1996) 770 – 776.

[31] Baur, W.H.: Variation of mean Si-O bond lengts in silicon-oxigen tetrahedra. *Acta Cryst.* **B34** (1978) 1751 – 1756.

[32] Roisnel, T., Rodriguez-Carvajal, J.: WinPLOTR and WinFullProf – Windows9x/NT tools for powder diffraction, May 2000.

7. The crystal structure of a mixed alkali phyllosilicate with composition $Na_{1.55}K_{0.45}Si_2O_5$

S. Rakic and V. Kahlenberg

Fachbereich Geowissenschaften (Kristallographie), Universität Bremen,
Klagenfurter Str., D - 28359 Bremen, Germany

Abstract

The crystal structure of $Na_{1.55}K_{0.45}Si_2O_5$ has been solved and refined to a final residual R1 of 0.048 for 1208 independent reflections. The compound is monoclinic with space group $P2_1/c$ (a = 4.845(1) Å, b = 8.647(2) Å, c = 11.992(3) Å, β = 90.31(4)°, V = 503.1(4) Å^3, M_r = 189.40 u, Z = 4, λ(MoK_α) = 0.71073 Å, D_x = 2.51 g/cm^3, μ(MoK_α) = 1.14 mm^{-1}). The crystal showed twinning by pseudo-merohedry according to $2_{[100]}$, a feature which was accounted for in the refinements. The compound belongs to the group of single layer silicates. Individual sheets can be described as being built by the condensation of Zweier single chains of SiO_4 - tetrahedra parallel to the a - axis or, alternatively, by condensation of Vierer single chains parallel to the b - axis. The layers contain six-membered rings in UUDUUD or DDUDDU conformation. The stacking of the layers parallel to the c - axis results in a three-dimensional structure in which the alkali cations reside between the layers for charge compensation. The distribution of the alkali atoms among the two crystallographically different M(1) and M(2) positions shows a definite preference by the larger potassium for the M(1) site. The smaller M(2) site is K-free.

Introduction

Alkali disilicates have been investigated frequently because of their complex polymorphism as well as for their interesting material science applications. Sodium disilicate, for example, shows at least eight different modifications as a function of pressure, temperature and synthesis conditions (Willgallis & Range [1]; Williamson & Glasser [2]; Hoffmann & Scheel [3]). For $K_2Si_2O_5$ two different phases have been reported (Schweinsberg & Liebau [4]; de Jong et al. [5]). Further structurally characterized alkali silicates with just one type of alkali atoms are $Li_2Si_2O_5$ (de Jong et al. [5]), $Rb_2Si_2O_5$ and $Cs_2Si_2O_5$ (deJong et al. [6]).

Among the group of mixed alkali disilicates of general composition $M(1)M(2)Si_2O_5$ the following compounds exists : $NaRbSi_2O_5$, $NaCsSi_2O_5$ (de Jong et al. [7]), $Cs_{1.33}Li_{0.67}Si_2O_5$ (Veldman et al. [8]) and $KLiSi_2O_5$ (de Jong e al. [9]). Information on possible crystalline mixed phases in the system $Na_{2-x}K_xSi_2O_5$ is limited, in contrast to the pure end-members which have been characterized in detail. Furthermore, several studies using Raman spectroscopy, EXAFS and solid state NMR have been performed on the glasses occurring in this system (Florian et al. [10]; Greaves [11]; Brawer & White [12]). The existence of a crystalline compound with composition $Na_{1..3}K_{0.7}Si_2O_5$ has been reported by Sakaguchi et al. [13]. The powder pattern of this phase was indexed based on a monoclinic cell with a=4.84, b=8.69, c=11.97 Å, β = 90.37°. However, up to date no structural characterization has been performed. The ion exchange properties of the phases $Na_{2-x}K_xSi_2O_5$ with x ~ 0.6-0.9 determined by Sakaguchi et al. [13] are comparable with those observed in δ-$Na_2Si_2O_5$, which is used as a builder in washing powders in combination with or as an alternative to zeolitic materials (Rieck [14]). In the course of an ongoing study on the crystal chemistry of sodium and potassium disilicates we obtained single crystals of $Na_{1.55}$ $K_{0.45}Si_2O_5$. Despite small differences in the chemical composition this phase seems to be identical with the compound described by Sakaguchi et al. [13]. Furthermore, the comparison between the unit cell parameters of $Na_{1.55}$ $K_{0.45}Si_2O_5$ and δ-$Na_2Si_2O_5$ given in Table 1 points to a structural relationship between the two phases.

Table 1. Lattice parameters and space groups for $Na_2Si_2O_5$-phases stable at ambient conditions and mixed alkali disilicates containing sodium.

Phase	Space group	*a* (Å)	*b* (Å)	*c* (Å)	Monoclinic angle	Reference
α-$Na_2Si_2O_5$	*Pcnb*	6.409	15.422	4.896		[28]
β-$Na_2Si_2O_5$	$P112_1/b$	8.133	12.329	4.848	104.2°	[29]
δ-$Na_2Si_2O_5$	$P12_1/n1$	8.393	12.083	4.843	90.37°	[18]
$NaRbSi_2O_5$	$P12_1/c1$	4.857	13.540	7.733	90.91°	[7]
$NaCsSi_2O_5$	$Pna2_1$	17.074	4.901	13.339		[7]
$Na_{1.5}K_{0.5}Si_2O_5$	$P12_1/c1$	4.845	8.647	11.992	90.31°	This work

The aim of the present paper is to determine the crystal structure of the new mixed Na-K-disilicate and to describe the differences and similarities with other single layer silicates.

Experimental Details

Starting materials for the single-crystal growth were Na_2CO_3 (Fluka, 99%), K_2CO_3 (Riedel deHaën, 99%) and SiO_2. The source of silica was fine grained quartz powder. The reagents were weighed in molar ratios to give a chemical composition $Na_{1.3}K_{0.7}Si_2O_5$ and carefully homogenized in an agate mortar. A sample of 1 g was placed in an open 50ml platinum crucible. The mixture was slowly heated from room temperature to 1000°C (2h) in a resistance heated furnace and quenched rapidly. To increase the homogeneity of the resulting glass the sample was re-ground, melted again at 800°C for 2h, and subsequently annealed at 550° C for eight days. Inspection of the synthesis product using a polarizing microscope revealed the presence of crystalline material embedded in a glass matrix. Single crystals of up to 0.05 x 0.15 x 0.30 mm could be mechanically separated from the glass. The optical quality of exclusively all crystals was only poor. No sharp extinction positions could be observed when viewed between crossed polarizers.

A platy crystal, about 0.07 x 0.10 x 0.18 mm in size was selected for the structural investigations. Single-crystal intensity measurements were performed using a STOE- imaging plate detector system IPDS. Experimental details pertaining to data collection and structure determination are summarized in Table 2.

Table 2. Data collection and refinement parameters

(A)	**Crystal data**	
	a (Å)	4.845(1)
	b (Å)	8.647(2)
	c (Å)	11.992(3)
	β (°)	90.31(4)
	V ($Å^3$)	503.1(4)
	Space group	$P\,2_1/c$
	Z	4
	Chemical formula	$Na_{1.55}\,K_{0.45}Si_2O_5$
	D_{calc} (g cm^{-3})	2.51
	μ (mm^{-1})	1.14

(B)	Intensity measurements	
	Crystal shape	Plate
	Diffractometer	Stoe – IPDS
	Monochromator	Graphite
	Radiation	MoKα, λ = 0.71073 Å
	X-ray power	50 kV, 40 mA
	Detector to sample distance	60 mm
	Rotation width in ϕ (°)	2.5
	No. of exposures	180
	Irradation time / exposure (min.)	5.00
	θ - range (°)	2.0° - 38.2°
	Reflection range	$\lvert h \rvert \leq 6 ; \lvert k \rvert \leq 10 ; \lvert l \rvert \leq 5$
	No. of measured reflections	7597
	No. of unique reflections in 2/*m*	2037
	R_{int} in 2/*m* after absorption correction	0.130
	No. of observed reflections ($I > 2\sigma(I)$)	1208
(C)	**Refinement of the structure**	
	No. of parameters used in the refinement	85
	R1 ($F_o > 4\sigma(F_o)$) ; R1 (all data)	0.055
	wR2 ($F_o > 4\sigma(F_o)$)	0.134
	Weighting parameter a	0.0714
	Goodness of Fit	0.902
	Final $\Delta\rho_{min}$ (e / Å^3)	-0.69
	Final $\Delta\rho_{max}$ (e / Å^3)	0.43
	$R1 = \Sigma \lvert\lvert F_o\rvert - \lvert F_c\rvert\rvert / \Sigma \lvert F_o\rvert$	$wR2 = (\Sigma(w(F_o^2 - F_c^2)^2) / \Sigma(w(F_o^2)^2))^{1/2}$
	$w = 1 / (\sigma^2 (F_o^2) + (aP)^2)$	$P = (2F_c^2 + \max(F_o^2,0)) / 3$

The crystal showed monoclinic Laue symmetry 2/*m*. The evaluation of the systematic extinction rules resulted in the space group $P12_1/c1$. Data reduction including intensity integration, background corrections, Lorentz and polarization correction was performed with the Stoe XRED program package. The reflections were numerically corrected for absorption using 9 external faces.

The structure was solved by direct methods with the program SIR92 (Altomare et al. [15]) using a multisolution process. The phase set with the maximum combined figure of merit resulted in an E-map, the most intense peaks of which could be interpreted as a partial structure containing the alkali, silicon and some of the oxygen atoms. The structure was completed by difference Fourier calculations providing the starting parameters for the least squares refinements performed with the program SHELXL-93 (Sheldrick [16]). Neutral-atom scattering factors and anomalous-dispersion corrections were taken from the *International Tables for X-ray crystallography* (Ibers & Hamilton [17]). Though the model seemed to be reasonable, iterative full matrix least squares calculations based on F^2 using isotropic displacement factors converged to the rather high unweighted R1 index of 0.17. The introduction of anisotropic thermal parameters did not significantly improve the refinement.

Based on these results, a possible twinning of the crystal was taken into consideration in order to explain the difficulties during the refinement. Actually, the reflections at higher θ angles showed a considerable anisotropic broadening which can be explained by twinning according to $2_{[100]}$ or $m_{(100)}$, respectively. This type of twinning by pseudo-merohedry is a feature often observed in compounds where the monoclinic angle β is very close to 90°. However, no splitting of reflections was detected and therefore, the overlapping reflections were processed like single reflections during the integration of the data. Assuming the twofold axis $2_{[100]}$ as the element of twinning, the fraction of the twin components with the total fraction restrained to 1.0 was introduced into the refinement calculation. Similar rotation twins have been observed in the structure of δ-$Na_2Si_2O_5$ (Kahlenberg et al. [18]). The value for R1 dropped to 0.065; the volume fraction α for twin component 1 refined to 0.38(2). In the next step, the site occupancies of the two alkali sites M(1) and M(2) were included into the refinement. No constraints on the bulk composition were applied. However, full occupancy for both sites was assumed. Within the experimental error no K-substitution on M(2) could be detected, leading to the chemical composition $(Na_{0.55}K_{0.45})NaSi_2O_5$ in crystal chemical notation. The error in the Na/K distribution for the M(1) site is ± 0.02 as derived from the occupancy refinements. Therefore, the composition of the crystal used for the structure solution is slightly depleted in K compared to the bulk composition of the glass. The final calculations using anisotropic displacement parameters converged at R1 = 0.055. The largest shift in the final cycle was < 0.001. The refined atomic coordinates, equivalent isotropic and anisotropic displacement parameters, as well as selected interatomic distances and angles are given in Tables 3 - 5. Drawings of structural details were prepared using the programs ATOMS (Dowty [19]) and ORTEP-3 (Farrugia [20]).

Table 3. Atomic coordinates and equivalent isotropic displacement factors. U_{eq} is defined as one third of the trace of the orthogonalized U_{ij} tensor. All atoms occupy general positions. M(1) is a mixed alkali site with site occupancies of 0.55(2) Na and 0.45(2) K. M(2) contains exclusively sodium.

Atom	*x*	*y*	*z*	U_{eq}
Si(1)	0.8016(5)	0.3255(3)	-0.1748(2)	0.0163(8)
Si(2)	0.2976(6)	0.4758(3)	-0.2840(2)	0.0147(8)
M(1)	0.7474(7)	0.8594(3)	-0.5369(3)	0.0227(12)
M(2)	0.7531(8)	0.3991(4)	-0.4486(3)	0.0237(14)
O(1)	0.2408(4)	0.4221(8)	-0.4089(5)	0.0313(21)
O(2)	0.7313(14)	0.3305(7)	-0.0461(5)	0.0230(19)
O(3)	0.2381(15)	0.6595(7)	-0.2614(5)	0.0250(20)
O(4)	0.6251(10)	0.4503(8)	-0.2503(5)	0.0270(20)
O(5)	0.1227(10)	0.3789(7)	-0.1895(6)	0.0263(17)

Table 4. Anisotropic displacement parameters ($Å^2$). The anisotropic displacement factor exponent takes the form: $-2\pi^2 [h^2 a^{*2} U_{11} + ... + 2 h k a^* b^* U_{12}]$

Atom	U_{11}	U_{22}	U_{33}	U_{23}	U_{13}	U_{12}
Si(1)	0.013(1)	0.019(2)	0.017(1)	0.001(1)	0.001(1)	-0.001(1)
Si(2)	0.011(1)	0.017(2)	0.016(1)	0.001(1)	0.003(1)	0.001(1)
M(1)	0.019(2)	0.023(2)	0.026(2)	-0.001(1)	-0.004(2)	0.000(1)
M(2)	0.015(2)	0.031(3)	0.025(2)	-0.005(2)	0.002(2)	-0.003(2)
O(1)	0.022(4)	0.046(4)	0.026(3)	-0.002(3)	-0.003(3)	0.008(4)
O(2)	0.018(3)	0.026(4)	0.025(3)	0.006(3)	0.006(3)	-0.003(3)
O(3)	0.024(4)	0.030(4)	0.021(4)	0.000(3)	0.000(4)	0.015(3)
O(4)	0.028(3)	0.022(4)	0.031(4)	-0.003(4)	-0.001(3)	-0.004(3)
O(5)	0.026(3)	0.031(5)	0.022(3)	-0.003(3)	-0.002(3)	-0.002(3)

Table 5. Selected bond distances (Å) and angles (deg.).

Si(1)	-O(2)	1.583(7)	Si(2)	-O(1)	1.591(7)
	-O(5)	1.633(6)		-O(3)	1.637(7)
	-O(3)	1.637(7)		-O(5)	1.648(7)
	-O(4)	1.645(7)		-O(4)	1.650(6)
Mean		1.625	Mean		1.632
M(1)	-O(1)	2.520(7)	M(2)	-O(1)	2.305(7)
	-O(2)	2.541(8)		-O(2)	2.306(7)
	-O(2)	2.685(7)		-O(1)	2.416(5)
	-O(2)	2.721(8)		-O(4)	2.500(7)
	-O(5)	2.789(8)		-O(1)	2.538(5)
	-O(4)	3.097(7)			

O – T – O angles			
O(5)-Si(1)-O(2)	107.9(4)	O(3)-Si(2)-O(1)	114.2(4)
O(3)-Si(1)-O(2)	117.0(3)	O(5)-Si(2)-O(1)	114.3(3)
O(3)-Si(1)-O(5)	107.9(4)	O(5)-Si(2)-O(3)	106.7(3)
O(4)-Si(1)-O(2)	113.8(3)	O(4)-Si(2)-O(1)	110.7(3)
O(4)-Si(1)-O(5)	104.4(3)	O(4)-Si(2)-O(3)	105.0(4)
O(4)-Si(1)-O(3)	105.0(3)	O(4)-Si(2)-O(5)	105.1(3)
Mean	109.3	Mean	109.3
T – O – T angles			
Si(1)-O(3)-Si(2)	142.5(4)		
Si(1)-O(4)-Si(2)	135.9(4)		
Si(1)-O(5)-Si(2)	135.4(4)		

Description of the structure

The structure of $Na_{1.55}$ $K_{0.45}Si_2O_5$ consists of a sequence of tetrahedral layers perpendicular to [001]. Each layer is composed of six membered rings of SiO_4 - tetrahedra in *UUDUUD* - and *DDUDDU* - conformation. Figure 1(a) shows a projection parallel to *c* of one of the two tetrahedral sheets in the unit cell. Alternatively, the single layers can be described as being built by condensation of Vierer single chains parallel [010] or Zweier single chains parallel [100] via common corners.

A single chain contains $Si(1)O_4$ - as well as $Si(2)O_4$ - tetrahedra. The Zweier single chains are similar to those observed in Na_2SiO_3 (McDonald & Cruickshank [21]). The eequatorial oxygen atoms of the sheets are not strictly coplanar and therefore, the layers are corrugated.

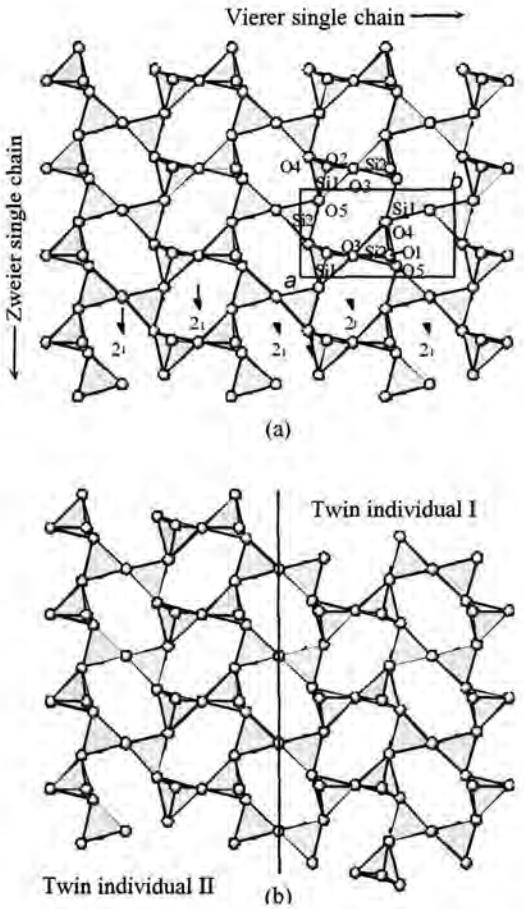

Figure 1.(a) Single layer of the SiO_4-tetrahedra in $Na_{1.55}K_{0.45}Si_2O_5$ containing pseudo 2_1-axes running parallel *a*. (b) Hypothetical twin boundary within a single layer between two individuals.

The twinning by pseudo-merohedry observed on a macroscopic scale can be explained microscopically by the existence of pseudo-symmetry elements within the layers (2_1-axes running parallel *a*). The resulting two twin individuals and the hypothetical twin boundary within a single layer are shown in Figure 1(b). The orientation and the sequence of directedness of the oval rings located directly at the twin boundary is unchanged.

The bonds between the two symmetrically independent silicon cations and the non-bridging oxygen atoms O(1) and O(2), respectively, are very short ($<Si\text{-}O_{nbr}>$: 1.586 Å) but are in good agreement with the values for the equivalent non-bridging oxygen atoms in the α -, β - and δ-modifications of $Na_2Si_2O_5$. The bond distances between Si(1) and Si(2), respectively, and the three bridging oxygen atoms of each tetrahedron are considerably longer (average 1.640 Å and 1.646 Å). While the average values of the O - Si - O angles for the two tetrahedra about Si(1) and Si(2) are very close to the ideal value of 109.47°, the individual O - Si - O angles range from 104° to 117° for the SiO_4 groups. This suggests that the polyhedra are slightly distorted. According to Robinson et al. [22] the distortion can be expressed numerically by means of the angle variance σ^2 . This parameter has values of 25.20 and 18.79, respectively, for the two $Si(1)O_4$ - and $Si(2)O_4$ - polyhedra. The angle variances can be compared with the corresponding values observed for the two crystallographically independent tetrahedra in δ - $Na_2Si_2O_5$ (σ^2 = 23.8 and 22.6, respectively).

The T-O-T angles are about 135° for the two oxygen atoms O(4) and O(5) within a Zweier single chain and 142° about O(3), the anion connecting neighboring chains. The differences between the inter- and intra chain Si-O-Si angles are less pronounced compared with the corresponding angles in δ-$Na_2Si_2O_5$ (134° and 155°) or α-$Na_2Si_2O_5$ (138° and 180°). The Si-O-Si angles agree well with the commonly observed Si-O-Si angle frequency distribution reported by Baur [23] resulting from a statistical analysis of a huge number of different silicate structures. Mean T-O distances of Si(1)-O = 1.625 Å and Si(2)-O = 1.632 Å are slightly larger than the value of 1.617(6) given by Baur [24] as a mean distance in phyllosilicates.

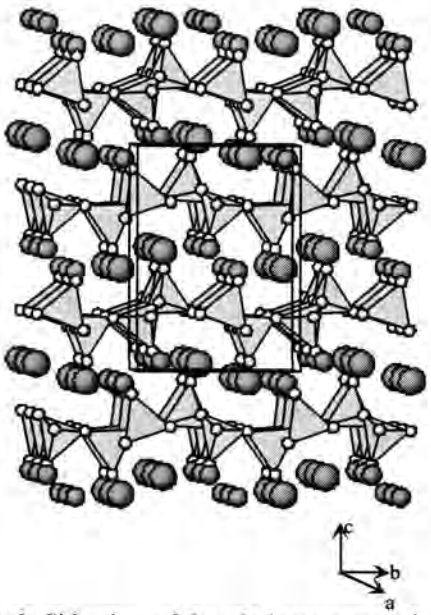

Figure 2. Side view of the whole structure of $Na_{1.55}K_{0.45}Si_2O_5$. The large and small spheres in the voids between the tetrahedral layers represent the M(1) and M(2) sites, respectively.

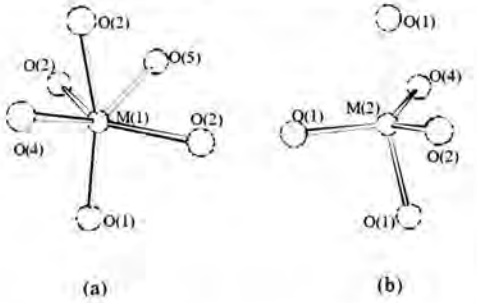

Figure 3. Coordination polyhedra surrounding the alkali cations. (a) distorted octahedron about M(1); (b) distorted trigonal bipyramid about M(2)

Charge balance in the structure is achieved by the incorporation of alkali ions in the channels between tetrahedral layers. The channels along [100] result from the folding of the layers. Figure 2 shows a side view of the whole structure almost parallel to this direction.

The potassium-free M(2) site has five oxygen ligands between 2.31 Å and 2.54 Å. The average value of 2.413 Å agrees well with typical Na-O bond lengths which average about 2.44 Å (Wilson [25]). The M(1) site shows a (5+1) coordination. The five inner oxygen neighbours have bond distances between 2.52 Å and 2.79 Å. Extending the limit for coordinating anions up to 3.2 Å, an additional sixth ligand at about 3.10 Å can be found.

The increased values of the individual M-O bond distances for M(1) correspond with the partial substitution of potassium with a cation radius of 1.38 Å (Shannon [26]) for sodium (1.00 Å) on this position. The coordination polyhedra about M(1) and M(2) are given in Figure 3. Bond valence calculations were performed using the

parameters given by Brese & O'Keefe [27] for Na-O and K-O pairs, and the bond distances of the first coordination sphere given in Table 5. For the contributions of the mixed M(1) site the results obtained for Na-O and K-O bonds were weighted by the site occupancies determined from the refinement. The bond valence sums (BVS) for the cations were close to the atomic valences: Si(1): 4.00 v.u., Si(2): 3.93 v.u., M(1): 0.91 v.u. and M(2): 0.99 v.u. The BVS values for the oxygen anions varied between 1.88 v.u. for O(2) and 2.07 v.u. for O(4).

Discussion

A comparison of the basic crystallographic data of the sodium disilicates stable at ambient pressure and the structurally characterized mixed alkali disilicates containing Na reveals that one very short lattice constant of about 4.9 Å is a common feature (cf. Table 1). This value corresponds to the translation period along the chain direction in $[Si_2O_6]$ Zweier single chains, being a common structural building element in all these compounds. However, all phases listed in Table 1 represent different structure types and the differences may be attributed to the various ways how the Zweier single chains can be linked to form bigger building units. The mixed disilicates $NaRbSi_2O_5$ and $NaCsSi_2O_5$, for example, consist of double chains forming 4-membered tetrahedral rings (deJong et al. [7]). The different $Na_2Si_2O_5$ polymorphs as well as the Na-K-disilicate discussed in this paper exhibit an increased connectivity of the chains resulting in the formation of folded tetrahedral layer structures.

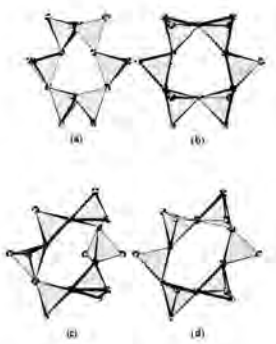

Figure 4. Comparison between the different S6R's in (a) α- $Na_2Si_2O_5$ [28], (b) δ- $Na_2Si_2O_5$ [18], (c) β- $Na_2Si_2O_5$ [29] and (d) $Na_{1.55}K_{0.45}Si_2O_5$.

In all four compounds neighbouring layers are twisted by 180° about the 2_1-axes parallel to the layers. Furthermore, each layer can be characterized by six-membered rings (S6R) forming honeycomb-like nets. As can be seen from Fig. 4 the S6R in α- and δ-$Na_2Si_2O_5$ have a ditrigonal configuration, whereas the rings in β-$Na_2Si_2O_5$ and $Na_{1.55}K_{0.45}Si_2O_5$ exhibit an oval configuration. Within a single oval S6R, the min./max. distances between opposite O-atoms are 3.97 and 6.17 Å (for $Na_{1.55}K_{0.45}Si_2O_5$), and 3.65 and 6.03 Å (for β- $Na_2Si_2O_5$), respectively, indicating that the rings in Na-K-disilicate have a larger aperture. However, concerning the sequence of directness of up and down pointing

vertices, $Na_{1.55}K_{0.45}Si_2O_5$ is more similar to δ-$Na_2Si_2O_5$. The sequence is UUDUUD and DDUDDU, respectively, in both phases.

The strikingly close relationship between the unit cell parameters of $Na_{1.55}K_{0.45}Si_2O_5$ and δ-$Na_2Si_2O_5$ is reflected by structural similarities. However, there remain pronounced differences between both materials, so that $Na_{1.55}$ $K_{0.45}Si_2O_5$ represents a new type of a tetrahedral single-layer structure.

Acknowledgement

Financial support for this work has been received from the Deutsche Forschungsgemeinschaft under the grant Ka1342/1.

References

[1] Willgallis, A.; Range, K.J.: Zur Polymorphie des $Na_2Si_2O_5$. *Glastechn. Ber.* **37** (1963) 194 - 200.

[2] Williamson, J.; Glasser, F.P.: The crystallisation of $Na_2O.2SiO_2$ - SiO_2 lasses. *Phys. Chem. Glasses* **7** (1966) 127 - 138.

[3] Hoffmann, W.; Scheel, H.J.: Über die γ - und δ - Modifikationen des Natriumdisilikates, $Na_2Si_2O_5$. *Z. Kristallogr.* **129** (1969) 396 - 404.

[4] Schweinsberg, H.; Liebau, F.: Darstellung und kristallographische Daten von $K_2Si_2O_5$, $KHSi_2O_5$-I und $K_2Si_4O_9$. *Z. Anorg. Allg. Chem.* **387** (1972) 241-251.

[5] deJong, B.H.W.S.; Supèr, H.T.J.; Spek, A.L.; Veldman, N.; Nachtegaal, G.; Fischer, J.C.: Mixed alkali systems: Structure and ^{29}Si MASNMR of $Li_2Si_2O_5$ and $K_2Si_2O_5$. *Acta Cryst.* **B54** (1998) 568 - 577.

[6] deJong, B.H.W.S.; Slaats, P.G.; Supèr, H.T.J.; Veldman, N.; Spek, A.L.: Extended structures in crystalline phyllosilicates: silica ring systems in lithium, rubidium and cesium and cesium/lithium phyllosilicate. *J. Non Crys. Sol.* **176** (1994) 65-171.

[7] deJong, B.H.W.S.; Supèr, H.T.J.; Frijhoff, R.M.; Spek, A.L.; Nachtegaal, G.: Mixed alkali systems: Dietzel's theorem, X-ray structure, hygroscopicity and ^{29}Si MAS NMR of $NaRbSi_2O_5$ and $NaCsSi_2O_5$. *Z. Kristallogr.* **215** (2000) 397-405.

[8] Veldman, N.; Spek, A.L.; Supèr, H.T.J.; deJong, B.H.W.S.: Cesium-Lithium Phyllosilicate, $Cs_{1.33}Li_{0.67}Si_2O_5$. *Acta Crystallogr.* **C51** (1995) 1972-1974.

[9] deJong, B.H.W.S.; Supèr, H.T.J.; Spek, A.L.; Veldman, N.; van Wezel W.; van der Mee, V.: Structure of $KLiSi_2O_5$ and the Hygroscopicity of Glassy Mixed Alkali Disilicates. *Acta Cryst.* **B52** (1996) 770-776.

[10] Florian, P.; Vermillion, K.E.; Grandinetti, P.J.; Farnan, I.; Stebbins, J.F.: Cation distribution in mixed alkali disilicate glasses. *J. Am. Chem. Soc.* **118** (1996) 3493 - 3497.

[11] Greaves, G.N.: Structural studies of the mixed alkali effect in disilicate glasses. *Solid State Ionics* **105** (1998) 243 - 248.

[12] Brawer, S.A.; White, W.B.: Raman spectroscopic investigations of the structure of silicate glasses. I. The binary alkali silicates. *J. Chem. Physics* **63** (1975) 2421 - 2432.

[13] Sakaguchi, M.; Sakamoto, I.; Akagi, R.: Powder data for potassium sodium silicate $Na_{1.3}K_{0.7}Si_2O_5$. *Powder Diffraction* **10** (1995) 290-292.

[14] Rieck, H.P.: Natriumschichtsilicate und Schichtkieselsäuren. *Nachr. Chem. Techn. Lab.* **44** (1996) 699-704.

[15] Altomare, A.; Cascarano, G.; Giacovazzo, C.; Guagliardi, A.; Burla, M.C.; Polidori, G.; Camalli, M.: SIR92 – a program for automatic solution of structures by direct methods. *J. Appl. Cryst.* **27** (1992) 435

[16] Sheldrick, G.M.: SHELXL-93. Program for the refinement of crystal structures. Universität Göttingen, (1993) Germany.

[17] Ibers, J.A.; Hamilton, W.C.: Eds.: International tables for X - ray crystallography, Volume IV, Kynock, (1974) Birmingham, U.K.

[18] Kahlenberg, V.; Dörsam, G.; Wendschuh-Josties, M.; Fischer, R.X.: The crystal structure of δ-$Na_2Si_2O_5$. *J. Sol. State Chem.* **146** (1999) 380-386.

[19] Dowty, E.: ATOMS - Shape Software (1997)

[20] Farrugia, L.J.: ORTEP-3 for Windows, *J. Appl. Cryst.* **30** (1997) 565.

[21] McDonald, W.S.; Cruickshank, D.W.J.: A reinvestigation of the structure of sodium metasilicate, Na_2SiO_3. *Acta Cryst.* **22** (1967) 37-43.

[22] Robinson, K.; Gibbs, G.V.; Ribbe, P.H.: Quadratic elongation : A quantitative measure of distortion in coordination polyhedra. *Science* **172** (1971) 567-570.

[23] Baur, W.H.: Straight Si-O-Si bridging bonds do exist in silicates and silicon dioxide polymorphs. *Acta Cryst.* **B36** (1980) 2198-2202.

[24] Baur, W.H.: Variation of mean Si-O bond lengths in silicon-oxygen tetrahedra. *Acta Cryst.* **B34** (1978) 1751-1756.

[25] Wilson, A.J.C.: Ed.: International Tables for Crystallography, Volume C, Mathematical, Physical and Chemical Tables, Kluwer, (1995) Dordrecht.

[26] Shannon, R.D.: Revised effective ionic radii and systematic studies of interatomic distances in halides and chalcogenides. *Acta Cryst.* **A32** (1976) 751-767.

[27] Brese, N.E.; O'Keefe, M.: Bond-Valence Parameters for Solids. *Acta Cryst.* **B47** (1991) 192-197.

[28] Pant, A.K.; Cruickshank, D.W.J.: The crystal structure of α-$Na_2Si_2O_5$. *Acta Cryst.* **B24** (1968) 13-19.

[29] Pant, A.K.: A reconsideration of the crystal structure of β-$Na_2Si_2O_5$. *Acta Cryst.* **B24** (1968) 1077-1083.

8. Single crystal structure investigation of twinned $NaKSi_2O_5$ - a novel single layer silicate

S. Rakic and V. Kahlenberg

Fachbereich Geowissenschaften (Kristallographie), Universität Bremen, Klagenfurter Str., D - 28359 Bremen, Germany

Abstract

A new synthetic crystalline mixed alkali disilicate of composition $NaKSi_2O_5$ has been prepared by re-crystallization of a glass of corresponding composition. The compound is monoclinic, space group $P2_1/n$ (a = 7.3005(8)Å, b = 17.389(2)Å, c = 12.353(2)Å, β = 91.14(1)°, V = 1567.9Å^3, Z = 12, D_{calc} = 2.52 g/cm^3). The crystal used for the data collection showed twinning by pseudo-merohedry according to $2_{[001]}$, a feature we took account of in the refinements. The structure was solved by direct methods and refined to a residual of R1=0.070 (170 parameters). The compound belongs to the group of tetrahedral single layer silicates. Individual sheets are parallel to (001). The stepped layers can be described as being built by the condensation of unbranched dreier double chains. The double chains in turn consist of two unbranched dreier single chains connected via common corners and exclusively containing tertiary (Q^3) tetrahedra. The stacking of the layers consisting of four-, six- and eight-membered rings results in a three-dimensional structure in which the alkali cations reside in the voids between neighboring sheets. The sodium and potassium atoms show an ordered distribution among the six symmetrically independent alkali sites. The coordination numbers for Na and K vary between 4 to 5 and 6 to 7, respectively.

Introduction

The ternary system Na_2O - K_2O -SiO_2 is of interest in both materials science and earth science. Especially the glasses formed in the compositional range between $Na_2Si_2O_5$ and $K_2Si_2O_5$ have been studied frequently using spectroscopic techniques like solid-state NMR [1] and EXAFS [2] to rationalize the so called "mixed alkali effect". This term is used for the observation that several physical properties such as electrical conductivity and the viscosity show a non-linear dependence from the chemical composition when adding alkali ions of a second type into a single alkali disilicate glass. Furthermore, melts with composition $(Na_{1-x}K_x)_2Si_2O_5$ have been used by geoscientists as models for silicate melt phases which are the essential component of nearly all igneous processes[3,4].

Crystalline phases in the system $Na_2Si_2O_5$ - $K_2Si_2O_5$ could provide model structures and analogue materials for interpreting the absorption spectra of the glasses and melts mentioned above [5]. While the crystal structures and different polymorphic forms of the two end-members have been studied in great detail (see [6] and references cited therein), there is a considerable lack of information concerning the existence of possible mixed sodium - potassium - disilicates. The crystal structure of $Na_{1.55}K_{0.45}Si_2O_5$ has been solved only recently [7]. In the course of our ongoing investigations on the crystal chemistry of phyllosilicates, we obtained single crystals of a previously unknown disilicate with composition $NaKSi_2O_5$. The object of the present work was to (1) characterize in detail the structure of $NaKSi_2O_5$; and (2) clarify relationships with other known silicates.

Experimental details

Starting materials for the single crystal growth were NaOH (Riedel-de Haën), KOH (Riedel-de Haën) and SiO_2. The source of silica was fine grained quartz powder. The reagents were weighed in molar ratios to give a chemical composition $NaKSi_2O_5$ and carefully homogenized in an agate mortar. The reagents for a sample of 1 g were placed in an open 50ml platinum crucible. The mixture was slowly heated from room temperature to 1100°C for 2h in a resistance heated furnace, quenched rapidly, and subsequently annealed at 550° C for eight days. Inspection of the product using a polarising microscope revealed the presence of crystalline material embedded in a glass matrix. Single crystals of up to 0.05 x 0.15 x 0.30 mm^3 could be mechanically separated from the glass. Exclusively all crystals showed a polysynthetic twinning with a lamellar domain structure when viewed between crossed polarizers. Therefore, the structure determination was performed using a specimen twinned by twofold rotation about [001].

Single crystal diffraction data were measured on a Stoe IPDS diffractometer using a platy crystal with principal dimensions of 0.05 x 0.1 x 0.1 mm^3. A relatively large sample - detector distance of 80mm was chosen to increase the resolution between the reflections belonging to the different twin individuals, i.e., to increase the number of non-overlapping reflections. Parameters of the data collection and of the subsequent structure refinement are summarized in Table 1. The program RECIPE of the Stoe software package was employed to isolate the diffraction spots coming from the two different orientations of the domains. The diffraction peaks were indexed independently and the two superimposed diffraction patterns were integrated simultaneously.

Table 1. Data collection and refinement parameters

(A)	**Crystal data**	
	a (Å)	7.3005(8)
	b (Å)	17.3894(18)
	c (Å)	12.3531(14)
	β (°)	91.139(14)
	V ($Å^3$)	1567.9(5)
	Space group	P $2_1/n$
	Z	12
	Chemical formula	$NaKSi_2O_5$
	D_{calc} ($g\ cm^{-3}$)	2.52
	μ (mm^{-1})	1.49
(B)	**Intensity measurements**	
	Crystal shape	Plate
	Diffractometer	Stoe – IPDS
	Monochromator	Graphite
	Radiation	MoKα, λ = 0.71073 Å
	X-ray power	50 kV, 40 mA
	Detector to sample distance	80 mm
	Rotation width in ϕ (°)	1.0
	No. of exposures	360
	Irridation time / exposure (min.)	6.00
	θ - range (°)	1.45° - 24.2°
	No. of measured reflections	18399
	No. of completely overlapped reflections	4727
	No. of separated reflections	7813
	R_{int} in *2/m*	0.096
	No. of unique observed reflections ($I > 2\ \sigma(I)$	2128
(C)	**Refinement of the structure**	
	No. of parameters used in the refinement	170
	R1 ($F_o > 4\ \sigma(F_o)$)	0.0697
	wR2 ($F_o > 4\ \sigma(F_o)$)	0.1386

Weighting parameter a	0.002
Goodness of Fit	0.874
Final $\Delta\rho_{min}$ (e / Å^3)	-0.62
Final $\Delta\rho_{max}$ (e / Å^3)	0.91
$R1 = \Sigma \lvert\lvert F_o\rvert - \lvert F_c\rvert\rvert / \Sigma \lvert F_o\rvert$	$wR2 = (\Sigma(w(F_o^2 - F_c^2)^2) / \Sigma(w(F_o^2)^2))^{1/2}$
$w = 1 / (\sigma^2 (F_o^2) + (aP)^2)$	$P = (2F_c^2 + \max(F_o^2, 0)) / 3$

The integration was repeated twice (with and without an overlapp check). From the combination of the resulting two data sets the non-overlapping as well as the completely overlapping reflections were extracted for the structure solution. Partially overlapped reflections occured almost exclusively for $|h| = 2$ or 3 and were rejected. Due to the low absorption coefficient of $NaKSi_2O_5$ no absorption correction was performed. Data reduction included Lorentz and polarization corrections. The symmetry of the intensity data set was consistent with Laue group $2/m$. The analysis of the systematic absences indicated the centrosymmetric space group $P12_1/n1$.

The structure was solved by direct methods using the program SHELXS-86 [8] using the non-overlapping reflections only. The phase set with the maximum combined figure of merit provided an E-map, the most intense peaks of which could be interpreted to give a reasonable crystal chemical model. This model was the starting point for the subsequent refinement calculations performed with the program SHELXL-93 [9] using the non-overlapping as well as the completely overlapping reflections (HKLF 5 data format of SHELXL-93). X-ray scattering factors for neutral atoms, together with real and imaginary anomalous-dispersion coefficients, were taken from the International Tables for X-ray Crystallography [10]. In the next step site occupancy refinements were performed, allowing substitution of sodium and potassium on the six crystallographically independent alkali positions. The refinement indicated a completely ordered distribution of Na and K. Within an error margin of five estimated standard deviations three of the six positions are exclusively occupied by Na, whereas the K atoms are located on the remaining three sites. The calculations using isotropic temperature factors converged to R1=0.103 for 110 parameters and 2128 independent reflections with $I > 2\sigma(I)$. The introduction of anisotropic displacement parameters for all atoms improved the residual index (R1=0.059). However, the temperature factors of two oxygen atoms became non-positive definite. We attribute the problems with the thermal motion of the two oxygens to an unfavorable ratio of parameters to observed reflections. To model the anisotropic thermal motion of each atom the total number of

parameters is increased to 245 and the over-determination is reduced to 2128 / 245 ~ 9. Therefore, in the final least squares calculations anisotropic displacement parameters were used for the cations only (170 parameters, R1 = 0.070). The refined atomic coordinates, anisotropic displacement factors as well as selected interatomic distances and angles are summarized in Table 2-4.

Table 2. Atomic coordinates and equivalent isotropic displacement factors. U_{eq} is defined as one third of the trace of the orthogonalized U_{ij} tensor. All atoms occupy general positions.

Atom	x	y	z	U_{eq}
Si(1)	0.0979(3)	0.6384(1)	0.6351(2)	0.0253(6)
Si(2)	-0.2617(3)	0.5575(1)	0.6630(2)	0.0277(7)
Si(3)	0.7523(3)	0.9285(1)	0.6686(2)	0.0254(6)
Si(4)	0.4543(3)	0.6691(1)	0.7546(2)	0.0298(6)
Si(5)	0.0224(3)	0.8048(1)	0.7446(2)	0.0245(6)
Si(6)	0.3932(3)	0.8312(1)	0.6529(2)	0.0261(6)
Na(1)	0.2031(4)	0.7477(2)	0.4255(3)	0.0382(8)
Na(2)	0.3957(4)	0.5846(2)	0.4612(3)	0.0366(9)
Na(3)	0.0689(4)	0.9112(2)	0.4878(3)	0.0426(10)
K(1)	0.0518(2)	0.5808(1)	0.9027(2)	0.0500(6)
K(2)	-0.2706(2)	0.7316(1)	0.5100(2)	0.0407(6)
K(3)	0.1156(3)	0.4364(1)	0.6175(2)	0.0611(7)
O(1)	0.0990(7)	0.6384(3)	0.5087(5)	0.0350(14)
O(2)	0.0276(7)	0.7202(3)	0.6842(5)	0.0367(15)
O(3)	-0.0439(7)	0.5730(3)	0.6825(5)	0.0272(14)
O(4)	0.2954(8)	0.6194(3)	0.6935(5)	0.0374(16)
O(5)	0.3261(7)	0.4409(3)	0.4576(4)	0.0344(14)
O(6)	-0.3521(8)	0.6206(3)	0.7406(5)	0.0414(16)
O(7)	0.3018(6)	0.5269(3)	0.2826(4)	0.0293(13)
O(8)	-0.1094(7)	0.8535(3)	0.6624(4)	0.0312(13)
O(9)	0.5461(3)	0.8952(3)	0.6910(5)	0.0342(16)
O(10)	-0.0795(8)	0.8161(3)	0.3760(5)	0.0415(15)
O(11)	0.4832(7)	0.7481(3)	0.6805(5)	0.0382(14)
O(12)	-0.0379(7)	0.8037(3)	0.8619(5)	0.0328(14)

O(13)	0.2257(8)	0.8456(3)	0.7358(5)	0.0347(15)
O(14)	0.3327(7)	0.8410(3)	0.5319(5)	0.0337(13)
O(15)	0.2290(6)	0.0230(3)	0.4344(4)	0.0323(13)

Table 3. Anisotropic displacement parameters ($Å^2$) for the cation sites. The anisotropic displacement factor exponent takes the form: $-2\pi^2 [h^2 a^{*2} U_{11} + ... + 2 h k a^* b^* U_{12}]$

Atom	U_{11}	U_{22}	U_{33}	U_{23}	U_{13}	U_{12}
Si(1)	0.0174(10)	0.0180(11)	0.0404(20)	0.0007(12)	0.0004(12)	-0.0002(10)
Si(2)	0.0163(10)	0.0145(12)	0.0524(21)	0.0036(12)	0.0045(12)	0.0014(10)
Si(3)	0.0201(10)	0.0173(11)	0.0389(18)	-0.0033(12)	-0.0004(12)	0.0012(10)
Si(4)	0.0161(10)	0.0204(12)	0.0529(20)	0.0005(13)	-0.0013(12)	0.0016(10)
Si(5)	0.0135(10)	0.0216(11)	0.0383(18)	-0.0058(12)	-0.0002(12)	0.0017(10)
Si(6)	0.0214(10)	0.0155(11)	0.0413(19)	0.0004(11)	0.0019(12)	-0.0007(10)
Na(1)	0.0314(14)	0.0323(17)	0.0512(22)	0.0006(18)	0.0080(18)	-0.0034(18)
Na(2)	0.0324(16)	0.0261(16)	0.0510(26)	0.0100(16)	-0.0073(20)	-0.048(16)
Na(3)	0.0351(16)	0.0308(17)	0.0617(28)	0.0043(18)	-0.0042(20)	-0.0130(17)
K(1)	0.0362(10)	0.0560(12)	0.0579(17)	-0.0068(13)	0.0025(12)	0.0027(11)
K(2)	0.0322(9)	0.0302(10)	0.0596(16)	0.0016(11)	0.0038(11)	0.0011(9)
K(3)	0.0581(12)	0.0557(13)	0.0696(19)	0.0020(13)	0.0024(14)	0.0099(13)

Table 4. Selected bond distances (Å) and angles (deg.).

Si(1)	-O(1)	1.562(6)	Si(2)	-O(5)	1.553(6)
	-O(2)	1.634(5)		-O(6)	1.609(6)
	-O(3)	1.652(5)		-O(7)	1.643(5)
	-O(4)	1.633(6)		-O(3)	1.626(6)
	Q.E.	1.004		Q.E.	1.007
	A.V.	17.1		A.V.	29.8
	Mean	1.620		Mean	1.608

Si(3)	-O(15)	1.536(5)		Si(4)	-O(10)	1.546(7)
	-O(7)	1.641(5)			-O(4)	1.621(6)
	-O(9)	1.641(6)			-O(11)	1.667(6)
	-O(8)	1.651(5)			-O(6)	1.658(6)
	Q.E.	1.007			Q.E.	1.005
	A.V.	28.1			A.V.	23.1
	Mean	1.617			Mean	1.623
Si(5)	-O(12)	1.523(6)		Si(6)	-O(14)	1.559(6)
	-O(8)	1.623(6)			-O(13)	1.630(6)
	-O(13)	1.651(6)			-O(11)	1.621(6)
	-O(2)	1.651(5)			-O(9)	1.638(6)
	Q.E.	1.007			Q.E.	1.004
	A.V.	29.9			A.V.	17.9
	Mean	1.612			Mean	1.612
Na(1)	-O(12)	2.247(6)		Na(2)	-O(5)	2.291(6)
	-O(14)	2.282(6)			-O(12)	2.353(6)
	-O(1)	2.297(6)			-O(1)	2.442(6)
	-O(10)	2.449(6)			-O(7)	2.507(6)
					-O(5)	2.550(5)
Na(3)	-O(14)	2.335(6)		K(1)	-O(10)	3.256(6)
	-O(10)	2.398(6)			-O(4)	3.236(6)
	-O(15)	2.370(6)			-O(14)	2.656(5)
	-O(15)	2.654(6)			-O(15)	2.736(5)
	-O(8)	2.732(6)			-O(3)	2.799(6)
					-O(15)	3.000(5)
K(2)	-O(10)	2.635(6)		K(3)	-O(5)	2.528(6)
	-O(12)	2.719(6)			-O(1)	2.546(6)
	-O(11)	2.810(5)			-O(13)	2.653(6)
	-O(5)	3.054(5)			-O(9)	2.760(7)
	-O(2)	3.037(6)			-O(3)	2.771(6)
	-O(8)	3.054(6)			-O(7)	3.371(5)
	-O(1)	3.147(6)				

O – T – O angles

O(3)-Si(1)-O(4)	105.0(3)	O(6)-Si(2)-O(3)	102.1(3)
O(2)-Si(1)-O(3)	105.3(3)	O(7)-Si(2)-O(3)	105.6(3)
O(2)-Si(1)-O(4)	107.0(3)	O(6)-Si(2)-O(7)	106.7(3)
O(1)-Si(1)-O(3)	111.8(3)	O(5)-Si(2)-O(7)	110.8(3)
O(1)-Si(1)-O(4)	114.9(3)	O(5)-Si(2)-O(3)	114.6(4)
O(1)-Si(1)-O(2)	112.2(3)	O(5)-Si(2)-O(6)	116.1(3)
Mean	109.4	Mean	109.3
O(7)-Si(3)-O(9)	102.1(3)	O(4)-Si(4)-O(6)	106.5(3)
O(7)-Si(3)-O(8)	106.8(3)	O(11)-Si(4)-O(6)	104.1(3)
O(9)-Si(3)-O(8)	107.0(3)	O(4)-Si(4)-O(11)	106.3(3)
O(15)-Si(3)-O(8)	109.3(3)	O(10)-Si(4)-O(6)	109.8(4)
O(15)-Si(3)-O(9)	115.5(3)	O(10)-Si(4)-O(4)	114.4(3)
O(15)-Si(3)-O(7)	115.4(2)	O(10)-Si(4)-O(11)	114.9(3)
Mean	109.3	Mean	109.3
O(8)-Si(5)-O(2)	101.6(3)	O(13)-Si(6)-O(9)	103.3(3)
O(8)-Si(5)-O(13)	104.9(3)	O(11)-Si(6)-O(9)	105.9(3)
O(2)-Si(5)-O(13)	108.9(3)	O(13)-Si(6)-O(11)	108.1(3)
O(12)-Si(5)-O(13)	110.2(3)	O(14)-Si(6)-O(13)	112.6(3)
O(12)-Si(5)-O(8)	115.0(3)	O(14)-Si(6)-O(11)	113.9(3)
O(12)-Si(5)-O(2)	115.3(3)	O(14)-Si(6)-O(9)	112.3(3)
Mean	109.3	Mean	109.4

T – O – T angles

Si(1)-O(3)-Si(2)	132.8(4)
Si(1)-O(4)-Si(4)	135.7(3)
Si(3)-O(8)-Si(5)	137.6(4)
Si(2)-O(7)-Si(3)	137.4(3)
Si(5)-O(13)-Si(6)	131.5(4)
Si(2)-O(6)-Si(4)	140.4(4)
Si(4)-O(11)-Si(6)	142.7(3)
Si(3)-O(9)-Si(6)	144.4(4)
Si(1)-O(2)-Si(5)	162.7(4)

The figures showing structural details were prepared using the program ATOMS [11]. The authors are aware of the fact that the precision of the bond distances and angles as well as for the thermal displacement parameters obtained from a twinned crystal is lower compared to the results which could be obtained when a high quality single crystal can be used. However, in the present case no such sample was available.

Description and discussion of the structure

The crystal structure of $NaKSi_2O_5$ can be classified as a single layer silicate. Basic building element of the tetrahedral layers are unbranched dreier single chains running parallel [100] similar to those observed in para-wollastonite [12]. Therefore, the *a* lattice constant of about 7.300 Å corresponds to the periodicity of the single chain. The stretching factor f_s of the chain as defined in [13] is 0.901.

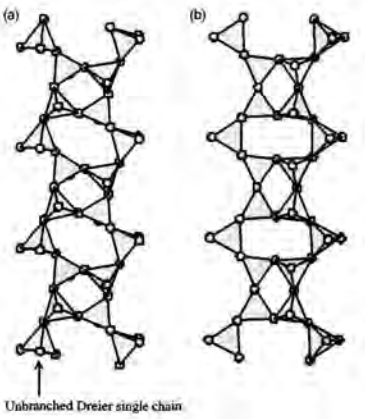

Figure 1. (a) Projection of a single four tetrahedra wide band including two unbranched Dreier single chains and (b) and the corresponding band in okenite.

Two adjacent dreier single chains are linked by sharing two out of three tetrahedra in each chain forming a four tetrahedra wide slab (see Fig. 1(a)). Using the nomenclature introduced by Liebau [13] the slab can be denoted as an unbranched dreier double chain. It is formed by alternating four (S4R)- and elliptical six-membered (S6R) rings. The sequence of directedness in the rings is UDUD and DUUDUU or UDDUDD, respectively. The double chains are related to those in the mineral okenite [14] (cf. Fig. 1(b)).

However, the conformation of the rings in okenite is different (UUDD and UUUDDD, respectively). In the next step the double chains are linked to build a two-dimensional layer: the wollastonite-type chains of neighboring bands are joined by sharing one oxygen per every third tetrahedron. As a result of this linking scheme, eight-membered rings (S8R) occur at the connecting points between the double chains. A projection of a single layer parallel [001] is given in Figure 2(a). In the case of the S4R and S6R's the directions perpendicular to the planes defined by the equatorial oxygen atoms of the rings are almost parallel to [001]. For the eight-membered rings the tilt angles between the corresponding ring directions and [001] are about ± 45°.

Therefore, the single layers are stepped and not planar, as can be seen in a projection parallel [100] (cf. Fig. 2(b)). The unit cell contains two of the single layers (cf. Fig. 3). The alkali cations are incorporated for charge compensation and reside in voids between the layers.

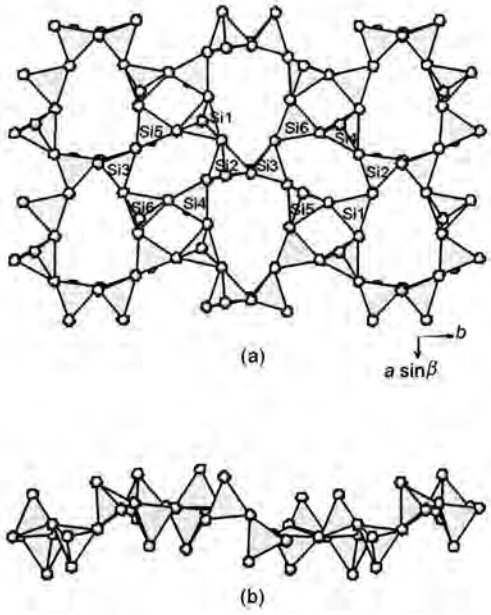

Figure 2. Projection of a single sheet containing SiO_4-tetrahedra perpendicular (a) and parallel (b) to the layer.

Individual Si-O bond distances cover a wide range between 1.52 - 1.66Å. The bonds between the Si and the non-bridging (nbr.) oxgens O(1), O(5), O(10), O(12), O(14) and O(15) are significantly shorter (<Si-O(nbr.)> = 1.547 Å) compared to the bridging (br.) Si-O bonds (<Si-O(br.)> = 1.638 Å).The bonds between Si and some of the non-bridging oxygen atoms are close to the lower limit observed in oxosilicates [13] . On the other hand, small Si-O distances of about 1.52 Å are not as rare as one may assume. For example, similar values have been encountered in minerals like deerite [15] or plagioclase [16] as well as synthetic compounds like $Ba_2Si_4O_{10}$ [17] or Ca_2SiO_4 [18]. Furthermore, the grand mean value of 1.615 for all Si-O bonds in the structure compares well with the value of 1.617(6) given in [19] as a mean distance in phyllosilicates.

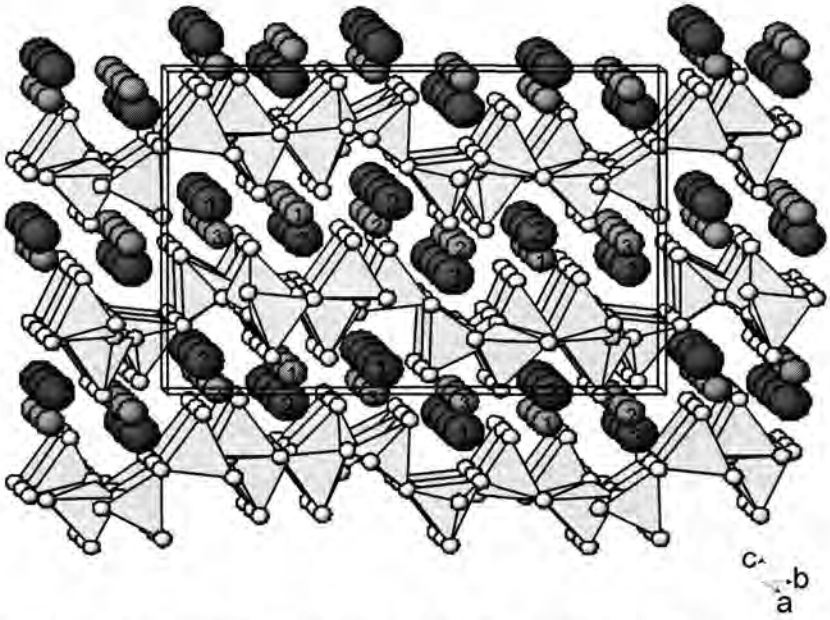

Figure 3. Side view of the whole structure of $NaKSi_2O_5$. Smaller medium grey spheres represent sodium atoms; bigger, dark grey spheres correspond to potassium ions; the numbers refer to the listing of the atomic positions in Table 2.

While the average values of the O - Si - O angles for the tetrahedra are very close to the ideal value of 109.47°, the individual O - Si - O angles range from 101° to 116° for the SiO_4-groups. This suggests that the polyhedra are slightly distorted. According to Robinson et al. [20] the distortion from ideal tetrahedral geometry can be expressed numerically by means of the quadratic elongation (Q.E.) and the angle variance (A.V.). These parameters have been calculated for each of the six symmetrically independent tetrahedra and are listed in Table 4. The results compare well with the corresponding values observed for the tetrahedra in $Na_{1.55}K_{0.45}Si_2O_5$ (A.V. = 25.2 and 18.5, respectively).

The Si-O-Si angles are between 131.5° and 162.7°; the <Si-O-Si> angle is about 140.6°, almost identical with the value for a bond angle of a strain-free Si-O-Si bond given in [13]. Furthermore, the Si-O-Si angles agree well with the commonly observed Si-O-Si angle frequency distribution reported by Baur [21] resulting from a statistical analysis of a huge number of different silicate structures. The difference between the Si-O-Si angles occurring within the dreier single chains ($<Si\text{-}O\text{-}Si>_{intra}$ = 137.2°) and the oxygen atoms connecting neighboring chains ($<Si\text{-}O\text{-}Si>_{inter}$ = 147.0°) is not very pronounced and only slightly larger compared to the values observed in $Na_{1.55}K_{0.45}Si_2O_5$: 135° and 142°, respectively. Bond valence sums (BVS) calculated using the parameters for the Si-O bond given by in [22] vary between 4.22 v.u. (for Si(4)) and 4.38 v.u. (for Si(2)), close to the expected value of 4 v.u.

The alkali cations are located between the tetrahedral layers. The cation distribution of the alkali atoms among the six possible M sites as derived from the site occupancy refinements is also reflected in the M-O bond lengths. The bond distances to the surrounding oxygen ligands for the three Na-positons are considerably shorter (<Na-O> = 2.415 Å) than the corresponding values for the K-sites (<K-O> = 2.880 Å). Na(2) and Na(3) are coordinated by five oxygen neighbors in form of distorted tetragonal pyramids. An interesting structural detail is the coordination sphere about Na(1): up to 3.2 Å only four oxygen ligands can be found. The coordination polyhedron can be described as a strongly distorted tetrahedron. The only other layered sodium disilicate with a similar coordination environment for Na is ε-$Na_2Si_2O_5$, a high pressure phase [23]. Inspite of the low coordination number, Pauling's second rule is fulfilled for Na(1): the BVS is about 1.01 v.u. The corresponding values for Na(2) and Na(3) are 0.95 v.u. and 0.83 v.u., respectively. The three different potassium ions are five-, six- and seven-fold coordinated. The bond valence sums are in the range between 0.80 v.u. (for K(1)) ans 1.31 v.u. (for K(3)).

Na(1) and K(2) are arranged in rows parallel [100], located above and below the bands containing the four- and six-membered rings. In a view perpendicular to the ring planes their

positions project almost on top of each other, close to the centres of the S4R and S6R. Within a single row, Na(1) and K(2) strictly alternate. However, in neighboring bands the Na/K sequence is reversed. The remaining alkali atoms Na(2), Na(3), K(1) and K(3) reside above and below the ring apertures of the S8R's. In contrast to Na(1) and K(2) their positions are significantly displaced relative to the centres of the rings. Once again the alkali atoms can be found in rows running parallel to the crystallographic *a*-axis.However, in this case the rows contain alternating pairs of K(1)/K(3) and Na(2)/Na(3), respectively.

Comparison with related structures

$NaKSi_2O_5$ represents a new structure type. Anhydrous silicate sheets with a 4-6-8-membered ring systems have not been observed before among the group of alkali single layer silicates. The tetrahedral sheets in the different modifications of $Na_2Si_2O_5$ as well as in $Na_{1.45}K_{0.55}Si_2O_5$ are exclusively composed of S6R's [6,7]. According to [24] layers with mixed ring types have been encountered in $Rb_2Si_2O_5$, $Cs_2Si_2O_5$ (4-8) and $Cs_{1.33}Li_{0.67}Si_2O_5$ (4-8-12). The only other known anhydrous layer silicate with sheets comprised of four-, six- and eight-membered rings is $K_2Ba_7[Si_{16}O_{40}]$ [25]. However, both compounds differ considerably in the relative proportions of the different ring types. The ratio of S4R:S6R:S8R is 1:6:1 in $K_2Ba_7[Si_{16}O_{40}]$ and 1:1:1 in $NaKSi_2O_5$, respectively. The shapes of the six-membered rings and the corresponding sequences of directedness of the S6R in $NaKSi_2O_5$ and $Na_{1.55}K_{0.45}Si_2O_5$ are identical. Furthermore, the min./max. distances between opposite O-atoms in the 6-fold rings are almost the same ($NaKSi_2O_5$: 4.03 Å / 6.37 Å; $Na_{1.55}K_{0.45}Si_2O_5$: 3.97 Å / 6.17 Å). Comparing the known mixed alkali disilicates with general composition $NaMSi_2O_5$ it is interesting to note that a layer silicate structure is realized only for the potassium member. The structures with M = Rb or Cs consist of isolated double chains of $[SiO_4]$ tetrahedra forming four-membered rings [26]. Among the sodium-potassium disilicates $(Na_xK_{1-x})_2Si_2O_5$ the change in the compositional parameter x from 0.225 to 0.5 involves a dramatic change in the topology of the silicate layer. Further studies in the pseudo binary system $Na_2Si_2O_5$ - $K_2Si_2O_5$ are currently in progress and may reveal new types of layer structures.

Acknowledgement

The authors would like to thank the two anonymous reviewers for their helpful comments.
Financial support for this work has been received from the Deutsche Forschungsgemeinschaft under the grant Ka1342/1.

References

[1] Florian, P.; Vermillion, K.E.; Grandinetti, P.J.; Farnan, I.; Stebbins, J.F.: Cation distribution in mixed alkali disilicate glasses. *J. Am. Chem. Soc.* **118** (1996) 3493 - 3497.

[2] Greaves, G.N.: Structural studies of the mixed alkali effect in disilicate glasses. *Solid State Ionics* **105** (1998) 243 - 248.

[3] Kanzaki, M.; Xue, X.; Stebbins, J.F.: Phase relations in Na_2O-SiO_2 and $K_2Si_4O_9$ systems up to 14 GPa and ^{29}Si NMR study of the new high-pressure phases: implications to the structure of high-pressure silicate glasses. Phys. Earth Planet. Int. **107** (1998) 9-21.

[4] Maekawa, H.; Yokokawa, T.: Effects of temperature on silicate melt structure: a high temperature ^{29}Si NMR study of $Na_2Si_2O_5$. Geochim. Cosmochim. Acta **61** (1997) 2569-2575.

[5] Sitarz, M.; Mozgawa, W.; Handke, M.J.: Rings in the structure of silicate glasses. Mol. Struct. **450** (1999) 281.

[6] Kahlenberg, V.; Dörsam, G.; Wendschuh-Josties, M.; Fischer, R.X.: The crystal structure of δ-$Na_2Si_2O_5$. *J. Sol. State Chem.* **146** (1999) 380-386.

[7] Rakic, S., Kahlenberg, V. submitted to Eur. J. Mineral.

[8] Sheldrick, G.M.: SHELXS-86. Universität Göttingen, Germany, 1986.

[9] Sheldrick, G.M.: SHELXL-93. A program for the refinement of crystal structures. Universität Göttingen, Germany, 1993.

[10] Ibers, J.A.; Hamilton, W.C.: Eds. International tables for X - ray crystallography, vol. IV, Kynoch, Birmingham, U.K.,1974.

[11] Dowty, E.: ATOMS5.1 – Shape Software, 2000.

[12] Trojer, F.J.: The crystal structure of parawollastonite. Z. Kristallogr., **127** (1968) 291-308.

[13] Liebau, F.: Structural chemistry of silicates. Springer-Verlag, Berlin, 1985.

[14] Merlino, S.: Okenite, $Ca_{10}Si_{18}O_{46}*18H_2O$: the first example of a chain and sheet silicate. Am. Mineral. **68** (1983) 614-622.

[15] Fleet, M.E.: The crystal structure of deerite. Am. Mineral. **62** (1977) 990.

[16] Berking, B.: Die Verfeinerung der Kristalstruktur eines lunaren Plagioklases An_{90}. Z. Kristallogr., **144** (1976) 198.

[17] Katscher, H.; Bissert, F.; Liebau, F.: The crystal structure of high-temperature $Ba_2[Si_4O_{10}]$. Z. Kristallogr. **137** (1973) 146.

[18] Cruickshank, D.W.J.: Refinements of structures containing bonds between Si, P, S or Cl and O or N. X.$^{\beta}$ -Ca_2SiO_4. Acta Cryst. **17** (1964) 685.

[19] Baur, W.H.: Variation of mean Si-O bond lengths in silicon-oxygen tetrahedra. *Acta Cryst.* **B34** (1978) 1751-1756.

[20] Robinson, K.; Gibbs, G.V.; Ribbe, P.H.: Quadratic elongation : A quantitative measure of distortion in coordination polyhedra. *Science* **172** (1971) 567-570.

[21] Baur, W.H.: Straight Si-O-Si bridging bonds do exist in silicates and silicon dioxide polymorphs. *Acta Cryst.* **B36** (1980) 2198-2202.

[22] Brese, N.E.; O'Keefe, M.: Bond-Valence Parameters for Solids. *Acta Cryst.* **B47** (1991) 192-197.

[23] Fleet, M.E.; Henderson, G.S.: Epsilon sodium disilicate: a high-pressure layer structure [$Na_2Si_2O_5$]. J Sol State Chem **119** (1995) 400-404

[24] deJong, B.H.W.S.; Slaats, P.G.; Supèr, H.T.J.; Veldman, N.; Spek, A.L.: Extended structures in crystalline phyllosilicates: silica ring systems in lithium, rubidium and cesium and cesium/lithium phyllosilicate. *J. Non Crys. Sol.* **176** (1994) 65-171.

[25] Cervantes Lee, F.J.; Dent Glasser, L.S.; Glasser, F.P.; Howie, R.A.: The structure of potassium barium silicate $K_2Ba_7Si_{16}O_{40}$. Acta Cryst., **B38** (1982) 2099.

[26] deJong, B.H.W.S.; Supèr, H.T.J.; Frijhoff, R.M.; Spek, A.L.; Nachtegaal, G.: Mixed alkali systems: Dietzel's theorem, X-ray structure, hygroscopicity and ^{29}Si MAS NMR of $NaRbSi_2O_5$ and $NaCsSi_2O_5$. *Z. Kristallogr.* **215** (2000) 397-405.

9. Structural characterization of high pressure C - $Na_2Si_2O_5$ by single crystal diffraction and ^{29}Si MAS NMR

S. Rakic[1], V. Kahlenberg[1], C. Weidenthaler[2], B. Zibrowius[2]

[1]Fachbereich Geowissenschaften (Kristallographie), Universität Bremen, Klagenfurter Str., D - 28359 Bremen, Germany

[2]Max-Planck-Institut für Kohlenforschung, Kaiser-Wilhelm-Platz 1, D - 45470 Mülheim an der Ruhr, Germany

Abstract

Single crystals of C-$Na_2Si_2O_5$ have been synthesized from the hydrothermal recrystallization of a glass. The title compound is monoclinic, space group $P2_1/c$ with Z = 8 and unit cell parameters a = 4.8521(4)Å, b = 23.9793(16)Å, c = 8.1410(6)Å, β = 90.15(1)°, V = 947.2(2)Å^3. The structure has been determined by direct methods and belongs to the group of phyllosilicates. It is based on layers of tetrahedra with elliptically six-membered rings in chair conformation. The sequence of directedness within a single ring is UDUDUD. The sheets are parallel to (010) with linking sodium cations in five- and six-fold coordination. Concerning the shape and the conformation of the rings C-$Na_2Si_2O_5$ is closely related to β-$Na_2Si_2O_5$. However, both structures differ in the stacking sequences of the layers. A possible explanation for the frequently observed polysynthetic twinning of phase C is presented. In the ^{29}Si MASNMR spectrum of C-$Na_2Si_2O_5$ four well-resolved lines of equal intensity are observed at -86.0, -86.3, -87.4, and -88.2 ppm. The narrow range of isotropic chemical shifts reflects the great similarity of the environments of the different Si sites. This lack of pronounced differences in geometry renders a reliable assignment of the resonance lines to the individual sites on the basis of known empiric correlations between and geometrical features impossible.

Introduction

Sodium disilicates are of interest in mineralogy and solid state chemistry as well. Melts with composition $Na_2Si_2O_5$, for example, have been used by geoscientists as models for silicate melt phases which are the essential components of nearly all igneous processes (Maekawa *et al.* [1]; Kanzaki *et al.* [2]).

Crystalline sodium disilicates and especially δ-$Na_2Si_2O_5$ have been studied because of their interesting high ion exchange capacity and selectivity (Wolf and Schwieger [3]). A review of the industrial applications can be found in the paper of Rieck [4]. Furthermore, a complex polymorphism with at least eight different stable and metastable phases has been reported for $Na_2Si_2O_5$ as a function of temperature, pressure and synthesis conditions (Willgallis and Range [5]; Williamson and Glasser [6]; Hoffmann and Scheel [7]). However, the crystal structures of several of these modifications remain to be solved.

The phase equilibrium diagram for the system $Na_2Si_2O_5$ in the range between room pressure and 400 bars has been investigated by Williamson and Glasser [6]. Three thermodynamically stable phases have been observed : α-$Na_2Si_2O_5$, β-$Na_2Si_2O_5$ and another high pressure polymorph designated 'phase C'. The triple point between the three phases is located at about 715°C and 90 bars. A preliminary investigation of phase C indicated monoclinic symmetry and a pseudo-orthorhombic metric (a = 8.12Å, b = 23.7 Å, c = 4.85 Å, β = 90°). However, no detailed structural characterization was performed. The results of Williamson and Glasser [6] concerning the existence of a sodium disilicate modification with a stability range starting at slightly elevated pressures were confirmed by Jacobsen [8]. The phase relations in the $Na_2Si_2O_5$ system especially at higher pressures have been studied by Kanzaki *et al.* [2]. According to their results the stability field of phase C extends to at least 25 kbar (at 900°C). At pressures of about 50-60 kbar a new phase (ε- $Na_2Si_2O_5$) appears.

In the course of an ongoing project on the crystal chemistry and the phase transitions in sodium and potassium disilicates we obtained single-crystals of phase C. The aim of the present work is to provide a description of the crystal structure of this compound and to show the relationships with known silicate structures. Preliminary results obtained by ^{29}Si MASNMR spectroscopy are also included.

Experimental Details

The single crystals in this study were synthesized from a glass of $Na_2Si_2O_5$ composition. The glass was prepared by fusing a stoichiometric mixture of Na_2CO_3 (Fluka, 99%) and SiO_2 (fine grained quartz powder) in a covered platinum crucible at 1000°C for 1h and quenching in air. The product was crushed and then ground in acetone. The melting process was repeated for two times in order to increase the homogeniety of the glass. Approximately 0.19g of the glass and 2ml of H_2O were loaded and sealed in a gold capsule (about 3 mm in diameter and 30 mm in height). The hydrothermal experiment was performed in an externally heated Morey-type autoclave.

The sample was taken at room temperature to a pressure of 1 kbar, and subsequently taken to a temperature of 750°C. The run duration at the final temperature was 24h. After quenching, the recovered sample consisting of transparent, colorless, platy crystals up to 0.3 mm in diameter was examined using a petrographic microscope. Almost all crystals showed a polysynthetic twinning.

For the structural investigations one of the rare untwinned crystals (0.24 x 0.12 x 0.006 mm in size) was selected. A total of 6124 reflections up to 24.2° θ were collected at 20°C on a Stoe imaging plate detector system IPDS (graphite-monochromatized MoK_α radiation). Table 1 contains a summary of the conditions for the data collection and of the subsequent structure refinement parameters. All the data were numerically corrected for absorption by use of 9 indexed external faces. Data reduction including intensity integration, background corrections, Lorentz and polarisation correction was performed with the Stoe XRED program package.

Table 1. Data collection and refinement parameters

(A)	**Crystal data**	
	a (Å)	4.8521(4)
	b (Å)	23.9793(16)
	c (Å)	8.1410(6)
	β (°)	90.15(1)
	V (Å^3)	947.2(2)
	Space group	$P\,2_1/c$
	Z	8
	Chemical formula	$Na_2Si_2O_5$
	D_{calc} (g cm^{-3})	2.56
	μ (mm^{-1})	0.86
(B)	**Intensity measurements**	
	Crystal shape	Plate
	Diffractometer	Stoe – IPDS
	Monochromator	Graphite
	Radiation	Mo-K_α, λ = 0.71073 Å
	X-ray power	50 kV, 40 mA
	Detector to sample distance	80 mm

	Rotation width in ϕ (°)	1.0
	No. of exposures	200
	Irridation time / exposure (min.)	5.00
	θ - range (°)	1.45° - 24.2°
	Reflection range	$\lvert h \rvert \leq 5 ; \lvert k \rvert \leq 27 ; \lvert l \rvert \leq 9$
	No. of measured reflections	6124
	No. of unique reflections in 2/m	1495
	R_{int} in 2/m after absorption correction	0.0354
	No. of observed reflections ($I > 2\sigma(I)$)	1113
(C)	**Refinement of the structure**	
	No. of parameters used in the refinement	163
	R1 ($F_o > 4\sigma(F_o)$) ; R1 (all data)	0.0261 ; 0.0391
	wR2 ($F_o > 4\sigma(F_o)$)	0.0658
	Weighting parameter a	0.0427
	Goodness of Fit	0.931
	Final $\Delta\rho_{min}$ (e / Å^3)	-0.26
	Final $\Delta\rho_{max}$ (e / Å^3)	0.39
	$R1 = \Sigma \lvert\lvert F_o \rvert - \lvert F_c \rvert\rvert / \Sigma \lvert F_o \rvert$	$wR2 = (\Sigma(w(F_o^2 - F_c^2)^2) / \Sigma(w(F_o^2)^2))^{1/2}$
	$w = 1 / (\sigma^2 (F_o^2) + (aP)^2)$	$P = (2F_c^2 + \max(F_o^2, 0)) / 3$

The diffraction symmetry of the crystal was consistent with Laue group 2/*m*. The systematic reflection conditions *h0l*: $l = 2n$; 0*k*0: $k = 2n$ unambiguously indicated the space group was $P2_1/c$ (No. 14). The structure was solved by direct methods with the program SIR92 (Altomare *et al.* [9]) using a multisolution process. The phase set with the maximum combined figure of merit resulted in an E-map, the most intense peaks of which could be interpreted as a layer structure. Least squares refinements were performed with the program SHELXL-93 (Sheldrick [10]). Neutral-atom scattering factors and anomalous-dispersion corrections were taken from the *International Tables for X-ray crystallography* (Ibers and Hamilton [11]). The final calculations using anisotropic diplacement parameters converged at R1 = 0.026 for 1113 independent reflections with $I > 2\sigma(I)$. The largest shift in the final cycle was < 0.001. The resulting fractional atomic coordinates, equivalent isotropic and anisotropic displacement parameters, as well as selected interatomic distances and angles are given in Tables 2 - 4.

Drawings of structural details were prepared using the program ATOMS (Dowty [12]).

The ^{29}Si MASNMR spectra of the powdered crystals were recorded on a BRUKER Avance 500WB spectrometer operating at 99.36MHz. A 4 mm MAS probe allowing stable spinning speeds of up to 15 kHz for several days was used. Since we obtained practically no signal after several hundred scans under the conditions used by Heidemann *et al.* [13] in a recent NMR study of sodium disilicates (p/4 pulses of 2 μs and a repetition time of 10 s), we performed a series of measurements with p/4 pulses and repetition times of between 60 s and 1800 s (at least 48 scans). From the dependence of the normalised intensity on the repetition time we estimated the longitudinal relaxation time T_1 to be of the order of 3000 s for all the silicon sites. Hence, the optimum flip-angle to maximise the signal intensity for a repetition time of 900 s is about p/4. These parameters were applied for the measurements at different MAS frequencies. The chemical shifts were referenced to neat TMS in a separate rotor.

Table 2. Atomic coordinates and equivalent isotropic displacement factors. U_{eq} is defined as one third of the trace of the orthogonalized U_{ij} tensor. All atoms occupy general positions.

Atom	x	y	z	U_{eq}
Si(1)	0.2961(2)	0.36325(4)	0.1966(1)	0.0146(2)
Si(2)	0.6843(2)	0.34077(4)	0.6429(1)	0.0145(2)
Si(3)	0.1831(2)	0.40821(4)	0.5373(1)	0.0145(2)
Si(4)	0.7948(2)	0.38941(4)	-0.0185(1)	0.0152(2)
Na(1)	0.2299(3)	0.26138(6)	0.5247(2)	0.0244(3)
Na(2)	0.2743(3)	0.51408(5)	0.3548(2)	0.0215(3)
Na(3)	0.2534(3)	0.47281(5)	-0.1019(2)	0.0225(3)
Na(4)	0.7548(3)	0.28108(5)	0.2783(2)	0.0229(4)
O(1)	0.1210(4)	0.3844(1)	0.0352(3)	0.0195(5)
O(2)	0.2339(4)	0.3015(1)	0.2523(3)	0.0199(6)
O(3)	0.6209(4)	0.3690(1)	0.1429(3)	0.0184(5)
O(4)	0.2440(4)	0.4105(1)	0.3392(3)	0.0182(5)
O(5)	0.7431(4)	0.3414(1)	-0.1590(3)	0.0192(5)
O(6)	0.7456(4)	0.2819(1)	0.5655(3)	0.0184(5)
O(7)	0.3573(4)	0.3561(1)	0.6162(3)	0.0182(5)
O(8)	-0.1423(4)	0.3920(1)	0.5597(3)	0.0180(5)
O(9)	0.2452(4)	0.4667(1)	0.6166(3)	0.0183(5)
O(10)	0.7336(4)	0.4511(1)	-0.0767(3)	0.0195(5)

Table 3. Anisotropic displacement parameters ($Å^2$). The anisotropic displacement factor exponent takes the form: $-2\pi^2 [h^2 a^{*2} U_{11} + ... + 2 h k a^* b^* U_{12}]$

Atom	U_{11}	U_{22}	U_{33}	U_{23}	U_{13}	U_{12}
Si(1)	0.0136(4)	0.0166(5)	0.0135(5)	-0.0002(4)	0.0012(3)	0.0002(4)
Si(2)	0.0134(5)	0.0156(5)	0.0145(5)	0.0000(4)	-0.0001(4)	0.0002(4)
Si(3)	0.0132(5)	0.0156(5)	0.0147(5)	0.0003(4)	0.0008(4)	0.0002(4)
Si(4)	0.0135(5)	0.0183(5)	0.0137(5)	-0.0003(4)	-0.0002(4)	-0.0001(4)
Na(1)	0.0240(8)	0.0246(7)	0.0247(8)	0.0049(6)	-0.0008(6)	-0.0009(8)
Na(2)	0.0215(7)	0.0208(7)	0.0221(8)	0.0024(6)	0.0015(6)	-0.0001(4)
Na(3)	0.0219(7)	0.0248(8)	0.0208(8)	-0.0031(6)	0.0002(6)	-0.0018(6)
Na(4)	0.0211(7)	0.0266(8)	0.0209(8)	-0.0027(6)	0.0005(6)	0.0006(6)
O(1)	0.0165(12)	0.0243(12)	0.0176(13)	0.0021(10)	0.0010(9)	-0.0006(10)
O(2)	0.0196(12)	0.0195(12)	0.0206(14)	-0.0018(10)	-0.0002(10)	-0.0007(9)
O(3)	0.0172(12)	0.0221(12)	0.0159(12)	0.0006(10)	-0.0011(9)	-0.0002(9)
O(4)	0.0204(12)	0.0182(12)	0.0159(13)	-0.0002(10)	0.0022(9)	-0.0002(9)
O(5)	0.0220(12)	0.0189(12)	0.0166(13)	0.0015(10)	-0.0006(9)	-0.0005(10)
O(6)	0.0194(12)	0.0179(12)	0.0179(14)	-0.0002(10)	0.0002(9)	0.0001(9)
O(7)	0.0160(12)	0.0187(12)	0.0199(13)	0.0020(10)	-0.0001(9)	-0.0004(9)
O(8)	0.0189(12)	0.0172(12)	0.0180(13)	0.0012(10)	0.0011(9)	0.0004(9)
O(9)	0.0196(12)	0.0203(12)	0.0149(13)	-0.0005(10)	0.0002(10)	-0.0004(10)
O(10)	0.0198(12)	0.0192(12)	0.0195(13)	-0.0006(10)	-0.0002(9)	0.0022(9)

Table 4. Selected bond distances (Å) and angles (deg.).

Si(1)	-O(2)	1.578(3)	Si(2)	-O(6)	1.575(3)
	-O(3)	1.642(2)		-O(8)	1.637(3)
	-O(4)	1.642(3)		-O(5)	1.637(3)
	-O(1)	1.643(3)		-O(7)	1.643(2)
Mean		1.626	Mean		1.623
Si(3)	-O(9)	1.573(3)	Si(4)	-O(10)	1.581(3)
	-O(8)	1.637(2)		-O(3)	1.638(3)
	-O(7)	1.639(3)		-O(5)	1.642(3)
	-O(4)	1.641(3)		-O(1)	1.645(2)
Mean		1.623	Mean		1.627

Na(1)	-O(2)	2.389(3)	Na(2)	-O(9)	2.387(2)
	-O(2)	2.417(3)		-O(10)	2.413(3)
	-O(6)	2.425(2)		-O(9)	2.420(3)
	-O(7)	2.468(3)		-O(8)	2.443(3)
	-O(6)	2.571(3)		-O(4)	2.491(3)
				-O(9)	2.574(2)
Na(3)	-O(9)	2.297(3)	Na(4)	-O(6)	2.299(3)
	-O(10)	2.334(3)		-O(6)	2.339(3)
	-O(10)	2.396(3)		-O(2)	2.386(2)
	-O(1)	2.481(3)		-O(3)	2.465(3)
	-O(10)	2.584(2)		-O(2)	2.583(2)
				-O(5)	2.982(3)

O – T – O angles

O(2)-Si(1)-O(4)	114.48(13)	O(6)-Si(2)-O(8)	114.17(13)
O(3)-Si(1)-O(2)	109.86(12)	O(5)-Si(2)-O(6)	111.71(13)
O(3)-Si(1)-O(4)	106.25(12)	O(5)-Si(2)-O(8)	108.20(13)
O(1)-Si(1)-O(2)	114.87(13)	O(7)-Si(2)-O(6)	109.34(12)
O(1)-Si(1)-O(4)	105.79(13)	O(7)-Si(2)-O(8)	105.94(12)
O(1)-Si(1)-O(3)	104.82(12)	O(7)-Si(2)-O(5)	107.10(12)
Mean	109.35	Mean	109.41
O(8)-Si(3)-O(9)	110.48(12)	O(3)-Si(4)-O(10)	115.03(13)
O(7)-Si(3)-O(9)	114.90(13)	O(5)-Si(4)-O(10)	114.77(13)
O(7)-Si(3)-O(8)	105.78(12)	O(5)-Si(4)-O(3)	105.74(13)
O(4)-Si(3)-O(9)	109.80(13)	O(1)-Si(4)-O(10)	109.13(12)
O(4)-Si(3)-O(8)	107.08(12)	O(1)-Si(4)-O(3)	105.20(12)
O(4)-Si(3)-O(7)	108.46(13)	O(1)-Si(4)-O(5)	106.20(12)
Mean	109.42	Mean	109.35

T – O – T angles	
Si(3)-O(8)-Si(2)	136.18(15)
Si(4)-O(1)-Si(1)	136.89(15)
Si(2)-O(7)-Si(3)	136.02(15)
Si(1)-O(3)-Si(4)	137.32(15)
Si(4)-O(5)-Si(2)	135.95(16)
Si(1)-O(4)-Si(3)	134.43(16)

Description of the structure

The structure of C-$Na_2Si_2O_5$ consists of a sequence of layers of tetrahedra perpendicular to *b*. A single layer can be described as being built by condensation of unbranched zweier single chains running parallel *a* or vierer single chains parallel *c* via common corners. Furthermore, each single tetrahedral sheet consists of elliptically distorted rings composed of six [SiO_4]-tetrahedra in chair conformation. The sequence of directedness for the up (U) and down (D) pointing tetrahedra within a single six-membered ring (S6R) is UDUDUD. The unit cell contains four layers of tetrahedra; a projection parallel *b* of a single sheet in the unit cell of C-$Na_2Si_2O_5$ is given in Figure 1(a).

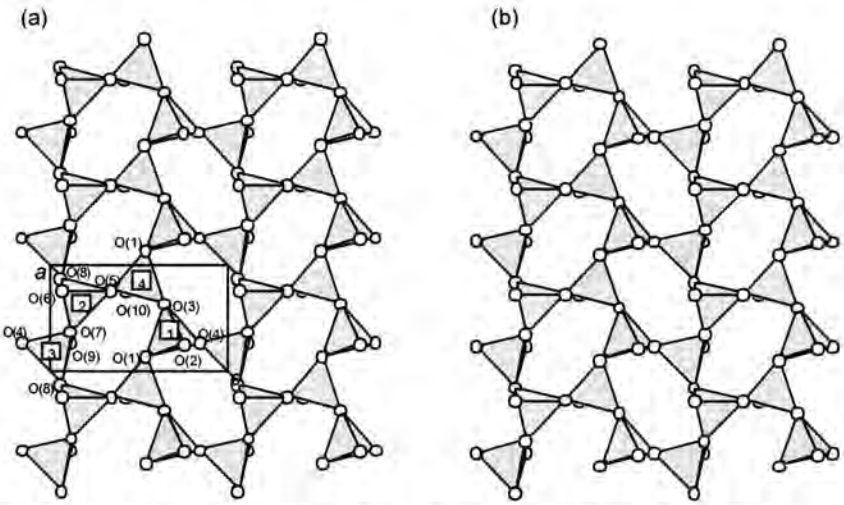

Figure 1.Single layer of tetrahedra in (a) C-$Na_2Si_2O_5$ and (b) β- $Na_2Si_2O_5$. The numbers within the tetrahedra of phase C correspond to the labels of the central Si atoms in Table 2.

The spread in the individual Si-O bond lengths follows the trend usually observed in silicate structures: the bond distances between Si and the terminal oxygens (O(2), O(6), O(9), O(10)) are considerably shorter than the bonds to bridging oxygen atoms.

The values for $\langle Si\text{-}O\rangle_{term.}$ = 1.576 Å and $\langle Si\text{-}O\rangle_{brid.}$ = 1.640 Å are in good agreement with those observed in the α -, β - and δ- modifications of $Na_2Si_2O_5$. Mean Si-O distances of the four tetrahedra given in Table 4 compare well with the value of 1.617(6) given by Baur [14] as a mean Si-O distance in phyllosilicates. While the average values of the O-Si-O angles for the four symmetrically independent tetrahedra are very close to the ideal value of 109.47°, the individual O-Si-O angles range from 104.8 to 115.0° for the SiO_4 groups. This suggests that the distortion of polyhedra is not very pronounced. According to Robinson *et al.* [15] the distortion can be expressed numerically by means of the quadratic elongation (Q.E.) and the angle variance (A.V.). The values of these parameters for the different tetrahedra are listed in Table 4. The Si-O-Si angles at the bridging oxygen atoms vary between 134.4 and 137.3°. Similar values have been observed for β-$Na_2Si_2O_5$: 135.1 – 136.5° (Pant [16]), whereas the corresponding values for the second known high-pressure modification ε- $Na_2Si_2O_5$ are considerably smaller: 127.0° - 129.3° (Fleet and Henderson [17]).

Linkage between the layers is provided by sodium cations. They reside between the sheets in about 1.6 Å wide slabs containing either Na(1) and Na(4) or Na(2) and Na(3), respectively. Within a single slab the Na cations are located in rows running parallel *a*.

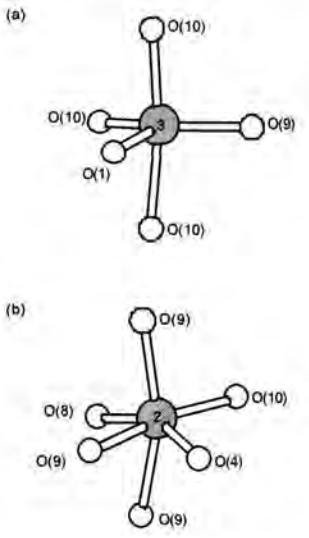

Figure 2. The two principally different coordination polyhedra for Na observed in C- $Na_2Si_2O_5$:
(a) distorted trigonal bipyramids (shown for Na(3) as an example) and (b) distorted octahedra (for Na(2)).

Na(1) and Na(3) are surrounded by five oxygen atoms at distances varying between 2.30 and 2.58 Å. Na(2) is coordinated to six oxygen anions. The Na(4) site shows a (5+1) coordination. The five inner oxygen neighbors have bond distances between 2.30 Å and 2.58 Å. Extending the limit for coordinating anions up to 3.0 Å, an additional sixth ligand at about 2.98 Å can be found. Since typical Na-O bond lengths average about 2.44 Å (Wilson [18]) the sixth Na(4)-O distance represents a weak bond. Coordination polyhedra around the sodium cations can be described as distorted trigonal bipyramids and distorted octahedra, respectively. (cf. Figure 2).

Bond valence sums (BVS) for the cations were calculated using the parameterization for the Si-O and the Na-O bond given by Brown and Altermatt [19].

The results range from 4.16 v.u. - 4.22 v.u. for Si and 0.87 v.u. - 1.04 v.u. for Na, close to the expected values of 4 v.u. for Si and 1 v.u. for Na, respectively. The BVS values for the oxygen anions vary between 1.91 v.u. for O(2) and 2.17 v.u. for O(7).

Results and Discussion

Comparison with β-$Na_2Si_2O_5$

A common feature of almost all structurally characterized sodium disilicates are tetrahedral layers of six-membered rings formed by the condensation of zweier single chains. The translation periods along the chains is reflected in a short lattice constant of about 4.8 - 4.9 Å (see Kahlenberg [20] and references cited in there). Comparing the shape of the S6R's, C-$Na_2Si_2O_5$ is closely related to β-$Na_2Si_2O_5$ (cf. Figure 1(a) and 1(b)). In both structures the rings exhibit an elliptically distortion, whereas the rings in α - and δ-$Na_2Si_2O_5$ have a ditrigonal form. The close relationship in the ring geometry is also responsible for the similar Si-O-Si angles mentioned above. However, the relationships between C- and β-$Na_2Si_2O_5$ are not limited to the geometry and the conformation of the single layers. As can be seen from Figures 3(a) and (b) in both structures identical blocks containing two layers A and B can be identified, which are related by inversion centers.

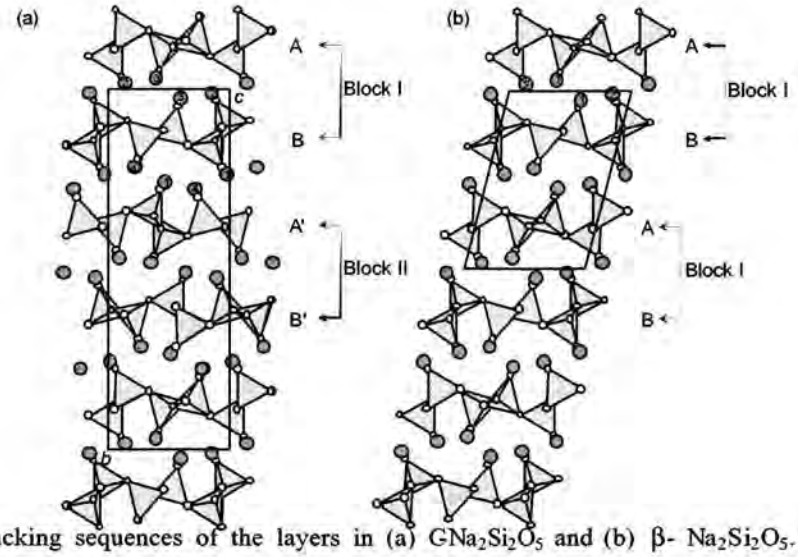

Figure 3. Stacking sequences of the layers in (a) C-$Na_2Si_2O_5$ and (b) β- $Na_2Si_2O_5$. Dark grey circles correspond to the Na-atoms linking the sheets. The labeling of the sodium cations in the β-phase follows the choice of Pant (1968)[16].

Furthermore, the number of oxygen ligands of the two different Na-atoms residing between the layers A and B are identical : five and six, respectively. A detailed comparison between the individual Na-O bond distances of the corresponding sodium atoms reveals, that there

exists an almost one-to-one correspondence of the Na(2) and Na(3) atoms in phase C and the cations Na(2) and Na(1) in the β-phase. The main difference between the two modifications results from the way in which the blocks are stacked. In contrast to β-$Na_2Si_2O_5$, where two adjacent blocks are translationally equivalent (resulting in a two layer stacking sequence), two neighboring blocks I and II in C-$Na_2Si_2O_5$ are related by the *c*-glide planes at y = ¼ and y = ¾, respectively. Therefore, a four layer stacking sequence is observed in this phase and the sodium atoms Na(1) and Na(4) at the interface between the blocks show a different coordination environment compared to Na(2) and Na(3). Whereas the 2_1-screw axes in β-$Na_2Si_2O_5$ are located within the single layers, running parallel to the zweier single chains, the corresponding symmetry elements in phase C are oriented perpendicular to the layers.

Twinning

Twinning by pseudo-merohedry is a feature frequently observed in monoclinic crystals where β is close to 90°. Actually, under the petrographic microscope almost all crystals of C-$Na_2Si_2O_5$ showed a polysynthetic twinning with composition planes parallel to (001). The twinning observed on a macroscopic scale may be microscopically rationalized by the existence of domains related by twofold axes running parallel [100] or mirror planes perpendicular to [001]. The resulting two types of twin individuals and the hypothetical twin boundary within a single layer for a twinning according to $2_{[100]}$ are shown in Figure 4.

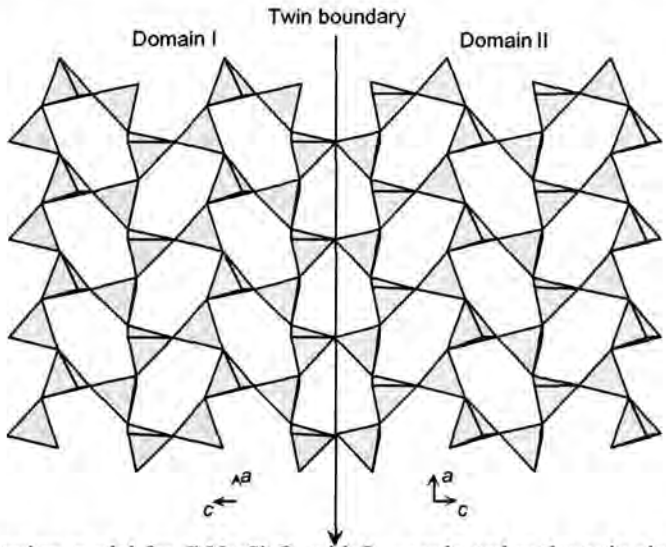

Figure 4. Possible twinning model for C-$Na_2Si_2O_5$ with $2_{[100]}$ selected as the twin element.

At the interfaces between the domains ditrigonally shaped, six-membered rings in UDUDUD conformation are formed. Twinning according to $m_{[001]}$ also results in rings of ditrigonal shape at the domain boundary.

However, the conformation of these rings would be UUDUDD. Since twinning by $2_{[100]}$ is not involved with a change the of sequence of directedness across the twin boundary this twinning model seems to be more appropriate.

^{29}Si MAS-NMR

The ^{29}Si MASNMR spectrum in Figure 5 shows four well-resolved lines with chemical shifts in the range between -86.0 ppm and -88.2 ppm. It can be fitted nicely using four Lorentzians with linewidths of 21 Hz and 24 Hz for the two low-field and the two high-field lines, respectively. The relative intensities thus obtained are 1 : 0.99 : 0.92 : 0.89. The small deviations from unity could easily be caused by the individual relaxation times in the various sites differing by not more than 10% from each other (cf. Experimental). The chemical shifts fall in the range observed for Q^3 groups in other alkali disilicates (Heidemann *et al.* [13], de Jong *et al.* [21]). The signal-to-noise ratio is sufficient to rule out any significant contributions from amorphous by-products.

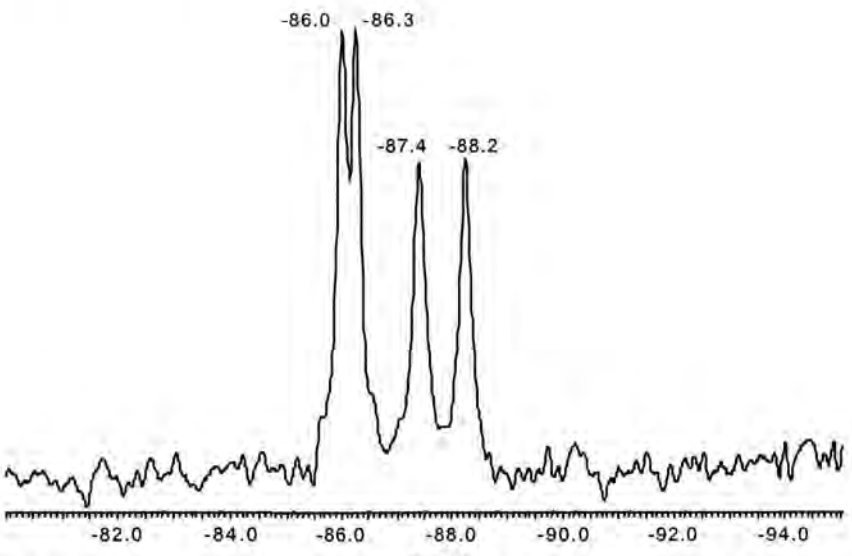

Figure 5. ^{29}Si MASNMR spectrum of C-$Na_2Si_2O_5$ recorded at an MAS frequency of 12 kHz (232 scans, p/4 pulses, repetition time: 900 s, cf. Experimental).

Although there was not quite enough sample to fill the 4 mm rotor we attempted to determine the parameters describing the anisotropy of the chemical shift (CSA), *i. e.* the anisotropy *?* and the asymmetry *?*. These parameters contain valuable information on the local geometry of different silicon sites (Grimmer [22]). The ^{29}Si MASNMR spectrum obtained at an MAS frequency of 2.2 kHz is given in Figure 6.

The spectral range in which the five spinning sidebands are observed indicates anisotropy values characteristic of Q^3 units (Heidemann *et al.* [13], Grimmer [22]). However, the signal-to-noise ratio achieved is too low for a reliable determination of the CSA parameters, in particular, to ascertain any subtle differences between the non-equivalent sites. To obtain an adequate signal-to-noise ratio in a reasonable time, the measurements have to be repeated with a larger amount of sample using a 7 mm rotor.

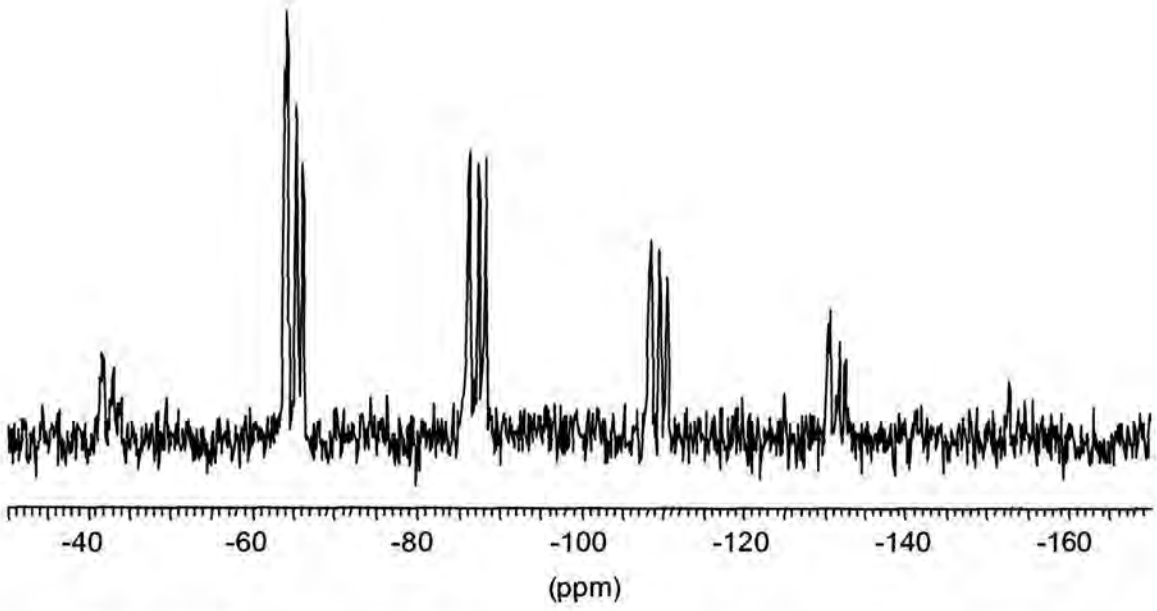

Figure 6. ^{29}Si MASNMR spectrum of C-$Na_2Si_2O_5$ recorded at an MAS frequency of 2.2 kHz (360 scans, p/4 pulses, repetition time: 900 s, cf. Experimental).

The four well-resolved lines in the ^{29}Si MASNMR spectrum (Figure 5) undoubtedly have to be attributed to the presence of the four non-equivalent sites. However, their actual assignment to the individual sites turns out to be a problem. Generally, the chemical shift-structure correlation is the main reason why the combination of X-ray diffraction with solid-state NMR spectroscopy is so efficient. The close correlation between ^{29}Si NMR chemical shift and geometrical properties such as Si-O bond lengths and Si-O-Si bond angles *a* was recognized soon after the first paper on the application of ^{29}Si MASNMR to silicates (Lippmaa *et al.* [23]) was published. Basic concepts and the early work on the theoretical interpretation of ^{29}Si NMR chemical shifts in zeolites and other silicates and quantitative correlations between chemical shift and structure parameters has been reviewed by Engelhardt and Michel [24]. We have applied several correlation equations established for Q^3 units using either the Si-O bond lengths or the bond angles *a*.

The results thus obtained are inconsistent with each other (see Table 5).

Table 5 Compilation of geometry data of the silicon sites and calculated isotropic chemical shifts using established empirical correlations

Parameter	Si(1)	Si(2)	Si(3)	Si(4)
<d(Si-O)> (Å)	1.6263	1.6230	1.6225	1.6265
Σ(EN)[a]	15.1974	15.1938	15.1827	15.2085
<∠Si-O-Si> (°)	136.21	136.05	135.54	136.72
<d(Si-Si)> (Å)	3.047	3.040	3.036	3.051
δ_{iso} = 844.2 <d(Si-O)>/Å - 1459.5 (ppm) (Smith *et al.* [29])	-86.58	-89.36	-89.79	-86.41
δ_{iso} = 1187 <d(Si-O)>/Å - 2014 (ppm) (Grimmer and Radeglia [26])	-83.58	-87.50	-88.09	-83.34
δ_{iso} = -24.336 Σ(EN) + 279.27 (ppm) (Janes and Oldfield [30])	-90.57	-90.49	-90.22	-90.84
δ_{iso} = -0.725 <∠Si-O-Si> + 9.054 (ppm) (de Jong *et al.* [21])	-89.70	-89.58	-89.21	-90.07

[a] Sum of bond electronegativities calculated according to Janes and Oldfield [30]: EN(Si-O) = ∠Si-O-Si / 136.79° + 2.9235 and EN(O-Na) = 3.4395.

The equations based on the Si-O distances predict a much wider range of chemical shifts than actually observed in the spectrum while those based on the bond angles predict a significantly narrower one than is observed. Furthermore, the two types of correlations suggest completely different sequences of the lines: From the bond-angle based correlations the order Si(3), Si(2), Si(1), and Si(4) (from low to high field) is obtained, whereas the Si-O distance based correlations produce the opposite sequence.

Heidemann *et al.* [13] have reported the similar discrepancy for β–$Na_2Si_2O_5$.

Using different siliceous zeolites for which high-quality structure data were available, Fyfe *et al.* [25] have critically evaluated several chemical shift-structure correlations for Q^4 units. Both the mean Si-Si distance, that is, the distance between the target silicon atom and its first nearest neighboring silicon atoms, and the mean value of the cos a / (cos a-1) function were found to have a linear relationship with the isotropic ^{29}Si NMR chemical shift with very high correlation coefficients. The main limitation in the structure-chemical shift correlations is the accuracy of the X-ray data, particularly when refinements of powder data are involved. Errors of 0.001 Å in the Si-O bond lengths (Grimmer and Radeglia [26], Engelhardt and Michel [24], Grimmer [22]), 0.01 Å in the Si-Si distances (Fyfe *et al.* [25]) or 2° in the mean bond angles (Engelhardt and Radeglia [27], Engelhardt and Michel [24]) correspond to comparatively large shift uncertainties of the order of 1 ppm. Very recently, Hochgräfe *et al.* [28] have demonstrated that improved structural data can be obtained from lattice energy minimization calculations compared to those from Rietveld analysis, provided that the topology of the framework is known. These authors pointed out that they used Si-Si distances since the true crystallographic Si-O distances are often obscured by static or dynamic disorder of the oxygen atoms, whereas a similar disorder has never been observed for silicon atoms in zeolite framework structures. Hence, the use of geometry data that do not depend on oxygen positions might be superior even if single-crystal data are available.

To the best of our knowledge, no quantitative correlation based on Si-Si distances has been established for Q^3 units. Assuming the same slope of the chemical shift *versus* mean Si-Si distance correlation (about -115 ppm/Å) as obtained for Q^4 units by Fyfe *et al.* [25], the difference of 0.015 Å between the mean Si-Si distances for Si(3) and Si(4) in the silicate under study corresponds to a chemical shift difference of 1.7 ppm. This value fits the experimentally observed shift difference of 2.2 ppm of the most separated lines (Figure 5) much better than the rather large differences derived from the Si-O bond lengths or the rather small ones derived from the Si-O-Si bond angles. Since the above given slope is negative, the resonance line at the lowest field should be assigned to Si(3) and that at the highest field to Si(4), giving the same sequence as the correlations based on the bond angles (cf. Table 5). However, this argument is rather tentative and further work is necessary to put the assignment on a firm footing. Considering the great similarity of the environments of the four silicon sites it might be a difficult problem to solve.

Acknowledgement

Financial support for this work has been received from the Deutsche Forschungsgemeinschaft under the grant Ka1342/1. The help of Prof. D. Lindsley (SUNY at Stony Brook) during the hydrothermal experiments is gratefully acknowledged. Furhermore, the authors would like to thank Dr. A.-R. Grimmer (Berlin) for helpful comments with regard to the applicability of the different chemical shift-structure correlations.

References

[1] Maekawa, H.; Yokokawa, T.: Effects of temperature on silicate melt structure: A high temperature Si-29 NMR study of $Na_2Si_2O_5$. Geochim Cosmochim Acta **61** (1997) 2569-2575

[2] Kanzaki, M.; Xue, X.; Stebbins, J.F.: Phase relations in Na_2O-SiO_2 and $K_2Si_4O_9$ systems up to 14 GPa and ^{29}Si NMR study of the new high-pressure phases: implications to the structure of high-pressure silicate glasses. Phys Earth Planet Int **107** (1998) 9-21

[3] Wolf, F.; Schwieger, W.: Zum Ionenaustausch einwertiger Kationen an synthetischen Natriumpolysilicaten mit Schichtstruktur. Z Anorg Allg Chem **457** (1979) 224-228.

[4] Rieck, H.P.: Natriumschichtsilicate und Schichtkieselsäuren. Nachr Chem Tech Lab **44** (1996) 699-704

[5] Willgallis, A.; Range, K.J.: Zur Polymorphie des $Na_2Si_2O_5$. Glastechn Ber **37** (1963) 194-200

[6] Williamson, J.; Glasser, F.P.: The crystallisation of $Na_2O{\cdot}2SiO_2$ - SiO_2 glasses. Phys Chem Glasses **7** (1996) 127-138

[7] Hoffmann, W.; Scheel, H.J.: Über die γ - und δ - Modifikationen des Natriumdisilikates, $Na_2Si_2O_5$. Z Kristallogr **129** (1969) 396-404

[8] Jacobsen, H.: Neue Untersuchungen an Natriumdisilikat ($Na_2Si_2O_5$). Diplomarbeit (1991) Universität Hannover.

[9] Altomare, A.; Cascarano, G.; Giacovazzo, C.; Guagliardi, A.; Burla, M.C.; Polidori, G.; Camalli, M.: SIR92 – a program for automatic solution of structures by direct methods. J Appl Cryst **27** (1992) 435

[10] Sheldrick, G.M.: SHELXL-93. Program for the refinement of crystal structures. Universität Göttingen (1993) Germany.

[11] Ibers, J.A.; Hamilton, W.C.: Eds. International tables for X - ray crystallography, Volume IV, Kynock, Birmingham, (1974) U.K.

[12] Dowty, E.: ATOMS, Version5.1 - Shape Software (2000).

[13] Heidemann, D.; Hübert, C.; Schwieger, W.; Grabner, P.; Bergk, K.H.; Sarv, P.: ^{29}Si- und ^{23}Na-Festkörper-MAS-NMR-Untersuchungen an Modifikationen des $Na_2Si_2O_5$. Z Anorg Allg Chem **617** (1992) 169-177

[14] Baur, W.H.: Variation of mean Si-O bond lengths in silicon-oxygen tetrahedra. Acta Cryst **B34** (1978) 1751-1756

[15] Robinson, K.; Gibbs, G.V.; Ribbe, P.H.: Quadratic elongation : A quantitative measure of distortion in coordination polyhedra. Science **172** (1971) 567-570

[16] Pant, A.K.: A reconsideration of the crystal structure of β-$Na_2Si_2O_5$. Acta Cryst **B24** (1968) 1077-1083

[17] Fleet, M.E.; Henderson, G.S.: Epsilon sodium disilicate: a high-pressure layer structure [$Na_2Si_2O_5$]. J Sol State Chem **119** (1995) 400-404

[18] Wilson, A.J.C.: Ed. International Tables for Crystallography, Volume C, Mathematical, Physical and Chemical Tables, (1995) Kluwer, Dordrecht.

[19] Brown, I.D.; Altermatt, D.: Bond-valence parameters obtained from a systematic analysis of the Inorganic Crystal Structure Database. Acta Cryst **B41** (1985) 244-247

[20] Kahlenberg, V.; Dörsam, G.; Wendschuh-Josties, M.; Fischer, R.X.: The crystal structure of δ-$Na_2Si_2O_5$. J Sol State Chem **146** (1999) 380-386

[21] de Jong, B.H.W.S.; Super, H.T.J.; Spek, A.L.; Veldman, N.; Nachtegaal, G.; Fischer, J.C.: Mixed alkali systems: Structure and ^{29}Si MAS NMR of $Li_2Si_2O_5$ and $K_2Si_2O_5$. Acta Cryst **B54** (1998) 568-577

[22] Grimmer, A-R.: Shielding tensor data and structure: the bond-related chemical shift concept. In: Tossell JA (ed) Nuclear magnetic shieldings and molecular structure. Kluwer, Dordrecht, (1993) pp 191-201

[23] Lippmaa, E.; Mägi, M.; Samoson, A.; Engelhardt, G.; Grimmer, A-R.: Structural studies of silicates by solid-state high-resolution ^{29}Si NMR. J Am Chem Soc **102**: (1980) 4889-4893

[24] Engelhardt, G.; Michel, D.: High-resolution solid state NMR of silicates and zeolites. Wiley, Chichester, (1987) pp 122-134

[25] Fyfe, C.A.; Müller, K.T.; Grondey, H.; Wongmoon, K.C.: Solid state double-resonance NMR experiments involving quadropolar and spin ½ nuclei. J Phys Chem **97** (1993) 13484-13495

[26] Grimmer, A-R.; Radeglia, R.: Correlation between the isotropic Si-29 chemical shifts and the mean silicon-oxygen bond length in silicates. Chem Phys Lett **106** (1984) 262-265

[27] Engelhardt, G.; Radeglia, R.: A semi-empirical quantum-chemical rationalization of the correlation between SiOSi angles and ^{29}Si NMR chemical shifts of silica polymorphs and framework aluminosilicates (zeolites). Chem Phys Lett **108** (1984) 271-274

[28] Hochgräfe, M.; Gies, H.; Fyfe, C.A.; Feng, Y.; Grondey, H.: Lattice energy-minimization calculation in the further investigation of XRD and NMR studies of zeolite frameworks. Chem Mater **12** (2000) 336-342

[29] Smith, K.A.; Kirkpatrick, R.J.; Oldfield, E.; Henderson, D.M.: High resolution silicon-29 nuclear magnetic resonance spectroscopic study of rock-forming silicates. Am Mineral **69** (1983) 1206-1215

[30] Janes, N.; Oldfield, E.: Prediction of silicon-29 nuclear magnetic resonance chemical shifts using a group electronegativity approach: application to silicate and aluminosilicate structures. J Am Chem Soc **107** (1985) 6769-6775

10. Hydrothermal synthesis and structural characterization of κ-$Na_2Si_2O_5$ and $Na_{1.84}K_{0.16}Si_2O_5$

S. Rakic[1], V. Kahlenberg[1,2] and B.C. Schmidt[3]

[1]Fachbereich Geowissenschaften (Kristallographie), Universität Bremen, Klagenfurter Str., D-28359 Bremen, Germany

[2]Institut für Mineralogie und Petrographie, Leopold-Franzens-Universität Innsbruck, Innrain 52, A-6020 Innsbruck, Austria

[3]Bayerisches Geoinstitut, Universität Bayreuth, D-95440 Bayreuth, Germany

Abstract

Single crystals of a new sodium disilicate modification labeled κ-$Na_2Si_2O_5$ have been prepared from the hydrothermal crystallization of a glass at 700°C and 3 kbar. The structure has been solved and refined to a residual of R(|F|) = 0.035 for 750 independent observed reflections. The compound is orthorhombic with space group $Pn2_1a$ (a = 8.128(1) Å, b = 4.8322(8) Å, c = 11.977(3) Å, V = 470.4(3) Å^3, Z = 4, D_x = 2.57 g/cm^3, μ(MoK_α) = 0.87 mm^{-1}) and belongs to the group of single layer silicates. Individual sheets can be described as being built by the condensation of *zweier* single chains of SiO_4 - tetrahedra parallel to the b - axis or, alternatively, by condensation of *vierer* single chains parallel to the a - axis. The layers contain six-membered rings in *UDUDUD* conformation. The stacking of the layers parallel to the c - axis results in a three-dimensional structure in which the alkali cations reside on two crystallographically independent sites (M(1) and M(2)) between the layers for charge compensation. The geometrical and topological features of the single tetrahedral sheets in κ-$Na_2Si_2O_5$ are almost identical to those observed in β- and C-$Na_2Si_2O_5$. Differences between the structures can be attributed to different ways of stacking of adjacent sheets and are discussed in detail. Small amounts of potassium can be substituted for sodium without changing the structure type. At slightly different synthesis conditions (600°C, 1kbar) we obtained an isostructural mixed alkali disilicate with composition $Na_{1.84}K_{0.16}Si_2O_5$ (a = 8.172(2) Å, b = 4.849(1) Å, c = 12.078(3) Å, V = 478.6(3) Å^3). The distribution of the alkali atoms among the two M(1) and M(2) positions shows a definite preference of the larger potassium for the M(1) site; the M(2) site is K-free.

Introduction

Alkali disilicates containing sodium have been investigated frequently because of their complex polymorphism as well as for their interesting material scientific applications. At ambient pressure, as many as six polymorphs of $Na_2Si_2O_5$ (phases α_{III}, α_{II}, α_I, β, γ, δ) are known to appear as a function of temperature and synthesis conditions [1-5]. Furthermore, the structures of the two high pressure phases C- and ε- $Na_2Si_2O_5$ have been described [6,7]. For potassium disilicate two different phases have been reported [8,9]. While the crystal structures of the above mentioned end-members of the system $Na_2Si_2O_5$ - $K_2Si_2O_5$ have been studied in detail, only limited information is available on the formation of intermediate compounds of general composition $Na_{2-x}K_xSi_2O_5$. Sakaguchi *et al.* [10] published an indexed powder pattern of a polycrystalline mixed phase with $x \sim 0.7$ prepared from the calcination of a slurry precipitated by adding NaOH and KOH to a sodium silicate solution. Single crystals of the same phase suited for structural investigations but with a slightly different general composition ($x = 0.45$) were obtained by Rakic and Kahlenberg [11] from the devitrification of a glass at 550°C and ambient pressure. Using a similar synthesis technique the same authors were able to prepare a novel compound with $x = 1.0$ [12]. Both phases belong to the group of single layer silicates but differ considerably concerning the topology of the tetrahedral layers. Whereas in $Na_{1.55}K_{0.45}Si_2O_5$ the conformation of up (*U*) and down (*D*) pointing tetrahedra within the six-membered rings is *UUDUUD*, the sheets in $NaKSi_2O_5$ are build up from four-, six- and eight-membered rings. The present paper is part of an ongoing study to elucidate the crystal chemistry of the Na- and Na - K - disilicates.

Experimental Details

The starting material for the single crystal growth experiments were glasses prepared from Na_2CO_3 (Fluka, 99%), K_2CO_3 (Riedel deHaën, 99%) and fine grained quartz powder. The reagents were weighted in molar ratios to give chemical compositions $Na_2Si_2O_5$ and $Na_{1.5}K_{0.5}Si_2O_5$, respectively, and were homogenized in an agate mortar. Subsequently, the mixtures were melted at 1000°C for 20 min. on platinum dishes in a resistance heating furnace, quenched to room temperature and re-ground. Melting, quenching and grinding were repeated three times to increase the homogeneity of the glass. Amounts of 0.20 g of the glass powders and about 1 wt% of water were loaded in gold capsules (5 mm diameter, 0.2 mm wall thickness, 22 mm length) and sealed by welding.

The hydrothermal synthesis was performed in an externally heated cold-seal pressure vessel operating in vertical configuration and being capable of rapid quenching. Synthesis experiments for both compositions were conducted for pressures of 1kbar as well as 3kbar and temperatures of 600°C and 700°C, respectively. At room temperature the samples were taken to the maximum pressure (water as pressure medium) and subsequently isobarically heated to the maximal temperature. After a run duration of 24 hours the samples were isobarically quenched to room temperature within a few seconds.

A first inspection of the eight synthesis products using a polarizing microscope revealed the presence of a polycrystalline material containing small amounts of glass. Only for the samples prepared at 700°C/3kbar (for $Na_2Si_2O_5$) and 600°C/1kbar (for $Na_{1.5}K_{0.5}Si_2O_5$) a few crystals with dimensions suitable for structural investigations were found and could be isolated from the matrix. The optical quality of the two samples was different. Whereas the pure sodium disilicate samples showed sharp extinction between crossed polarizers, the potassium containing crystals exhibited a pronounced undulous extinction. However, we could not observe any indications for a polysynthetic twinning, which is frequently encountered in alkali disilicates.

For the structural investigations crystals, about 0.02 x 0.06 x 0.18 mm^3 (for the Na-K-silicate sample) and 0.2 x 0.25 x 0.12 mm^3 (for the pure Na silicate) in size were selected. Single crystal x-ray diffraction (XRD) intensity measurements were performed using a STOE-imaging plate detector system (IPDS). Experimental details pertaining to data collections and structure determinations are summarized in Table 1.

Table 1. Data collection and refinement parameters

		κ-$Na_2Si_2O_5$	$Na_{1.84}K_{0.16}Si_2O_5$
(A)	**Crystal data**		
	a (Å)	8.128(1)	8.172(2)
	b (Å)	4.8322(8)	4.8493(9)
	c (Å)	11.977(3)	12.078(3)
	V ($Å^3$)	470.4(3)	478.6(3)
	Space group	$Pn2_1a$	$Pn2_1a$
	Z	4	4
	D_{calc} ($g\ cm^{-3}$)	2.572	2.564
	μ (mm^{-1})	0.87	0.975

(B)	**Intensity measurements**		
	Crystal shape	Plate	Plate
	Diffractometer	Stoe - IPDS	Stoe - IPDS
	Monochromator	Graphite	Graphite
	Radiation	MoK_α, $\lambda = 0.71073$ Å	MoK_α, $\lambda = 0.71073$ Å
	X-ray power	50 kV, 40 mA	50 kV, 40 mA
	Detector to sample distance	70 mm	70 mm
	Rotation width in ϕ (°)	2.0	2.0
	No. of exposures	100	100
	Irridation time / exposure (min.)	3.0	10.0
	2θ - range (°)	3.3° - 52.1°	3.3° - 52.1°
	Reflection range	$\lvert h \rvert \leq 10 ; \lvert k \rvert \leq 5 ; \lvert l \rvert \leq 14$	$\lvert h \rvert \leq 10 ; \lvert k \rvert \leq 5 ; \lvert l \rvert \leq 14$
	No. of measured reflections	3627	3738
	No. of unique reflections in *m2m*	905	945
	R_{int} in m2m after absorption correction	0.047	0.118
	No. of observed reflections ($I>2\sigma(I)$)	750	531
(C)	**Refinement of the structure**		
	No. of parameters used in the refinement	83	85
	R1 ($F_o > 4\ \sigma(F_o)$) ; R1 (all data)	0.035 ; 0.046	0.054; 0.106
	wR2 ($F_o > 4\ \sigma(F_o)$)	0.080	0.127
	Weighting parameter a	0.049	0.1256
	Goodness of Fit	1.048	0.885
	Final $\Delta\rho_{min}$ (e / Å^3)	-0.41	-0.58
	Final $\Delta\rho_{max}$ (e / Å^3)	0.51	0.70

Due to the smaller size of the K-containing crystal comparatively long exposing times of 10 minutes per frame were used. Both crystals showed orthorhombic Laue symmetry. The evaluation of the systematic extinction rules and the intensity statistics ($<|E^2-1>$) resulted in the space group $Pn2_1a$ for each phase.

Data reduction including intensity integration, background corrections, as well as Lorentz and polarization correction was performed with the Stoe XRED program package. All data were numerically corrected for absorption using a face absorption correction.

Attempts were made to determine the exact chemical composition of the K-containing crystal selected for the XRD measurements using an electron microprobe (EMP) as well as analytical scanning electron microscope (SEM). Although for the electron microprobe analysis (Cameca SX 50) low acceleration voltage and beam current (10kV, 5nA) were used we still observed significant beam damage of the crystal, which subsequently resulted in low analysis totals (88 to 92 %). Only in one part of the crystal beam damage was greatly reduced with resulting totals between 96 and 99 %. The chemical composition for these spots is about $Na_{1.86}K_{0.14}Si_{2.2}O_{5.4}$. The non-ideal (Na+K):Si ratio of 2:2.2 may be the result of some residual alkali loss under the electron beam. To obtain further constraints on the chemical composition of the investigated crystal we also used the EDX system of a SEM (LEO 1530). Due to the much lower beam current (about 0.2 nA) this technique caused no visible beam damage of the crystal. The disadvantage of these measurements was that we did not recalibrate the system but used the factory made calibration for the X-ray intensity to concentration relationship. On the basis of 43 analyses we observed an average Na:K ratio of 1.84:0.16, which is very close to the most trustworthy results of our EMP analysis. However, the SEM data give an average (Na+K):Si ratio of 2:2.56. Since the ideal value of 2:2 for a disilicate was confirmed by the subsequent structure analysis, the deviation from the ideal value may be due to some alkali loss under the beam or may be the artifact of the (for our crystal) incorrect x-ray intensity to concentration calibration of the used EDX system. Nonetheless the analyses indicated (a) the presence of a homogeneous phase and (b) the incorporation of minor amounts of potassium into the structure. Therefore, the crystal used for the structure solution is considerably depleted in potassium compared to the bulk composition of the starting glass.

Structure solution and refinements

The crystal structure of the pure sodium silicate was solved by direct methods with the program SIR92 [13] using a multi solution process. The phase set with the maximum combined figure of merit resulted in an E-map, the most intense peaks of which could be interpreted as a partial structure containing the sodium, silicon and some of the oxygen atoms. The structure was completed by difference Fourier calculations providing the starting

parameters for the least squares refinements performed with the program SHELXL-93 [14]. Neutral-atom scattering factors and anomalous-dispersion corrections were taken from the *International Tables for X-ray crystallography* [15]. Iterative full matrix least squares calculations based on F^2 using anisotropic displacement factors and a Larson-type extinction correction converged to an unweighted R1 index of 0.035. The correct absolute configuration was checked by inspection of the Flack parameter. The obtained structural model showed the typical features of a tetrahedral single layer disilicate. Due to the close relationship between the basic crystallographic data of the two compounds investigated in this study the structural model of the pure $Na_2Si_2O_5$ phase was used as a starting point for least squares refinements of the crystal structure of the potassium containing phase. Actually, the calculations confirmed the hypothesis that both compounds are isotypic. Initial refinements included the atomic parameters and the isotropic displacement factors as well. In the next step the site occupancies of the two alkali sites M(1) and M(2) were included in the refinement. According to SEM analysis, a constraint on the bulk composition was applied, and full occupancy for both sites was assumed. Within the experimental error no K-substitution on M(2) could be detected, leading to the following crystal chemical formula: $(Na_{0.84}K_{0.16})NaSi_2O_5$. The error in the Na/K distribution for the M(1) site is ± 0.02, as derived from the occupancy refinements. The final calculations using anisotropic displacement parameters converged at R1 = 0.053. The refined atomic coordinates, equivalent isotropic and anisotropic displacement parameters, as well as selected interatomic distances and angles are given in Tables 2 - 4.

Table 2. Atomic coordinates and equivalent isotropic displacement factors. The first and the second line of each atom correspond to the data of κ-$Na_2Si_2O_5$ and $Na_{1.84}K_{0.16}Si_2O_5$, respectively. U_{eq} is defined as one third of the trace of the orthogonalized U_{ij} tensor. All atoms occupy general positions. In case of $Na_{1.84}K_{0.16}Si_2O_5$, M(1) is a mixed alkali site with site occupancies of 0.84(2) Na and 0.16(2) K. M(2) contains exclusively sodium.

Atom	x	y	z	U_{eq}
Si(1)	0.1081(2)	0.1388(3)	0.5256(1)	0.0168(3)
	0.1084(4)	0.1373(7)	0.5257(3)	0.0338(9)
Si(2)	0.0528((2)	0.5254(3)	0.9324(1)	0.0160(3)
	0.0531(3)	0.5272(7)	0.9326(3)	0.0288(8)
M(1)	-0.0650(2)	0.0727(5)	0.7728(2)	0.0264(5)
	-0.0676(5)	0.0739(11)	0.7692(5)	0.0618(21)

M(2)	0.1890(2)	0.5978(5)	0.6911(2)	0.0242(5)
	0.1900(5)	0.5955(11)	0.6898(4)	0.0414(19)
O(1)	-0.0273(4)	0.6983(8)	0.0365(3)	0.0216(9)
	-0.0296(9)	0.7006(18)	0.0339(7)	0.0375(24)
O(2)	-0.0263(4)	0.5879(8)	0.8162(3)	0.0204(8)
	-0.0236(8)	0.5881(19)	0.8169(6)	0.0301(21)
O(3)	0.1644(4)	0.0791(9)	0.6490(3)	0.0217(8)
	0.1628(10)	0.0750(22)	0.6478(6)	0.0421(21)
O(4)	-0.0553(4)	0.9649(8)	0.4867(3)	0.0203(9)
	-0.0533(9)	0.9613(18)	0.4861(7)	0.0381(23)
O(5)	0.2509(4)	0.5837(8)	0.9303(3)	0.0205(8)
	0.2514(8)	0.5857(18)	0.9305(6)	0.0341(19)

Table 3. Anisotropic displacement parameters ($Å^2$). The anisotropic displacement factor exponent takes the form: $-2\pi^2 [h^2 a^{*2} U_{11} + ... + 2 h k a^* b^* U_{12}]$. The first and the second line of each atom correspond to the data of κ-$Na_2Si_2O_5$ and $Na_{1.84}K_{0.16}Si_2O_5$, respectively.

Atom	U_{11}	U_{22}	U_{33}	U_{23}	U_{13}	U_{12}
Si(1)	0.0111(6)	0.0153(8)	0.0240(7)	0.0006(7)	0.0011(6)	-0.0001(6)
	0.024(1)	0.029(2)	0.049(2)	0.000(2)	0.003(2)	0.000(1)
Si(2)	0.0119(6)	0.0153(8)	0.0209(7)	-0.0000(6)	0.0005(6)	0.0000(6)
	0.024(1)	0.028(2)	0.035(2)	0.000(2)	0.005(2)	0.000(2)
M(1)	0.020(1)	0.027(1)	0.032(1)	-0.002(1)	0.0049(8)	0.000(1)
	0.054(3)	0.038(4)	0.093(4)	-0.005(3)	0.038(3)	-0.004(3)
M(2)	0.0172(9)	0.024(1)	0.031(1)	-0.001(1)	0.0038(7)	-0.001(1)
	0.034(3)	0.033(3)	0.058(4)	0.000(3)	0.008(2)	0.000(3)
O(1)	0.016(2)	0.026(3)	0.022(2)	-0.000(2)	0.004(1)	-0.001(1)
	0.027(4)	0.043(6)	0.043(6)	0.003(4)	-0.009(4)	-0.013(4)
O(2)	0.013(2)	0.021(2)	0.027(2)	-0.002(2)	-0.002(1)	-0.000(2)
	0.026(4)	0.025(5)	0.039(5)	0.003(4)	0.002(3)	-0.002(4)
O(3)	0.017(2)	0.022(2)	0.026(2)	-0.001(2)	-0.000(1)	0.001(2)
	0.042(5)	0.031(5)	0.053(5)	0.001(6)	0.003(4)	0.000(4)

O(4)	0.013(2)	0.020(2)	0.028(2)	0.001(2)	-0.001(2)	0.002(1)
	0.029(4)	0.034(5)	0.051(5)	0.004(4)	0.007(4)	-0.005(3)
O(5)	0.011(2)	0.028(2)	0.023(2)	-0.001(2)	0.003(1)	-0.003(2)
	0.028(3)	0.035(5)	0.039(5)	0.001(5)	-0.001(3)	0.004(4)

Table 4. Selected bond distances (Å) and angles (deg.).

κ-$Na_2Si_2O_5$

Si(1)	-O(3)	1.573(4)	Si(2)	-O(2)	1.562(4)
	-O(4)	1.638(4)		-O(5)	1.635(3)
	-O(4)	1.640(4)		-O(1)	1.636(4)
	-O(5)	1.640(4)		-O(1)	1.637(4)
	Mean	1.623		Mean	1.618
M(1)	-O(3)	2.383(4)	M(2)	-O(2)	2.305(4)
	-O(3)	2.392(4)		-O(2)	2.316(4)
	-O(2)	2.420(5)		-O(3)	2.388(5)
	-O(1)	2.480(4)		-O(4)	2.476(4)
	-O(2)	2.562(5)		-O(3)	2.564(5)
				-O(5)	2.910(4)

O - Si - O angles

O(4)-Si(1)-O(3)	109.7(2)	O(1)-Si(2)-O(2)	114.6(2)
O(5)-Si(1)-O(3)	114.9(2)	O(1)-Si(2)-O(1)	105.6(2)
O(5)-Si(1)-O(4)	106.0(2)	O(1)-Si(2)-O(2)	109.7(2)
O(4)-Si(1)-O(3)	114.1(2)	O(5)-Si(2)-O(2)	111.0(2)
O(4)-Si(1)-O(4)	104.8(1)	O(5)-Si(2)-O(1)	108.4(2)
O(4)-Si(1)-O(5)	106.6(2)	O(5)-Si(2)-O(1)	107.1(2)
Mean		Mean	

Si - O - Si angles

Si(2)-O(1)-Si(2)	135.8(3)
Si(1)-O(4)-Si(1)	137.0(2)
Si(1)-O(5)-Si(2)	134.9(2)

$Na_{1.84}K_{0.16}Si_2O_5$

Si(1)	-O(3)	1.569(9)	Si(2)	-O(2)	1.561(8)
	-O(4)	1.641(10)		-O(1)	1.632(10)
	-O(4)	1.644(9)		-O(1)	1.645(10)
	-O(5)	1.642(8)		-O(5)	1.646(8)
	Mean	1.624		Mean	1.621
M(1)	-O(3)	2.387(8)	M(2)	-O(2)	2.324(8)
	-O(3)	2.420(9)		-O(2)	2.342(8)
	-O(2)	2.452(11)		-O(3)	2.390(11)
	-O(1)	2.581(10)		-O(4)	2.487(9)
	-O(2)	2.584(10)		-O(3)	2.584(11)
				-O(5)	2.951(9)

O - Si - O angles

O(4)-Si(1)-O(3)	110.1(5)	O(1)-Si(2)-O(2)	114.1(5)
O(5)-Si(1)-O(3)	115.5(4)	O(1)-Si(2)-O(1)	105.3(5)
O(5)-Si(1)-O(4)	106.1(4)	O(1)-Si(2)-O(2)	110.8(3)
O(4)-Si(1)-O(3)	113.7(5)	O(5)-Si(2)-O(2)	110.4(4)
O(4)-Si(1)-O(4)	104.5(3)	O(5)-Si(2)-O(1)	109.3(4)
O(4)-Si(1)-O(5)	106.1(4)	O(5)-Si(2)-O(1)	106.5(4)
Mean	109.3	Mean	109.4

Si - O - Si angles

Si(2)-O(1)-Si(2)	136.8(6)
Si(1)-O(4)-Si(1)	138.0(6)
Si(1)-O(5)-Si(2)	134.6(5)

We are aware of the fact that the values for thermal parameters for $Na_{1.84}K_{0.16}Si_2O_5$ are larger compared with the pure sodium disilicate. However, a re-examination of the diffraction data, the absorption correction and the resulting bond distances and angles did not reveal any indications that a wrong space group symmetry had been chosen nor did we detect any evidence for a systematic error during the data reduction. We attribute the higher values for the thermal motion to the considerably smaller sized of the crystal, reducing the diffracted intensity especially at higher diffraction angles. Drawings of structural details were prepared using the program ATOMS [16].

Results

The comparison of the sodium disilicate studied in this paper and the structurally characterized $Na_2Si_2O_5$ phases mentioned in the introduction revealed that the present compound represents a previously unknown modification which is named κ-$Na_2Si_2O_5$. Since κ-$Na_2Si_2O_5$ and $Na_{1.84}K_{0.16}Si_2O_5$ are isostructural we will focus the discussion of the structural details on the pure sodium disilicate phase.

The structure of κ-$Na_2Si_2O_5$ consists of a sequence of tetrahedral layers perpendicular to [001]. Each layer is composed of six membered rings of SiO_4 - tetrahedra in *UDUDUD* conformation. Figures 1a and b show projections parallel and perpendicular to *c* of one of the two tetrahedral sheets in the unit cell, respectively.

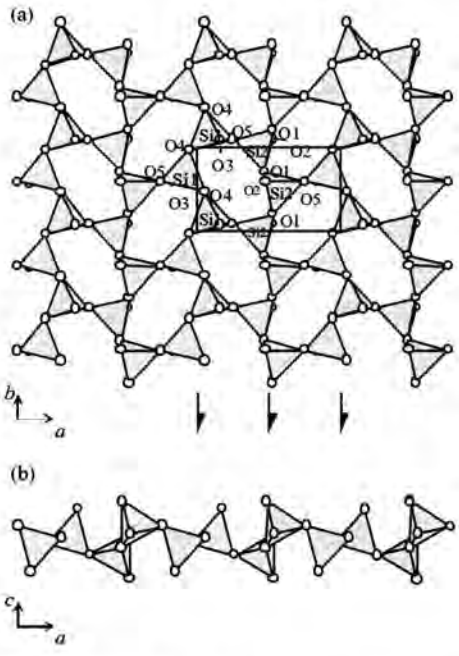

Figure 1. Single layer of the SiO_4-tetrahedra in κ-$Na_2Si_2O_5$ in projections perpendicular (a) and parallel (b) to the sheet.

Alternatively, the single layers can be described as being built by condensation of *vierer* single chains parallel [100] or *zweier* single chains parallel [010] via common corners. A single *zweier* chain contains either $Si(1)O_4$ or $Si(2)O_4$ - tetrahedra. The equatorial oxygen atoms of the sheets are not strictly coplanar. The bonds between the two symmetrically independent silicon cations and the non-bridging oxygen atoms O(2) and O(3), respectively, are short ($<Si\text{-}O_{nbr}>$: 1.568 Å) but are in good agreement with the values for the equivalent non-bridging oxygen atoms in the α -, β - and δ- modifications of $Na_2Si_2O_5$. The bond distances between Si(1) and Si(2), respectively, and the three bridging oxygen atoms of each tetrahedron are considerably longer (average 1.639 Å and 1.636 Å). The average T-O distances <Si(1)-O> = 1.623 Å and <Si(2)-O> = 1.618 Å are only slightly larger than the value of 1.617(6) given by Baur [17] as a mean distance in phyllosilicates.

While the average values of the O-Si-O angles for the two tetrahedra around Si(1) and Si(2) are very close to the ideal value of 109.47°, the individual angles range from 106° to 115° suggesting a slight distortion of the polyhedra. According to Robinson *et al.* [18] the distortion can be expressed numerically by means of the angle variance σ^2 . This parameter has values of 18.55 and 10.17, respectively, for the two polyhedra around Si(1)and Si(2).

The differences between the inter- and intra- chain Si-O-Si angles are almost negligible: the Si-O-Si angles are about 136.5° for the two oxygen atoms O(1) and O(4) within a zweier single chain, and 135° about O(5), the anion connecting neighboring chains. The Si-O-Si angles agree well with the commonly observed Si-O-Si angle frequency distribution reported by resulting from a statistical analysis of a large number of different silicate structures [19].

Charge balance in the structure is achieved by the incorporation of alkali ions located between the tetrahedral layers. Figure 2 shows a projection of the whole structure parallel to the layers.

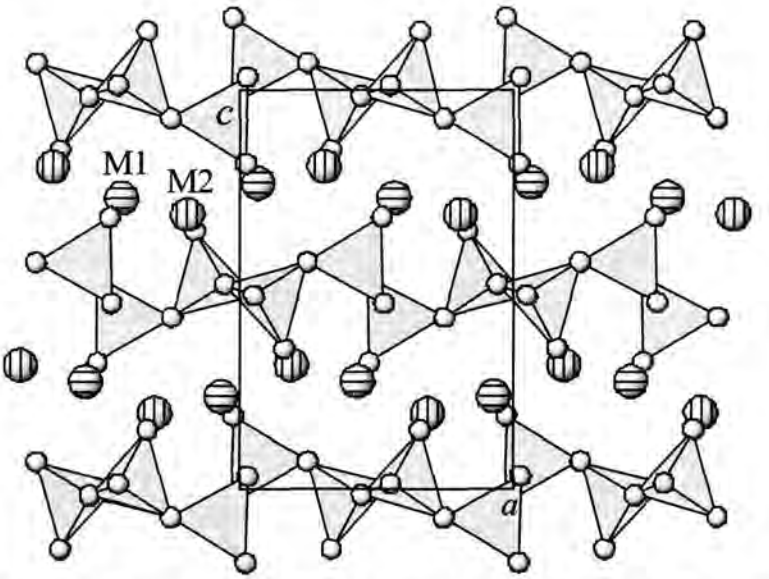

Figure 2. Projection of the whole structure of κ-$Na_2Si_2O_5$ parallel [010]. Horizontally and vertically hatched spheres correspond to the cation sites M(1) and M(2), respectively.

For the M(1)- as well as for M(2)-site five oxygen ligands between 2.30 Å and 2.60 Å can be found. Extending the limit for the coordinating anions up to 3.0 Å, M(2) has an additional sixth oxygen neighbor at about 2.91 Å. Since typical Na-O bond lengths average to about 2.44 Å [20] this latter bond would be weak. The coordination polyhedra can be approximately described as distorted trigonal bipyramids and distorted octahedra, respectively.

Each distorted $M(2)O_6$ octahedron shares four corners with neighboring octahedra in such a way that a single strongly folded perovskite-like layer is formed. Further linkage between the octahedra is provided by the $M(1)O_5$ groups. A single bipyramid shares four edges with the four adjacent octahedra. The tetrahedral layers alternate with the sheets containing the $M(2)O_6$ and $M(1)O_5$ polyhedra.

These intermediate layers are located at about z = 0.25 and 0.75. Projections of a single intermediate sheet parallel to [001] and [010] are given in Figures 3a and 3b, respectively.

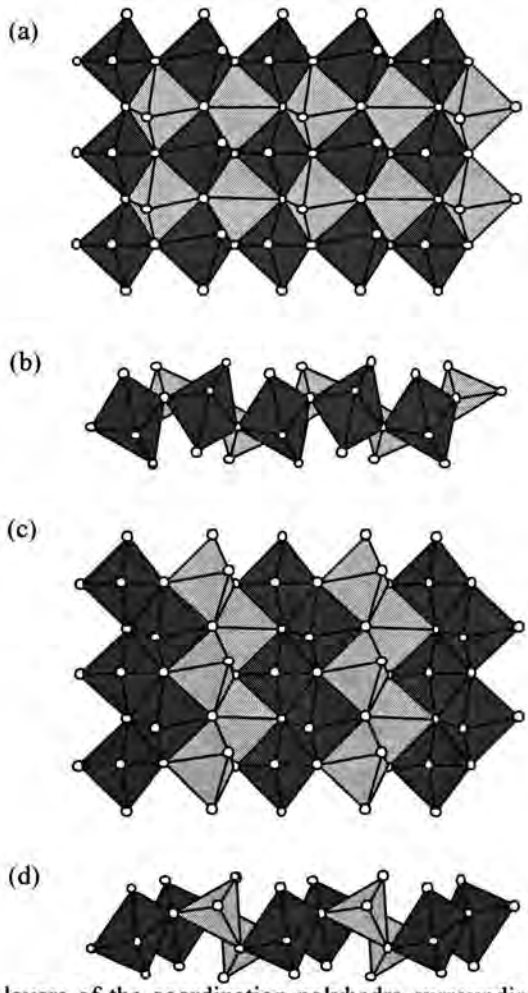

Figure 3. Intermediate layers of the coordination polyhedra surrounding the alkali cations in κ- $Na_2Si_2O_5$ (a,b) and β-$Na_2Si_2O_5$ (c,d). For each phase a projection perpendicular as well as parallel to the layers is shown. Octahedra and bipyramids are drawn in dark and medium grey color, respectively.

The incorporation of a small amount of potassium on the M(1) site in $Na_{1.84}K_{0.16}Si_2O_5$ is also reflected in the mean M-O distances. The average M(1)-O distance is increased from 2.447 Å in κ-$Na_2Si_2O_5$ to 2.485 Å in $Na_{1.84}K_{0.16}Si_2O_5$. The corresponding values for the potassium-free site M(2) are almost the same in both phases (2.410 Å and 2.425 Å, respectively).

Bond valence calculations were performed using the parameters given by Brese and O'Keeffe [21] for Si-O as well as Brown and Altermatt [22] for Na-O and K-O pairs and the bond distances of the first coordination sphere summarized in Table 4. The bond valence sums (BVS) for the atoms in both materials were close to the atomic valences.

In κ-$Na_2Si_2O_5$, for example, the following values were obtained: Si(1): 4.03 v.u., Si(2): 4.09 v.u., M(1): 0.89 v.u. and M(2): 1.05 v.u.. The BVS values for the oxygen anions varied between 1.89 v.u. for O(3) and 2.09 v.u. for O(1). When a site like M(1) in $Na_{1.84}K_{0.16}Si_2O_5$ is occupied by two different atoms a comparison of the bond valence sums calculated for each of the disordered atoms can be used to estimate the relative occupancies of the two atom species. The determination of the relative amounts of Na and K on M(1) based on the BVS resulted in occupancies of 84 at% Na and 16at % K. These values are in excellent agreement with the outcome of the structure refinements.

Discussion and comparison with related structures

The existence of a very short lattice constant of about 4.9 Å is a common feature of almost all alkali disilicates including the present compounds (see [11] and references therein). From a structural point of view this metrical parameter corresponds to the translation period of the tetrahedral *zweier* single chains within the layers of the phyllosilicates. More or less pronounced differences between the disilicates can be attributed to different layer topologies and/or different stacking schemes of the layers.

Concerning the geometrical and topological aspects of the tetrahedral layers, κ-$Na_2Si_2O_5$ is closely related with β- $Na_2Si_2O_5$ [23]. In both compounds the layers can be characterized by elliptically distorted six-membered rings in *UDUDUD* conformation. For β-$Na_2Si_2O_5$ as well as for κ- $Na_2Si_2O_5$ the 2_1-axes within the structure are running along the *zweier* single chains. The similarities between the arrangements of the tetrahedra in the layers are also reflected in the observed Si-O-Si angles falling into the same narrow range between 134° and 138° for each phase. Furthermore, the sodium atoms in both modifications are coordinated by either five or six oxygen ligands.

The main differences result from the ways in which adjacent layers are stacked (cf. Fig. 4). In κ- and β-$Na_2Si_2O_5$ an ABABA... stacking sequence has been realized. However, neighboring layers in the β-phase are related by inversion centers, whereas the corresponding sheets in κ- $Na_2Si_2O_5$ are mapped onto each other by *a*-glide planes perpendicular to [001]. Due to the different type of stacking in the β-phase the intermediate layers containing the $M(1)O_5$ and $M(2)O_6$ polyhedra are also transformed. The $M(2)O_6$ octahedra in β-$Na_2Si_2O_5$ are connected by common edges and form double chains or bands running parallel [010]. The octahedral bands in turn are linked by slabs containing edge sharing $M(1)O_5$ bipyramids.

The alternating sequence of octahedral and bipyramidal bands of a single intermediate layer in β-$Na_2Si_2O_5$ are shown in Figures 3c and 3d.

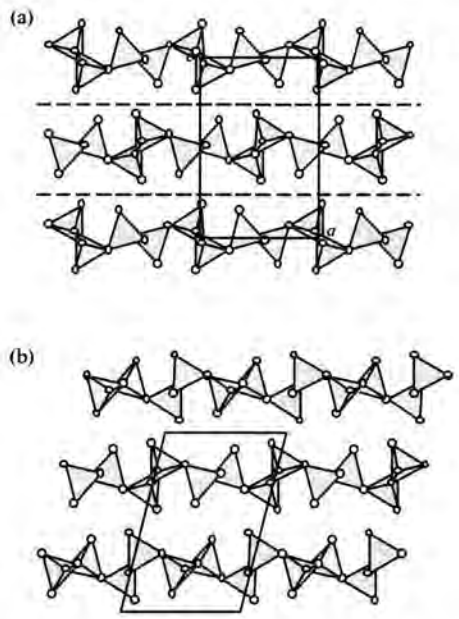

Figure 4. Comparison between the stacking of the tetrahedral layers in (a) κ- and (b) β-$Na_2Si_2O_5$.

Another interesting structural relationship can be obtained from the comparison with the recently solved structure of C-$Na_2Si_2O_5$ [6]. As can be seen from Figure 5 the C-phase can be considered as being built from a sequence of alternating blocks cut from the κ- and the β-modification, respectively. According to the phase diagram given by Williamson and Glasser [2] the β-phase is a low pressure modification. At pressures of 0.1 - 0.4 kbar the C-phase becomes stable. Although we did not study the stability region of the κ-phase in detail it is obviously that its field of existence is shifted to even higher pressures.

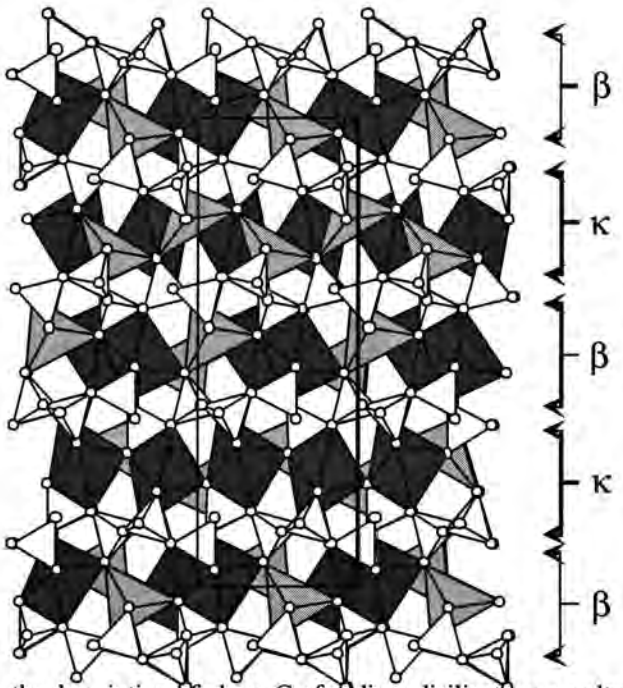

Figure 5. Modular approach for the description of phase C of sodium disilicate as an alternate stacking of blocks corresponding to κ- and β-$Na_2Si_2O_5$.

From a structural point of view a pressure dependent sequence β - C - κ may be rationalized as follows. Since the topology and the geometry of the tetrahedral layers in the three sodium disilicates are almost identical we can focus on the intermediate layers containing the NaO_x-polyhedra. Whereas the octahedra in β- and κ-$Na_2Si_2O_5$ have almost the same volume (18.1 $Å^3$ and 18.4 $Å^3$, respectively) the NaO_5-bipyramids in the κ-phase are significantly smaller (10.2 $Å^3$) compared with the corresponding polyhedra in the β-phase (11.5 $Å^3$). Therefore, with increasing pressure the κ-modification of sodium disilicate should be more stable. Since phase C contains equal amounts of building blocks of β- and k- $Na_2Si_2O_5$ as well, its existence is limited to intermediate pressure regions. However, it has to be pointed out that at pressures above 50 kbar a new phase (ε-disilicate) appears which can not be directly related to the sodium disilicates mentioned above [7]. In summary one can say that even in comparatively simple binary systems like Na_2O-SiO_2 there are still a lot of open questions concerning the number, the phase relationships and the crystal structures of the sodium silicates.

Acknowledgement

Financial support for this work has been received from the Deutsche Forschungsgemeinschaft under the grant Ka1342/1. BCS acknowledges funding by the visiting scientist program of the Bayerisches Geoinstitut.

References

[1] Willgallis, A.; Range, K.J.: Zur Polymorphie des $Na_2Si_2O_5$. Glastechn Ber **37** (1963) 194-200

[2] Williamson, J.; Glasser, F.P.: The crystallisation of $Na_2O·2SiO_2$ - SiO_2 glasses. Phys Chem Glasses **7** (1996) 127-138

[3] Hoffmann, W.; Scheel, H.J.: Über die γ - und δ - Modifikationen des Natriumdisilikates, $Na_2Si_2O_5$. Z Kristallogr **129** (1969) 396-404

[4] Jacobsen, H.: "Neue Untersuchungen an Natriumdisilikat ($Na_2Si_2O_5$)", Master thesis, University of Hannover (1991).

[5] Kahlenberg, V.; Dörsam, G.; Wendschuh-Josties, M.; Fischer, R.X.: The crystal structure of δ-$Na_2Si_2O_5$. J Sol State Chem **146** (1999) 380-386

[6] Rakic, S.; Kahlenberg, V.; Weidenthaler, C.; Zibrowius, B.: Structural characterization of high-pressure C-$Na_2Si_2O_5$ by single-crystal diffraction and ^{29}Si MAS NMR *Phys. Chem. Mineral.* **29** (2002) 477.

[7] Fleet, M.E.; Henderson, G.S.: Epsilon sodium disilicate: a high-pressure layer structure [$Na_2Si_2O_5$]. J Sol State Chem **119** (1995) 400-404

[8] Schweinsberg, H.; Liebau, F.: Darstellung und kristallographische Daten von $K_2Si_2O_5$, $KHSi_2O_5I$ und $K_2Si_4O_9$. Z. Anorg. Allg. Chem. **387** (1972) 241.

[9] de Jong, B.H.W.S.; Super, H.T.J.; Spek, A.L.; Veldman, N.; Nachtegaal, G.; Fischer, J.C.: Mixed alkali systems: Structure and ^{29}Si MAS NMR of $Li_2Si_2O_5$ and $K_2Si_2O_5$. Acta Cryst **B54** (1998) 568-577

[10] Sakaguchi, M.; Sakamoto, I.; Akagi, R.: Powder data for potassium sodium silicate $Na_{1.3}K_{0.7}Si_2O_5$. Powder Diffraction **10** (1995) 290-292.

[11] Rakic, S.; Kahlenberg, V.: The crystal structure of a mixed alkali phyllosilicate with composition $Na_{1.55}K_{0.45}Si_2O_5$. Eur. J. Mineral. **13** (2001a) 1215-1221.

[12] Rakic, S.; Kahlenberg, V.: Single crystal structure investigation of twinned $NaKSi_2O_5$ - a novel single layer silicate. Solid State Sci. **3** (2001b) 659-667.

[13] Altomare, A.; Cascarano, G.; Giacovazzo, C.; Guagliardi, A.; Burla, M.C.; Polidori, G.; Camalli, M.: SIR92 – a program for automatic solution of structures by direct methods. J Appl Cryst **27** (1992) 435

[14] Sheldrick, G.M.: SHELXL-93. Program for the refinement of crystal structures. Universität Göttingen, Germany (1993).

[15] Ibers, J.A., Hamilton, W.C.: Eds. International tables for X - ray crystallography, vol. IV, Kynoch, Birmingham, U.K.,1974.

[16] Dowty, E.: ATOMS Version5.1 - Shape Software (2000).

[17] Baur, W.H.: Variation of mean Si-O bond lengths in silicon-oxygen tetrahedra. *Acta Cryst.* **B34** (1978) 1751-1756.

[18] Robinson, K.; Gibbs, G.V.; Ribbe, P.H.: Quadratic elongation : A quantitative measure of distortion in coordination polyhedra. *Science* **172** (1971) 567-570.

[19] Baur, W.H.: Straight Si-O-Si bridging bonds do exist in silicates and silicon dioxide polymorphs. *Acta Cryst.* **B36** (1980) 2198-2202.

[20] Wilson, A.J.C.: (Ed.) International Tables for Crystallography, Volume C, Mathematical, Physical and Chemical Tables, Kluwer, Dordrecht (1995).

[21] Brese, N.E.; O'Keefe, M.: Bond-Valence Parameters for Solids. *Acta Cryst.* **B47** (1991) 192-197.

[22] Brown, I.D.; Altermatt, D.: Bond-valence parameters obtained from a systematic analysis of the Inorganic Crystal Structure Database. Acta Cryst **B41** (1985) 244-247

[23] Pant, A.K.: A Reconsideration of the Crystal Structure of β-$Na_2Si_2O_5$. Acta Cryst. **B24** (1968) 1077.

11. High pressure mixed alkali disilicates in the system $Na_{2-x}K_xSi_2O_5$: hydrothermal synthesis and crystal structures of $NaKSi_2O_5$-II and $Na_{0.67}K_{1.33}Si_2O_5$.

S. Rakic[1], V. Kahlenberg[1] and B.C. Schmidt[2]

[1]Fachbereich Geowissenschaften (Kristallographie), Universität Bremen, Klagenfurter Str., D - 28359 Bremen, Germany

[2]Bayerisches Geoinstitut, Universität Bayreuth, D-95440 Bayreuth, Germany

Abstract

Single crystal growth experiments for $NaKSi_2O_5$ and $Na_{0.67}K_{1.33}Si_2O_5$ have been successfully performed by hydrothermal crystallization of two stoichiometric glasses at 500°C and 1 kbar during 24 hours. For the glass with a Na:K ratio of 1:1 a previously unknown $NaKSi_2O_5$ modification named phase II was obtained. The structure of $NaKSi_2O_5$-II has been solved from a single crystal diffraction data set and refined to a residual of R(|F|) = 0.032 for 1186 independent reflections. The compound is monoclinic with space group $P2_1/c$ (a = 4.852(1) Å, b = 13.594(2) Å, c = 7.463(1) Å, β = 91.20(2)° V = 492.1(2) Å^3, M_r = 198.27 u, Z = 4, D_x = 2.68 g/cm^3, $\mu(MoK_\alpha)$ = 1.58mm^{-1}) and belongs to the group of double chain silicates. Individual double chains can be described as being built by the condensation of *zweier* single chains of SiO_4 - tetrahedra running parallel to the a - axis. Each chain contains four-membered rings. Alkali-atoms are 6- and 8-fold coordinated by the oxygen ligands. $NaKSi_2O_5$-II is isotypic with the structure of $NaRbSi_2O_5$ which has been synthesized at room-pressure. Hydrothermal treatment of a second glass with composition $Na_{0.5}K_{1.5}Si_2O_5$ resulted in the formation of single-crystalline material of $Na_{0.67}K_{1.33}Si_2O_5$, slightly Na-richer than the starting composition. The platy crystals showed twinning by pseudo-merohedry, a feature we took account of by separating the reflections from the different twin individuals during the data collection. Structure solution has been accomplished by direct methods. The subsequent refinement converged to a residual of R(|F|) = 0.037 for 1543 independent reflections. The compound is monoclinic as well with space group $I2/a$ (a = 12.731(2) Å, b = 7.321(1) Å, c = 17.827(3) Å, β = 100.85(2)° V = 1631.9(6) Å^3, M_r = 206.32 u, Z = 12, D_x = 2.53 g/cm^3, $\mu(MoK_\alpha)$ = 1.78mm^{-1}) and belongs to the group of single layer silicates. A single layer consists of four-, six- and eight- membered rings, which are parallel to (100), and can be described as being built by the condensation of unbranched *dreier* single chains running along the b-axis. The stacking of the layers results in a three-dimensional structure in which the

alkali cations reside between the layers for charge compensation. The distribution of the alkali atoms among the three crystallographically different positions M(1), M(2) and M(3) shows a definite preference of the larger potassium for the M(1) and M(2) site; the M(3) site is K-free. The alkali-atoms are 5- and 6- fold coordinated by the oxygen atoms. The geometrical and topological features of the single tetrahedral sheets in $Na_{0.67}K_{1.33}Si_2O_5$ are very similar to those observed in the phase I of $NaKSi_2O_5$. Differences can be attributed to different ways of stacking of adjacent sheets, and different sequences of up and down pointing tetrahedra within the rings.

Introduction

In contrast to the mixed alkali Na-K-disilicate glasses information on possible crystalline phases in the system $Na_2Si_2O_5$ - $K_2Si_2O_5$ is rather limited. The glasses of the system $Na_{2-x}K_xSi_2O_5$ have been intensively studied by several spectroscopic techniques like Raman scattering (Brawer and White [1]), EXAFS (Greaves [2]) or solid state NMR (Florian et al. [3]) in order to explain the so-called mixed alkali effect. This term is used for the observation, that several physical properties show a non-linear dependence from the chemical composition. Furthermore, the comparatively simple amorphous sodium and potassium disilicates have been used for molecular-dynamics computer simulations to study the dynamics of the alkali ions embedded in the SiO_2 matrix (Horbach et al. [4]) or for inelastic neutron scattering measurements to understand the microscopic nature of the low-energy excitations observed in the amorphous systems (Dove et al. [5]). Basic crystallographic data for the first crystalline intermediate compound with $x \sim 0.7$ have been obtained by Sakaguchi et al. [6] who reported an indexed powder pattern of a sample prepared from the calcination of precipitated precursors. Single crystals of the same phase suited for structural investigations but with a slightly different general composition ($x = 0.45$) were synthesized by Rakic and Kahlenberg [7] from the devitrification of a glass at 550°C and room pressure. Using a similar approach the same authors were able to prepare a Na-K-disilicate with $x = 1.0$ (Rakic and Kahlenberg [8]). In the following course of the manuscript this compound will be denoted $NaKSi_2O_5$-I. Furthermore, the existence of a potassium-poor compound with $x = 0.16$ has been shown only recently by Rakic et al. [9]. All three phases belong to the group single layer silicates .

The present paper is part of an ongoing study to elucidate the crystal chemistry of the mixed Na-K-disilicates and represents an extension of structural and preparative studies into the field of phases stable at elevated pressures.

Experimental Details

Starting materials for the single crystal growth were glasses prepared from fusing Na_2CO_3 (Fluka, 99%), K_2CO_3 (Riedel deHaën, 99%) and fine grained quartz powder. The reagents were weighed in molar ratios to give chemical compositions of $NaKSi_2O_5$ and $Na_{0.5}K_{1.5}Si_2O_5$ and were homogenized in an agate mortar. Subsequently, the mixtures were melted at 1000°C for 20 min. in a resistance heated furnace, quenched to room temperature and re-ground. Melting, quenching and grinding were repeated for three times to increase the homogeneity of the glass. Amounts of 0.21 g of the glass powders were loaded together with about 1 wt% of water into gold capsules (5 mm diameter, 0.2 mm wall thickness, 22 mm length) and were sealed by welding. The hydrothermal syntheses were performed in externally heated cold-seal pressure vessels operating in vertical configuration and being capable of rapid quenching. At room temperature the samples were taken to a pressure of 1 kbar (water as pressure medium) and subsequently isobarically heated to 500°. After run durations of 24 hours the samples were isobarically quenched to room temperature within a few seconds.

For both compositions, a first inspection of the synthesis products with a polarizing microscope revealed the presence of crystalline material containing only small amounts of glass. A few crystals with dimensions suitable for structural investigations were found and could be isolated from the matrix. Concerning the habit of the crystals and their optical quality the samples differed considerably. The crystals recovered from the more potassium rich run adopted the platy habit typical for phyllosilicates. For the glass with composition $NaKSi_2O_5$, on the other hand, prismatic fibrous crystals similar to those observed for actinolite or anthophyllite (Evans and Yang [10]; Walitzki et al. [11]) were obtained. Whereas the needles showed sharp extinction between crossed polarizers, a pronounced polysynthetic twinning was encountered for the platy crystals. The chemical compositions resulting from the subsequent structure analysis (see below) can be written as $NaKSi_2O_5$ (for the needles) and $Na_{0.67}K_{1.33}Si_2O_5$ (for the plates), respectively. Therefore, the composition of the second phase is slightly Na-richer than the starting composition of the corresponding glass.

From the differences in the morphology between the phase reported in present manuscript and the results of our previous study on $NaKSi_2O_5$ (Rakic and Kahlenberg [8]) we concluded that this compound may show polymorphism. Actually, this early hypothesis was confirmed by the subsequent structure analysis. The new modification will be named $NaKSi_2O_5$-II.

For the structural investigations on $NaKSi_2O_5$-II a needlelike crystal, about 0.03 x 0.13 x 0.19 mm in size was selected. Unfortunately, we could not find any untwinned crystal of $Na_{0.67}K_{1.33}Si_2O_5$. Therefore, a polysynthetic twinned sample with dimensions of about 0.3 x 0.2 x 0.1 mm was used for this compound. Single crystal intensity measurements were performed using a STOE- imaging plate detector system IPDS. Since the crystals of $Na_{0.67}K_{1.33}Si_2O_5$ were subject to twinning by pseudo-merohedry a comparatively large sample-detector distance of 70 mm was chosen in order to reduce the number of partially or completely overlapping reflections. Experimental details pertaining to data collection and structure determination are summarized in Table 1. The program RECIPE of the Stoe software package was employed to isolate the diffraction spots coming from the two different orientations of the twin domains in $Na_{0.67}K_{1.33}Si_2O_5$. The diffraction peaks were indexed independently and the two superimposed diffraction patterns were integrated simultaneously including an overlapp check. For the structure solution only the non-overlapping reflections of the larger twin individual were used. Data reduction included background corrections, Lorentz and polarization correction as well as a face absorption correction.

Table 1. Data collection and refinement parameters for $NaKSi_2O_5$-II and $Na_{0.67}K_{1.33}Si_2O_5$.

(A) Crystal data	$NaKSi_2O_5$-II	$Na_{0.57}K_{1.33}Si_2O_5$
a (Å)	4.852(1)	12.731(2)
b (Å)	13.594(2)	7.321(1)
c (Å)	7.463(1)	17.827(3)
β (°)	91.20(2)	100.85(2)
V (Å^3)	492.1(2)	1631.9(6)
Space group	$P2_1/c$	$I2/a$
Z	4	12
Chemical formula	$NaKSi_2O_5$	$Na_{0.67}K_{1.33}Si_2O_5$
D_{calc} (g cm^{-3})	2.68	2.53
μ (mm^{-1})	1.58	1.78

(B)	**Intensity measurements**		
	Crystal shape	Needle	Plate
	Diffractometer	Stoe - IPDS	Stoe - IPDS
	Monochromator	Graphite	Graphite
	Radiation	MoK_α, $\lambda = 0.71073$ Å	MoK_α, $\lambda = 0.71073$ Å
	X-ray power	50 kV, 40 mA	50 kV, 40 mA
	Detector to sample distance	60 mm	70 mm
	Rotation width in ϕ (°)	2.0	2.0
	No. of exposures	100	100
	Irridation time / exposure (min.)	3.0	3.0
	θ - range (°)	3.8° - 56.3°	3.3° - 52.1°
	Reflection range	$\|h\| \leq 6$; $\|k\| \leq 17$; $\|l\| \leq 9$	$\|h\| \leq 15$; $\|k\| \leq 8$; $\|l\| \leq 21$
	No. of measured reflections	4697	5414
	No. of observed reflections ($I > 2\ \sigma(I)$)	3247	3612
	No. of unique reflections	1186	1543
	R_{int} in *2/m* after absorption correction	0.049	0.056
(C)	**Refinement of the structure**		
	No. of parameters used in the refinement	82	127
	R1 ($F_o > 4\ \sigma(F_o)$) ;	0.032	0.037
	R1 (all data)	0.054	0.051
	wR2 ($F_o > 4\ \sigma(F_o)$)	0.083	0.097
	Weighting parameter a	0.0522	0.0708
	Goodness of Fit	0.926	1.063
	Final $\Delta\rho_{min}$ (e / Å^3)	-0.37	-0.36
	Final $\Delta\rho_{max}$ (e / Å^3)	0.54	0.55

Both phases showed monoclinic Laue symmetry *2/m*. The evaluation of the systematic extinction rules and the intensity statistics resulted in the assignment of the space groups $P2_1/c$ (for $NaKSi_2O_5$-II) and *I2/a* (for $Na_{0.67}K_{1.33}Si_2O_5$), respectively. Initial stuctural models

that conform to these space group symmetries were found by direct methods using the program SIR92 (Altomare et al. [12]). The phase sets with the maximum combined figure of merit resulted in an E-map, the most intense peaks of which could be interpreted as a partial structure containing the alkali, silicon and some of the oxygen atoms. The structures were completed by difference Fourier calculations providing the starting parameters for the least squares refinements performed with the program SHELXL-93 (Sheldrick [13]). Neutral-atom scattering factors and anomalous-dispersion corrections were taken from the *International Tables for X-ray crystallography* (Ibers and Hamilton [14]). Iterative full matrix least squares calculations based on F^2 using anisotropic displacement parameters converged to R1 = 0.032 for $NaKSi_2O_5$-II and 0.037 for $Na_{0.67}K_{1.33}Si_2O_5$, respectively. The final calculations included site occupancy refinements to study the Na/K distribution among the different alkali sites. No constraints on the bulk chemical composition were applied. However, full occupancy of the alkali sites was assumed. The results of the refinements indicate that within one standard deviation no Na - K substitution is observed for the different alkali positions in both compounds. The largest shift in the final cycle was < 0.001. The refined atomic coordinates, equivalent isotropic and anisotropic displacement parameters, as well as selected interatomic distances and angles are given in Tables 2-4. Drawings of structural details were prepared using the program ATOMS (Dowty [15]).

Table 2a. Atomic coordinates and equivalent isotropic displacement factors for $NaKSi_2O_5$-II. U_{eq} is defined as one third of the trace of the orthogonalized U_{ij} tensor. All atoms occupy general positions.

Atom	x	y	z	U_{eq}
Si(1)	0.1965(2)	0.0486(1)	-0.2160(1)	0.0137(2)
Si(2)	0.7022(2)	0.1301(1)	-0.0142(1)	0.0138(2)
K(1)	0.2043(2)	0.2002(1)	0.2861(1)	0.0264(2)
Na(1)	0.7241(3)	0.4056(1)	0.0264(2)	0.0198(4)
O(1)	0.8735(5)	0.4302(2)	0.3332(3)	0.0170(6)
O(2)	0.7785(6)	0.2408(2)	0.0082(4)	0.0217(6)
O(3)	0.2504(5)	0.4262(2)	0.0824(3)	0.0181(6)
O(4)	0.3756(5)	0.1144(2)	-0.0703(3)	0.0182(6)
O(5)	0.7474(6)	0.0692(2)	0.1768(3)	0.0178(6)

Table 3a. Anisotropic displacement parameters ($Å^2$) for $NaKSi_2O_5$-II. The anisotropic displacement factor exponent takes the form: $-2\pi^2 [h^2 a^{*2} U_{11} + ... + 2 h k a^* b^* U_{12}]$

Atom	U_{11}	U_{22}	U_{33}	U_{23}	U_{13}	U_{12}
Si(1)	0.0125(5)	0.0135(4)	0.0151(5)	0.0001(4)	0.0006(4)	0.0006(4)
Si(2)	0.0132(5)	0.0132(5)	0.0150(5)	-0.0005(4)	0.0004(4)	0.0006(4)
K(1)	0.0282(5)	0.0251(4)	0.0259(5)	-0.0030(4)	0.0020(4)	-0.0020(4)
Na(2)	0.0207(8)	0.0176(7)	0.0213(7)	0.0005(5)	0.0006(6)	-0.0004(6)
O(1)	0.0127(13)	0.0202(13)	0.0180(13)	0.0011(10)	0.0018(10)	-0.0011(10)
O(2)	0.0253(16)	0.0160(12)	0.0238(15)	0.0003(10)	0.0024(12)	-0.0022(11)
O(3)	0.0171(14)	0.0208(13)	0.0165(12)	-0.0012(10)	0.0018(10)	-0.0022(10)
O(4)	0.0146(14)	0.0185(12)	0.0215(13)	-0.0032(10)	0.0007(10)	0.0023(10)
O(5)	0.0224(15)	0.0155(12)	0.0155(12)	0.0002(9)	0.0017(10)	0.0021(10)

Table 4a. Selected bond distances (Å) and angles (deg.) for $NaKSi_2O_5$-II.

Si(1)	-O(3)	1.570(2)	Si(2)	-O(2)	1.557(3)
	-O(1)	1.643(3)		-O(4)	1.640(3)
	-O(4)	1.645(3)		-O(1)	1.643(3)
	-O(5)	1.649(3)		-O(5)	1.659(3)
	Mean	1.627		Mean	1.625
K(1)	-O(2)	2.793(3)	Na(1)	-O(2)	2.259(3)
	-O(3)	2.805(3)		-O(3)	2.361(3)
	-O(4)	2.856(3)		-O(1)	2.411(3)
	-O(5)	2.945(3)		-O(3)	2.431(3)
	-O(2)	2.949(3)		-O(3)	2.594(3)
	-O(4)	3.036(3)		-O(5)	2.636(3)
	-O(5)	3.296(3)			
	-O(2)	3.311(3)			

O - Si - O angles			
O(3)-Si(1)-O(1)	110.8(1)	O(2)-Si(2)-O(4)	112.3(2)
O(3)-Si(1)-O(4)	114.7(1)	O(2)-Si(2)-O(1)	115.7(2)
O(3)-Si(1)-O(5)	110.6(1)	O(2)-Si(2)-O(5)	111.3(2)
O(1)-Si(1)-O(4)	104.6(1)	O(4)-Si(2)-O(1)	104.9(1)
O(1)-Si(1)-O(5)	106.6(2)	O(4)-Si(2)-O(5)	105.3(1)
O(4)-Si(1)-O(5)	109.1(1)	O(1)-Si(2)-O(5)	106.7(1)
Mean	109.4	Mean	109.4
Si - O - Si angles			
Si(1)-O(1)-Si(2)	137.9(2)	Si(1)-O(4)-Si(2)	137.3(2)
Si(1)-O(5)-Si(2)	130.9(2)		

Table 2b. Atomic coordinates and equivalent isotropic displacement factors for $Na_{0.67}K_{1.33}Si_2O_5$. U_{eq} is defined as one third of the trace of the orthogonalized U_{ij} tensor. The oxygen atom O(7) is located on the special Wyckoff site 4(e). All other atoms occupy general positions.

Atom	x	y	z	U_{eq}
Si(1)	0.3475(1)	-0.1048(2)	0.3484(1)	0.0216(5)
Si(2)	0.3180(1)	0.2486(1)	0.4334(1)	0.0200(5)
Si(3)	0.2906(1)	-0.0497(2)	0.1745(1)	0.0262(5)
K(1)	0.6023(1)	0.1225(2)	0.4384(1)	0.0326(6)
K(2)	0.5845(1)	-0.1786(2)	0.2492(1)	0.0432(8)
Na(1)	0.4881(2)	0.4129(3)	0.5811(1)	0.0326(6)
O(1)	0.2812(2)	-0.0369(4)	0.2649(2)	0.0291(11)
O(2)	0.4715(2)	-0.1125(5)	0.3563(2)	0.0435(13)
O(3)	0.3064(2)	0.0293(4)	0.4117(2)	0.0246(10)
O(4)	0.2995(3)	-0.3035(4)	0.3661(2)	0.0374(12)
O(5)	0.4354(2)	0.3158(5)	0.4575(2)	0.0435(13)
O(6)	0.4051(3)	-0.0872(5)	0.1600(2)	0.0441(14)
O(7)	0.2500	0.2737(6)	0.5000	0.0540(23)
O(8)	0.2559(3)	0.3490(4)	0.3564(2)	0.0434(14)

Table 3b. Anisotropic displacement parameters ($Å^2$) for $Na_{0.67}K_{1.33}Si_2O_5$. The anisotropic displacement factor exponent takes the form: $-2\pi^2 [h^2 a^{*2} U_{11} + ... + 2 h k a^* b^* U_{12}]$

Atom	U_{11}	U_{22}	U_{33}	U_{23}	U_{13}	U_{12}
Si(1)	0.0238(9)	0.0190(10)	0.0218(9)	-0.0011(7)	0.0037(6)	0.0014(7)
Si(2)	0.0238(9)	0.0160(10)	0.0207(9)	-0.0001(7)	0.0056(6)	0.0000(7)
Si(3)	0.0383(10)	0.0185(10)	0.0217(9)	0.0015(7)	0.0053(7)	0.0002(7)
K(1)	0.0296(9)	0.0356(11)	0.0322(10)	0.0025(7)	0.0045(6)	0.0067(7)
K(2)	0.0297(10)	0.0527(13)	0.0492(12)	0.0007(8)	0.0124(7)	0.0076(8)
Na(1)	0.0523(17)	0.0293(17)	0.0338(15)	0.0002(11)	0.0174(12)	0.0044(12)
O(1)	0.0382(25)	0.0198(25)	0.0296(26)	0.0030(20)	0.0073(19)	0.0061(20)
O(2)	0.0282(26)	0.0582(36)	0.0434(30)	-0.0105(25)	0.0047(21)	0.0057(23)
O(3)	0.0325(25)	0.0173(24)	0.0248(22)	-0.0005(17)	0.0076(18)	-0.0017(19)
O(4)	0.0596(32)	0.0203(27)	0.0296(25)	0.0013(20)	0.0014(22)	-0.0099(23)
O(5)	0.0246(25)	0.0299(31)	0.0753(37)	-0.0177(26)	0.0073(23)	0.0003(20)
O(6)	0.0419(29)	0.0605(38)	0.0326(27)	0.0030(24)	0.0143(22)	0.0000(26)
O(7)	0.0984(62)	0.0097(37)	0.0712(53)	0.0000(0)	0.0601(47)	0.0000(0)
O(8)	0.0757(38)	0.0170(28)	0.0297(26)	0.0010(20)	-0.0101(24)	0.0020(24)

Table 4b. Selected bond distances (Å) and angles (deg.) for $Na_{0.67}K_{1.33}Si_2O_5$.

Si(1)	-O(2)	1.559(2)	Si(2)	-O(5)	1.555(3)
	-O(4)	1.631(3)		-O(7)	1.606(2)
	-O(1)	1.644(4)		-O(8)	1.625(4)
	-O(3)	1.653(3)		-O(3)	1.652(3)
	Mean	1.622		Mean	1.609
Si(3)	-O(6)	1.552(3)			
	-O(4)	1.638(3)			
	-O(1)	1.641(4)			
	-O(8)	1.640(3)			
	Mean	1.618			

K(1)	-O(5)	2.628(3)	K(2)	-O(6)	2.613(4)
	-O(2)	2.638(4)		-O(2)	2.643(3)
	-O(6)	2.746(4)		-O(8)	2.898(4)
	-O(3)	2.925(4)		-O(1)	2.928(3)
	-O(3)	2.946(3)		-O(8)	3.025(4)
	-O(4)	3.307(3)		-O(1)	3.167(3)

Na(1)	-O(5)	2.292(4)
	-O(6)	2.298(4)
	-O(5)	2.371(4)
	-O(2)	2.476(4)
	-O(4)	2.807(3)

O - Si - O angles

O(2)-Si(1)-O(4)	111.1(2)	O(5)-Si(2)-O(7)	112.5(2)
O(2)-Si(1)-O(1)	115.6(2)	O(5)-Si(2)-O(8)	112.3(2)
O(2)-Si(1)-O(3)	113.9(2)	O(5)-Si(2)-O(3)	114.3(2)
O(4)-Si(1)-O(1)	107.3(2)	O(7)-Si(2)-O(8)	109.2(2)
O(4)-Si(1)-O(3)	102.7(2)	O(7)-Si(2)-O(3)	104.3(2)
O(1)-Si(1)-O(3)	105.3(2)	O(8)-Si(2)-O(3)	103.5(2)
Mean	109.3	Mean	109.4
O(6)-Si(3)-O(4)	114.3(2)		
O(6)-Si(3)-O(1)	114.7(2)		
O(6)-Si(3)-O(8)	113.2(2)		
O(4)-Si(3)-O(1)	107.3(2)		
O(4)-Si(3)-O(8)	105.1(2)		
O(1)-Si(3)-O(8)	101.0(2)		
Mean	109.3		

Si - O - Si angles

Si(1)-O(1)-Si(3)	138.8(2)	Si(1)-O(4)-Si(3)	139.1(2)
Si(1)-O(3)-Si(2)	135.3(2)	Si(2)-O(7)-Si(2)	166.9(3)
Si(2)-O(8)-Si(3)	140.9(2)		

Results and discussion

$NaKSi_2O_5$-II

The structure of $NaKSi_2O_5$-II consists of a sequence of tetrahedral double chains running parallel to [100]. Each double chain contains four-membered rings of SiO_4 tetrahedra. Alternatively, the double chains can be described as being built by condensation of *zweier* single chains. A single sub-chain contains $Si(1)O_4$ as well as $Si(2)O_4$ - tetrahedra and is almost identical to those observed in the single chain silicate Na_2SiO_3 (see Fig. 1).

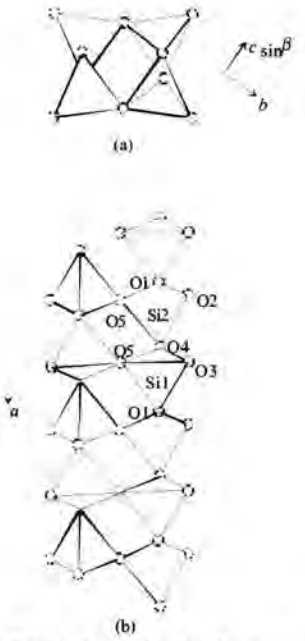

Figure 1. Projection of a single *zweier* double chain in $NaKSi_2O_5$-II (a) parallel and (b) perpendicular to [100].

The bonds between the two symmetrically independent silicon atoms and the non-bridging oxygen atoms O(2) and O(3), respectively, are short ($<Si\text{-}O_{nbr}>$: 1.564 Å) but are in good agreement with the values for the equivalent non-bridging oxygen atoms in other disilicates. The bond distances between Si(1) and Si(2), respectively, and the three bridging oxygen atoms of each tetrahedron are considerably longer (average 1.645 Å and 1.649 Å). While the average values of the O-Si-O angles for the two tetrahedra about Si(1) and Si(2) are very close to the ideal value of 109.47°, the angles range from 104° to 116° for the SiO_4 groups (Table 4a). This suggests that the polyhedra are slightly distorted. According to Robinson et al. [16] the distortion can be expressed numerically by means of the angle variance σ^2 . This parameter has values of 13.012 and 20.020 for the two polyhedra around Si(1)and Si(2), respectively. The differences between the inter- and intra- chain Si-O-Si angles are almost negligible: the Si-O-Si angles are about 137° for the two oxygen atoms O(1) and O(4) within a *zweier* single chain, and about 131° for O(5), the anion connecting neighboring chains. The Si-O-Si angles agree well with the commonly observed tetrahedral angle frequency distribution reported by Baur [17]) resulting from a statistical analysis of a large number of different silicate structures.

Charge balance in the structure is achieved by the incorporation of alkali ions. The Na atoms are surrounded by six oxygen ligands between 2.20 Å and 2.70 Å, forming distorted octahedra. Each NaO_6-octahedron shares two common edges with adjacent octahedra.

The condensation of the octahedra, in turn, results in bands running parallel [100], which can be classified as double ReO_3 chains (Wells, [18]). A single ribbon provides linkage between four adjacent tetrahedral double chains. The potassium cation is also surrounded by six oxygen ligands with distances between 2.80 Å and 3.10 Å. Furthermore, two additional oxygen neighbors can be found up to 3.3 Å. Focussing on the inner six oxygen ligands the KO_6-polyhedra can be also described as distorted octahedra. Octahedral chains are also formed via sharing of two common edges. However, for the potassium ions the ribbons have a different orientation: they are extending along [001]. A side view of the whole structure of $NaKSi_2O_5$-II is given in Figure 2.

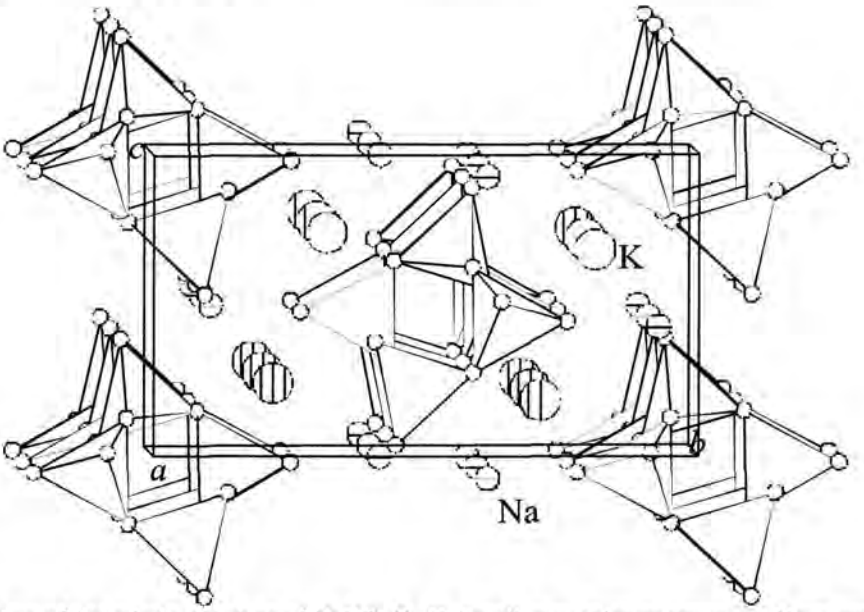

Figure 2. Side view of the whole structure of $NaKSi_2O_5$-II. Small grey spheres represent Na-atoms, the larger spheres correspond to the K-atoms.

Bond valence calculations were performed using the parameters given by Brown and Altermatt [19] for Si-O, Na-O and K-O pairs and the bond distances of the first coordination sphere summarized in Table 4. The bond valence sums (BVS) for the cations are in good agreement with atomic valences: Si(1): 4.16 v.u., Si(2): 4.19 v.u., Na(1): 1.11 v.u. and K(1): 0.86 v.u. The BVS values for the oxygen anions varied between 1.86 v.u. for O(2) and 2.21 v.u. for O(4).

The structure of $NaKSi_2O_5$-II is isotypic with $NaRbSi_2O_5$ (de Jong et al. [20]). However, the present structural investigation exhibits a considerably higher precision which is reflected in lower residuals and smaller standard deviations for the atomic coordinates and the bond distances/angles.

The close relationship is expressed by small deviations between their atomic positions calculated from an interpenetrating model of the structures based on the lattice constants of $NaKSi_2O_5$-II. The mean separation between the Si atoms of the two structures is 0.058 Å, between the O atoms it is 0.076 Å, and between the alkali ions it is 0.095 Å. The differences between the average values of the Si-O bond lengths ($NaRbSi_2O_5$: 1.622 Å; $NaKSi_2O_5$: 1.626 Å) as well as the Si-O-Si angles (136.7° and 135.3°, respectively) in the tetrahedra are negligible. The comparison between the lattice constants of both phases given in Table 5 shows the expected trend for the unit cell volumes resulting from the substitution of the smaller K (r = 1.51 Å) by the larger Rb (r = 1.61 Å; the values for ionic radii of the monovalent cations were taken from the corresponding tables of Shannon [21]).

Table 5. Comparison between the lattice constants of $NaKSi_2O_5$-II and $NaRbSi_2O_5$ (de Jong et al. [20]).

	a (Å)	b(Å)	c(Å)	β(deg.)	V(Å^3)
$NaKSi_2O_5$-II	4.852(1)	13.594(2)	7.463(1)	91.20(2)	492.1(2)
$NaRbSi_2O_5$	4.857(1)	13.540(1)	7.733(1)	90.91(1)	508.5(1)

The existence of two polymorphic forms of $NaKSi_2O_5$ as a function of the pressure used for the preparation can be attributed to pronounced differences in the densities between both modifications. The comparison between the unit cell volumes per formula unit of the layer silicate $NaKSi_2O_5$-I (V_I = 130.8 Å^3) prepared at ambient pressure and the double chain silicate structure observed in $NaKSi_2O_5$-II (V_{II} = 123.0 Å^3) shows clearly, that the latter phase exhibits a considerably higher density. Therefore, the formation of $NaKSi_2O_5$-II is favored by the application of increased pressure. It is noteworthy that this finding contradicts a trend in silicate crystal chemistry described by Ghose and Wan [22] that layers tend to result from hydrothermal synthesis and chains from atmospheric, high-temperature crystallization experiments.

$Na_{0.67}K_{1.33}Si_2O_5$

$Na_{0.67}K_{1.33}Si_2O_5$ belongs to the single layer silicate structures and represents a new structural variation among this group. The layers are parallel (100) and can be described as being built from the condensation of unbranched *dreier* single chains running along [010].

Hence, the *b* lattice constant of about 7.3 Å corresponds to the translation period of the single chains. Two neighboring chains share two out of three tetrahedra to form the four tetrahedra wide band shown in Figure 3a. Using Liebau's nomenclature (Liebau [23]) these ribbons can be addressed as unbranched *dreier* double chains.

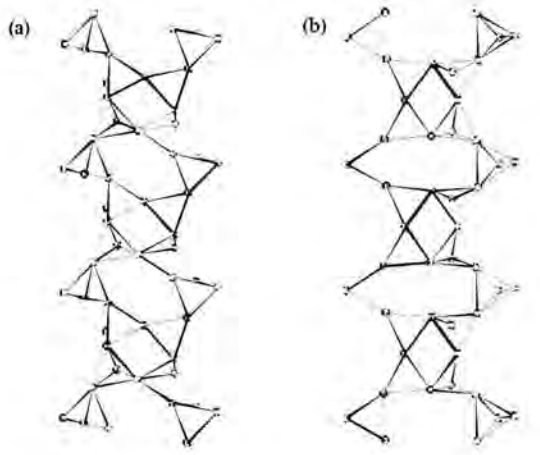

Figure 3. Projection of a single four tetrahedra wide ribbon including two unbranched *dreier* single chains in (a) $Na_{0.67}K_{1.33}Si_2O_5$ and (b) okenite.

A single band consists of an alternating sequence of four- and six-membered tetrahedral rings in UUDD and UUUDDD conformation, respectively. The same sequence of directedness can be found in the double chains of the mineral okenite (Merlino, [24]), a hydrous calcium silicate with composition $Ca_5Si_9O_{23}*9H_2O$ (see Figure 3b). The six-membered rings in $Na_{0.67}K_{1.33}Si_2O_5$ show a pronounced elliptical distortion. The planes defined by the equatorial oxygen atoms of both ring types are slightly inclined relative to (100). Adjacent ribbons are linked by the common oxygen atoms O(7) located on the twofold axis parallel *b* to build up the tetrahedral single layers.

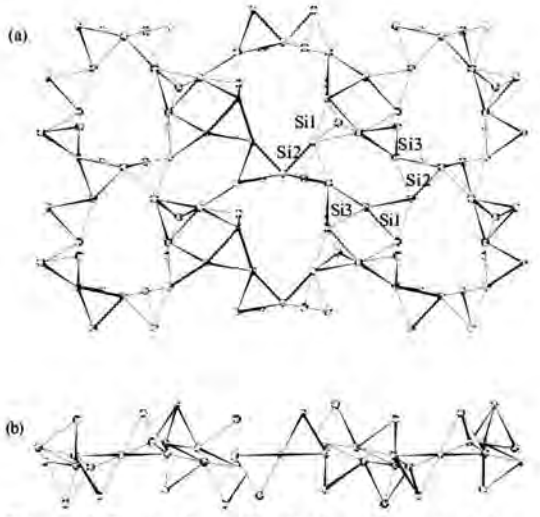

Figure 4. Projection of a single sheet containing SiO_4-tetrahedra (a) perpendicular and (b) parallel to the layer.

At the interface between two bands eight-membered tetrahedral rings are formed (see Fig. 4a). A projection of the corresponding single layer parallel [100] is given in Figure 4b. The unit cell contains two of these single layers in which all SiO_4 tetrahedra have three bridging and one terminating oxygen vertex (see Figure 5). The sodium and potassium atoms reside in voids between the tetrahedral sheets. No mixing of the two different alkali species has been observed: two out of three alkali sites are exclusively occupied by potassium, while the third position is a pure sodium site. The tetrahedra themselves exhibit rather typical bond lengths: the average $Si\text{-}O_{term.}$ and $Si\text{-}O_{br.}$ distances are 1.555 Å and 1.637 Å, respectively. The difference between the two averages of about 0.08 Å is also quite typical for silicate structures and reflects the stronger bonding between Si and $O_{term.}$ compared with that between K and O (or between Na

and O).

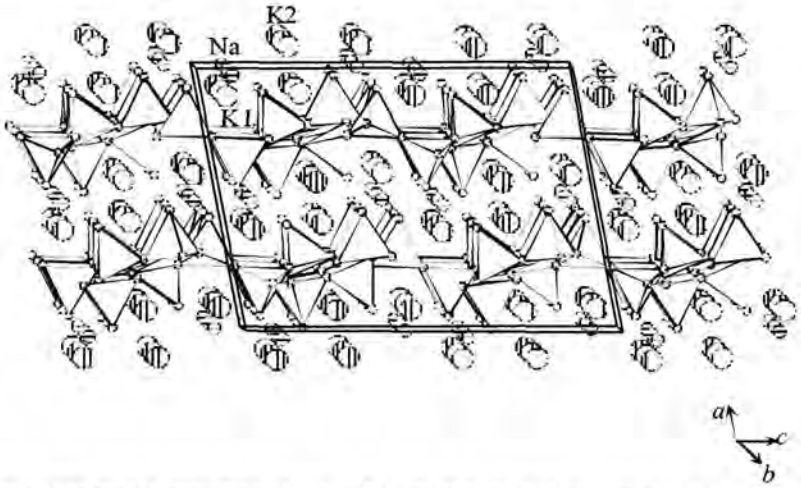

Figure 5. Side view of the whole structure of $Na_{0.67}K_{1.33}Si2O5$. Small grey spheres represent Na-atoms, the larger spheres correspond to the K-atoms.

In addition, the O-O distances (2.531 to 2.710 Å) and the O-Si-O bond angles (101.0° to 115.6°, Table 4b), respectively, are also very similar to the values reported in the literature (Liebau [23]). The angle variances σ^2 for the tetrahedra about the three Si atoms are 25.88 for Si(1), 20.58 for Si(2) and 32.15 for Si(3), indicating that the differences in the angle distortions are not very pronounced. Most of the Si-O-Si angles in Table 4 are close to 140°, the value which has been reported by Liebau [23] for an unstrained Si-O-Si bond angle. The only exception with about 167° is the angle around O(7) occurring at the interface between the neighboring double chains. It is interesting to note, that the probability ellipsoid defined by the adp's of this oxygen ligand shows a pronounced elongation perpendicular to the Si-O-Si bond. This may indicate that the ellipsoids for O(7) do not represent a true thermal motion and that the elongation is rather due to a disorder process.

The remaining atoms in the structure, the two crystallographically independent potassium ions as well as the sodium cations, are located in interstitial sites between the layers, such that the Na and K(1) atoms reside in planes defined by z ˜ 0.06, 0.44, 0.56, 0.94 and the K(2) atoms within the planes defined by z ˜ 0.25 and 0.75, respectively. Na and K(1) adopt positions above and below the eight-membered rings. Each sodium atom has five nearest oxygen neighbors; the distorted tetragonal NaO_5-pyramids are linked pairwise via a common edge. K(1) is coordinated by six oxygen ligands with distances up to 3.3 Å. However, no easy polyhedral approximation for the description of the coordination sphere could be found. The K(2) atoms, on the other hand, reside about 2.1 Å above and below the six-membered rings, slightly displaced from the center towards the O(1) atoms.

The $K(2)O_6$ polyhedra can be approximately described as distorted pentagonal pyramids. Two adjacent pyramids appear to share a common face. These dimers, in turn, are linked to each other by common oxygen corners.

The calculated bond valence sums (BVS, based on the data set of Brown and Altermatt [19]) for the three tetrahedral sites cations, as well as the alkali positions were close to the expected values of 4.0 v.u. and 1.0 v.u., respectively: Si(1): 4.22 v.u., Si(2): 4.36 v.u., Si(3):4.27 v.u., K(1):0.98 v.u. K(2):0.95 v.u. and Na(1): 0.97 v.u.. The BVS values for the oxygen anions varied between 1.91 v.u. for O(2) and 2.26 v.u. for O(8).

Unbranched *dreier* single layers containing four-, six- and eight-membered rings are comparatively rare building units among the group of layer silicates. The first representative of this group has been discovered by Fleet [25] in the structure of the mineral dalyite ($K_2ZrSi_6O_{15}$). Further examples can be found in the paper of Haile and Wuensch [26] on compounds belonging to the series $A_xMSi_6O_{15}$ with A: Na,K and M: Y, Nd. Concerning the structural relationships with the silicate layers observed in $Na_{0.5}K_{1.5}Si_2O_5$, the following three phases are of special interest: $K_3NdSi_6O_{15}$ (Pushcharovskii et al. [27]), $NaKSi_2O_5$-I (Rakic and Kahlenberg [8]) and $Na_2HCeSi_6O_{15}$ x nH_2O (Shumyatskaya et al. [28]). A common feature of all four materials are lattice constants of about 7.3 Å and 15.8 Å within the planes parallel to the tetrahedral sheets, corresponding to the translation periods of slightly folded *dreier* and strongly corrugated *achter* single chains. Neglecting different degrees of corrugation, the individual layers differ primarily in the directedness of the tetrahedra, i.e. in the distribution of "up" and "down" pointing tetrahedra (see Figure 6).

With regard to the phyllosilicates in the system $Na_2Si_2O_5$ - $K_2Si_2O_5$, there is a trend of an increasing stability of the eight-membered tetrahedral rings with increasing potassium content of the compounds. Whereas the single layers in the K-poor phases with x = 0.16 and x = 0.45 exhibit only six-membered rings (with different sequences of directedness), the corresponding layers for x = 1.0 and x = 1.33 consist of four- and eight-membered rings as well. It may be anticipated that $K_2Si_2O_5$ should adopt a single layer silicate structure, where no six-membered rings occur within the tetrahedral sheets. Actually, the metrical parameters of the potassium disilicate modification first described by Schweinsberg and Liebau [29] point to that direction. Structural investigations on this unknown phase are currently in progress and may reveal if the hypothesis mentioned above is justified.

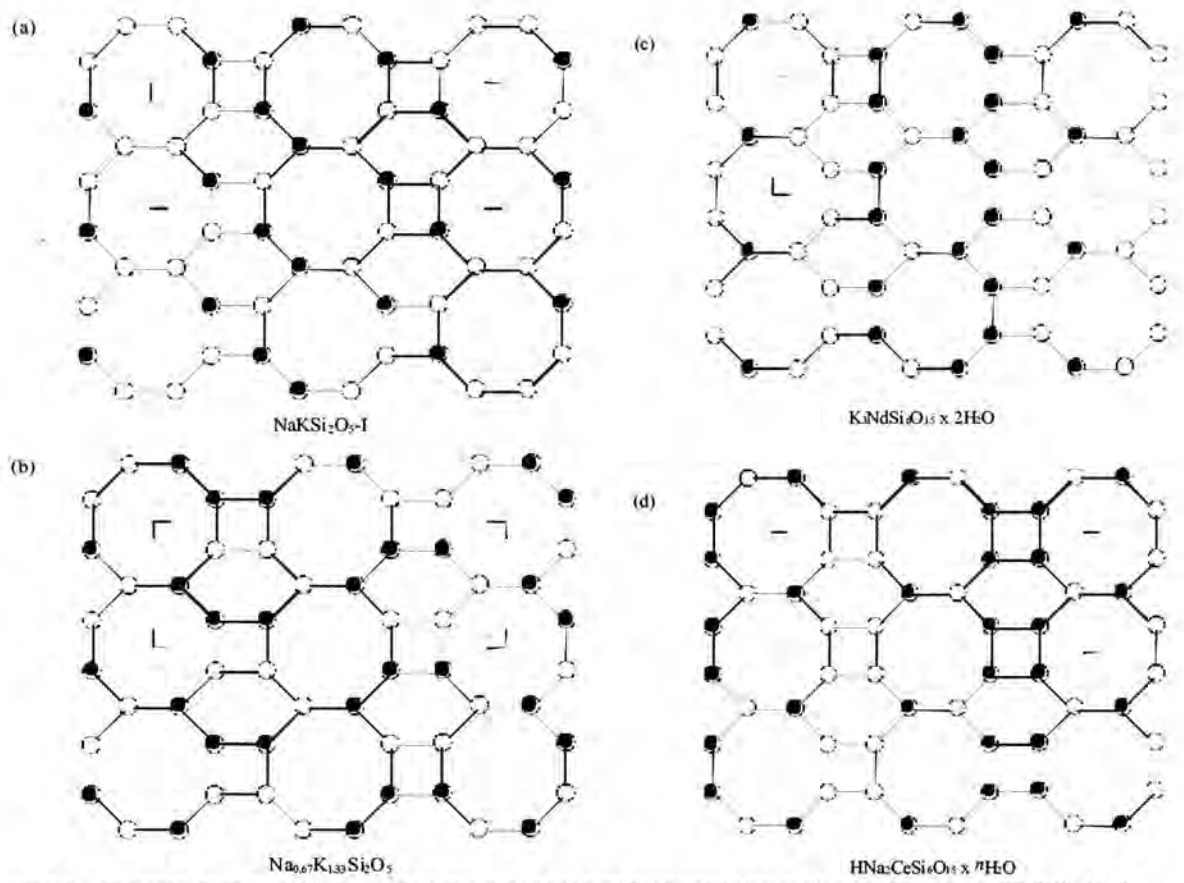

Figure 6. Idealized representation of the topology of the unbranched *dreier* single layers in (a) $NaKSi_2O_5$-I, (b) $Na_{0.67}K_{1.33}Si_2O_5$, (c) $K_3NdSi_6O_{15}$ x $2H_2O$ and (d) $Na_2HCeSi_6O_{15}$ x nH_2O. The directedness of each tetrahedron is indicated by either „?" for „up" or „?" for „down". The unit meshes within the idealized layers are indicated by the rectangles inscribed.

Acknowledgement

Financial support for this work has been received from the Deutsche Forschungsgemeinschaft under the grant Ka1342/1. BCS acknowledges funding by the visiting scientist program of the Bayerisches Geoinstitut.

References

[1] Brawer, S.A.; White W.B.: Raman spectroscopic investigations of the structure of silicate glasses. I. The binary alkali disilicates. J. Chem. Phys. **63** (1975) 2421-2432.

[2] Greaves, G.N.: Structural studies of the mixed alkali effect in disilicate glasses. Solid. State Ionics **105** (1998) 243-248.

[3] Florian, P.; Vermillion, K.E.; Grandetti, P.J.; Farnan, I.; Stebbins, J.F.: Cation distribution in mixed alkali disilicate glasses. J. Am. Chem. Soc. **118** (1996) 3493-3497.

[4] Horbach, J.; Kob W.; Binder, K.: Dynamics of sodium in sodium disilicate: channel relaxation and sodium diffusion. Phys. Rev. Lett. **88** (2002) art.no. 125502.

[5] Dove, M.T.; Harris, M.J.; Hannon, A.C.; Parker, J.M.; Swainson, I.P.; Gambhir, M.: Floppy Modes in crystalline and amorphous silicates. Phys. Rev. Lett., **78** (1997) 1070-1073.

[6] Sakaguchi, M.; Sakamoto, I.; Akagi, R.: Powder data for potassium sodium silicate $Na_{1.3}K_{0.7}Si_2O_5$. Powder Diffraction **10** (1995) 290-292.

[7] Rakic, S.; Kahlenberg, V.: The crystal structure of a mixed alkali phyllosilicate with composition $Na_{1.55}K_{0.45}Si_2O_5$. Eur. J. Mineral. **13** (2001a) 1215-1221.

[8] Rakic, S.; Kahlenberg, V.: Single crystal structure investigation of twinned $NaKSi_2O_5$ - a novel single layer silicate. Solid State Sci. **3** (2001b) 659-667.

[9] Rakic, S; Kahlenberg, V.; Schmidt, B.C.: Hydrothermal synthesis and structural characterization of an alkali disilicate with composition $Na_{1.84}K_{0.16}Si_2O_5$. submitted to Eur. J. Mineral. (2002).

[10] Evans, B.W.; Yang, H.X.: Fe-Mg disorder in tremolite-actinolite-ferro-actinolite at ambient and high temperature. Am. Mineral. **83** (1998) 458-475.

[11] Walitzki, E.M., Walter, F. & Ettinger, K.: Verfeinerung der Kristallstruktur von Anthophyllit vom Ochsenkogel/Gleinalpe, Österreich. Z. Kristallogr. **188** (1989) 237-244.

[12] Altomare, A.; Cascarano, G.; Giacovazzo, C.; Guagliardi, A.; Burla, M.C.; Polidori, G.; Camalli, M.: SIR92 - a program for automatic solution of structures by direct methods. J. Appl. Crystallogr. **27** (1992) 435.

[13] Sheldrick, G.M.: SHELXL-93. Program for the refinement of crystal structures. Universität Göttingen, Germany (1993).

[14] Ibers, J.A.; Hamilton, W.C., Eds.: International tables for X - ray crystallography, Volume IV, The Kynoch Press, Birmingham, U.K. (1974).

[15] Dowty, E.: ATOMS Version5.1 - Shape Software (2000).

[16] Robinson, K.; Gibbs, G.V.; Ribbe, P.H.: Quadratic elongation : A quantitative measure of distortion in coordination polyhedra. Science **172** (1971) 567-570.

[17] Baur, W.H.: Straight Si-O-Si bridging bonds do exist in silicates and silicon dioxide polymorphs. Acta Crystallogr. B**36** (1980) 2198-2202.

[18] Wells, A.F.: Structural inorganic chemistry. Clarendon Press, Oxford (1995).

[19] Brown, I.D.; Altermatt, D.: Bond-valence parameters obtained from a systematic analysis of the inorganic crystal structure database. Acta Crystallogr. B**41** (1985) 244-247.

[20] DeJong, B.H.W.S.; Supèr, H.T.J.; Frijhoff, R.M.; Spek, A.L.; Nachtegaal, G.: Mixed alkali systems: Dietzel's theorem, X-ray structure, hygroscopicity and ^{29}Si MAS NMR of $NaRbSi_2O_5$ and $NaCsSi_2O_5$. Z. Kristallogr. **215** (2000) 397-405.

[21] Shannon, R.D.: Revised effective ionic radii and systematic studies of interatomic distances in halides and chalcogenides. Acta Crystallogr. **A32** (1976) 751-767.

[22] Ghose, S.; Wan, C.: Zekterite, $NaLiZrSi_6O_{15}$: a silicate with six-tetrahedral-repeat double chains. Am. Mineral. **63** (1978) 304-310.

[23] Liebau, F.: Structural chemistry of silicates. Springer Verlag, Berlin (1985).

[24] Merlino, S.: Okenite, $Ca_{10}Si_{18}O_{46}*18H_2O$: the first example of a chain and sheet silicate. Am. Mineral. **68** (1983) 614-622.

[25] Fleet, M.E.: The crystal structure of Dalyite. Z. Kristallogr. **121** (1965) 349 - 368.

[26] Haile, S.M.; Wuensch, B.J.: Comparison of the crystal chemistry of selected MSi_6O_{15}-based silicates. Am. Mineral. **82** (1997) 1141-1149.

[27] Pushcharovskii, D.Y.; Karpov, O.G.; Pobedimskaya, E.A.; Belov, N.V.: The crystal structure of $K_3NdSi_6O_{15}$. Sov. Phys. Dokl. **22** (1977) 292-293.

[28] Shumyatskaya, N.G.; Voronkov, A.A.; Pyatenko, Y.A.: Sazhinite, $Na_2Ce[Si_6O_{14}(OH)]\cdot nH_2O$: a new representative of the dalyite family in crystal chemistry. Sov. Phys. Crystallogr. **25** (1980) 419-423.

[29] Schweinsberg, H.; Liebau, F.: Darstellung und kristallographische Daten von $K_2Si_2O_5$, $KHSi_2O_5$-I und $K_2Si_4O_9$. Z. anorg. allg. Chem. **387** (1972) 241-251.

12. Room - and high - temperature single crystal diffraction studies on γ - $Na_2Si_2O_5$: an interrupted framework with exclusively Q^3-units.

V. Kahlenberg[1,2], S. Rakic[2] and C. Weidenthaler[3]

[1]Institut für Mineralogie und Petrographie, Leopold-Franzens-Universität Innsbruck, Innrain 52, A - 6020 Innsbruck, Austria

[2]Fachbereich Geowissenschaften (Kristallographie), Universität Bremen, Klagenfurter Str., D - 28359 Bremen, Germany

[3]Max-Planck-Institut für Kohlenforschung, Kaiser-Wilhelm-Platz 1, D - 45470 Mülheim an der Ruhr, Germany

Abstract

Single crystals of γ-$Na_2Si_2O_5$ have been obtained from the crystallization of a stoichiometric glass at 520°C. The monoclinic crystals belong to space group *C2/c* (a = 33.326(2)Å, b = 14.1457(7)Å, c = 26.206(2)Å, β = 108.60(2)°, V = 11709.0(1.5)Å^3, Z = 96, D_{calc} =2.48 gcm^{-3}). The diffraction pattern showed the typical features of a superstructure. The structure was solved by direct methods including the pseudo-translational effects as a prior information for the normalization process and subsequently refined to a residual of RI = 0.058. The compound can be classified as an interrupted tetrahedral framework with exclusively Q^3-units. Basic building units are spiral *achter* single chains running parallel [010]. Every four of these chains are linked via common corners, surrounding a central tunnel where the sodium atoms are located for charge compensation. The framework density has a value of 16.4 T-atoms/1000Å^3. At 563°C the monoclinic phase undergoes a structural phase transition into a tetragonal high temperature modification (space group $I4_1/a$, a = 11.869(2)Å, c = 7.176(2)Å, V = 1011.0(6)Å^3, Z = 4). The transition is induced by cooperative rotations of the tetrahedra and involves a bisection of the translation period along the spiral chains. The symmetries of both modifications are in a close relationship: the space group of the *RT*-phase is a subgroup of index 24 of the space group of the *HT*-phase. Focussing on the connectivity of the tetrahedra the two phases are identical. Topologically they can be described as three dimensional 3-connected nets of a type which has been already observed in the intermetallic compounds LiGe and LiSi, as well as in the mineral grumantite.

Introduction

Since the early investigations of Kracek [1] the system Na_2O - SiO_2 has been the subject of many studies focussing on the phase relationships between sodium silicates [2-5]. Especially the disodium disilicates, $Na_2Si_2O_5$, have attracted considerable attention because these phases can occur during the devitrification of the technical important soda-lime glasses [6]. Furthermore, they are used as ion exchangers in washing powders in combination with or as an alternative to zeolitic materials [7,8] and have been investigated as possible Na ionic conductors [9]. In the field of earth science, glasses and melts of disodium disilicate composition have been frequently studied as comparatively simple model systems to understand the processes in igneous melts [10-11]. According to the investigations mentioned above at least nine different modifications of $Na_2Si_2O_5$ have to be distinguished. A more detailed comparison of the polymorphic forms can be found in [12] and the references cited therein.

Apart from the phases discussed in the present paper all disodium disilicates studied so far belong to the group of single layer silicates. Although the complex polymorphism of the disilicates has been known for more than fifty years, detailed crystallographic characterizations for several of the $Na_2Si_2O_5$ phases have been performed only recently [12,13]. The reason that these phases have not been studied earlier can be attributed to the low quality of the crystals hindering a structure determination by diffraction techniques. Especially twinning by pseudo-merohedry and/or diffuse scattering phenomena due to stacking faults of the tetrahedral single layers are frequently encountered.

One of the last unsolved structural problem within the group of the known disodiumdisilicates was the crystal structure of γ-$Na_2Si_2O_5$, a metastable modification which can be obtained from the crystallization of glasses in the range between 500°C - 580°C [2]. Several authors have tried to synthesize this compound in a pure form [2,3]. However, the simultaneous formation of other disodium disilicates or SiO_2 phases seems to be unavoidable. Hitherto, only one more detailed crystallographic investigation based on precession films has been performed for γ-$Na_2Si_2O_5$ by Hoffmann and Scheel [14]. According to their results the diffraction pattern of the γ-phase can be subdivided into (a) main reflections belonging to a monoclinic *P*-cell (a = 23.46 Å, b = 7.08 Å, c = 26.12 Å, β = 116.7°) and (b) additional satellite reflections parallel to [010] with incommensurate components with respect to b^*. Unfortunately, no structure determination even on the average structure has been performed.

Further complications arise from thermal analyses (DTA) showing three reversible thermal effects occurring at 555°C, 574°C and 595°C [2]. Willgallis and Range [2] attributed these effects to structural phase transitions and distinguished four sub-phases γ_{IV} - γ_I. The interpretation of the heat effects as polymorphic transformations has been challenged by Williamson and Glasser [3], who did not observe any significant differences between high-temperature diffraction patterns collected in stability regions of the postulated γ-polymorphs. However, both groups agree that at temperatures above about 670°C γ- $Na_2Si_2O_5$ is irreversibly converted to the β-phase of disodium disilicate.

The aim of the present study was (a) to synthesize single crystals suited for structural investigations, (b) to re-examine and discuss the crystal structure of the γ-phase at room conditions, (c) to compare the structure of γ- $Na_2Si_2O_5$ with the other modifications and (d) to investigate the existence of possible phase transitions at elevated temperatures.

Experimental details

First synthesis experiments to obtain single crystals were based on the approach already proposed by Hoffmann and Scheel [14]. Starting materials were (a) powdered glasses prepared from melting and quenching of a stoichiometric mixture of sodium carbonate (Fluka, 99%) and fine grained quartz powder and (b) dried water glass solution with disilicate composition. Both materials were fused on to sintered oxide plates of TiO_2, SnO_2, SiO_2 and GeO_2. Subsequently the glazed ceramic plates were devitrified for 24h in the range between 550°C and 650°C as described by Hoffmann and Scheel. Crystal growth was observed to start at the glass - ceramic interface. In contrast to the results reported by Hoffmann and Scheel we could not reproduce the formation of any single crystalline material of the γ-phase. Apart from traces of polycrystalline material of γ- $Na_2Si_2O_5$ the yield contained larger amounts of the α-phase as well as several single crystals of the oxidic substrate. Alternatively, we tried to obtain γ- $Na_2Si_2O_5$ directly from the crystallization of a disodium disilicate glass at a relatively low temperature of 520°C. In contrast to previous investigations [2] a comparatively long time of devitrification (10 days) was used in order to obtain single crystals with dimensions suitable for a single crystal diffraction experiment. The reaction product contained a significant amount of glass as well as two crystalline phases which could be easily distinguished under the polarizing microscope: numerous platy crystals of α- $Na_2Si_2O_5$ and some rare xenomorphic, optically biaxial crystals of a second compound.

Differential scanning calorimetry (DSC) studies of the material obtained from the crystallization experiments was performed on a Netzsch STA 449c. A powdered sample was placed into an alumina crucible and heated in air at a rate of 10°C/min from R.T. up to 620°C. After reaching 620°C the sample was cooled down to 400°C at a rate of 10°C/min.

A single crystal of the unknown crystalline phase with dimensions of 0.20 x 0.15 x 0.05 mm^3 was mounted in a glass capillary. Diffraction data were recorded on a Stoe imaging plate detector system (IPDS). Data collections at elevated temperatures were accomplished by means of a heating device based on the principle of immersing the crystal in a hot nitrogen stream, as proposed by Tuinstra and Storm [15]. A detailed description of the furnace can be found in [16]. An initial temperature calibration was performed using a chromel-alumel thermocouple placed at the position of the sample. The gas flow was regulated through a flow valve at a rate of 50 l/h.

Parameters of the data collection at room temperature and of the subsequent structure refinement are summarized in Table 1.

Table 1. Data collection and refinement parameters of the *RT*-phase.

(A)	Crystal data	
	a (Å)	33.326(2)
	b (Å)	14.1457(7)
	c (Å)	26.206(2)
	β (°)	108.60(2)
	V ($Å^3$)	11709.0(1.5)
	Space group	*C*12/*c*1
	Z	96
	Chemical formula	$Na_2Si_2O_5$
	D_{calc} (g cm^{-3})	2.48
	μ (mm^{-1})	0.83
(B)	Intensity measurements	
	Crystal shape	
	Diffractometer	Stoe - IPDS
	Monochromator	Graphite
	Radiation	MoKα, λ = 0.71073 Å
	X-ray power	50 kV, 40 mA
	Detector to sample distance	80 mm

	Rotation width in ϕ (°)	1.0
	No. of exposures	360
	Irridation time / exposure (min.)	3.00
	θ - range (°)	1.45° - 24.2°
	Reflection range	$\lvert h \rvert \leq 38$; $\lvert k \rvert \leq 16$; $\lvert l \rvert \leq 29$
	No. of measured reflections	67286
	No. of unique reflections in 2/m	9122
	R_{int} in 2/m	0.0627
	No. of observed reflections ($I > 2\,\sigma(I)$)	6191
(C)	Refinement of the structure	
	No. of parameters used in the refinement	
	R1 ($F_o > 4\,\sigma(F_o)$) ; R1 (all data)	0.058 ; 0.0936
	wR2 ($F_o > 4\,\sigma(F_o)$)	0.1140
	Weighting parameter a	0.08
	Goodness of Fit	0.975
	Final $\Delta\rho_{min}$ (e / Å^3)	-0.44
	Final $\Delta\rho_{max}$ (e / Å^3)	0.72
	$R1 = \Sigma \lVert F_o \rvert - \lvert F_c \rVert / \Sigma \lvert F_o \rvert$	$wR2 = (\Sigma(w(F_o^2 - F_c^2)^2) / \Sigma(w(F_o^2)^2))^{1/2}$
	$w = 1 / (\sigma^2 (F_o^2) + (aP)^2)$	$P = (2F_c^2 + \max(F_o^2, 0)) / 3$

Indexing resulted in an unusually large unit cell with a volume of about 11709 Å^3 (a = 33.326(2) Å, b = 14.1457(7) Å, c = 26.206(2) Å, β = 108.60(2)°). The analysis of the systematic absences implicated the diffraction symbol *2/mC-c-*. An inspection of the diffraction pattern revealed an unequal distribution of intensities among different classes of reflections, a characteristic feature of superstructures. Actually, the strong reflections correspond to a monoclinic, pseudo-tetragonal subcell with a' = 11.752, b' = 11.739, c' = 7.073 and γ' = 90.36°. The relationship between the real unit cell and the subcell can be formulated with the following matrix equation:

$$(\mathbf{a'}\ \ \mathbf{b'}\ \ \mathbf{c'}) = (\mathbf{a}\ \ \mathbf{b}\ \ \mathbf{c}) \times \begin{pmatrix} -1/6 & 1/3 & 0 \\ 0 & 0 & 1/2 \\ 1/3 & 1/3 & 0 \end{pmatrix}$$

Due to the low linear absorption coefficient of $\mu = 8.3$ cm^{-1} for MoK$_\alpha$- radiation no absorption correction has been applied. Data reduction included Lorentz and polarization corrections.

The structure was solved by direct methods using the program SIR97 [17]. Evaluation of the intensity statistics ($|E^2-1|$) did not clearly indicate the presence or absence of a center of symmetry. Both possible monoclinic space groups, *C*2/*c* and *Cc*, were tested. However, only in the noncentrosymmetric case a phase set could be found, the most intense peaks of which could be interpreted as the atomic positions of a partial model containing the silicon, sodium and some of the oxygen atoms. The structure was completed by difference Fourier calculations (program SHELX97, [18]). An inspection of the atomic coordinates obtained using the MISSYM subroutine of the program PLATON [19] revealed, that after applying an origin shift, pairs of atoms of the same kind can be found which fulfill the symmetry requirements of *C*2/*c* within a maximum deviation of about four estimated standard deviations. Therefore, the coordinates were transformed and the structure refinement was performed in space group *C*2/*c*. Neutral-atom scattering factors and anomalous dispersion corrections were taken from the International Tables for X-ray Crystallography [20]. The calculations using isotropic temperature factors converged to *R1* = 0.081 for 433 parameters and 6191 independent reflections with $I > 2\sigma(I)$. The introduction of anisotropic displacement parameters improved the residual index significantly (*R1* = 0.044). However, to model the anisotropic thermal motion of each atom the total number of parameters increased to 973 and the over-determination is reduced to 6191/973 ~ 6, if the reflections with $I > 2\sigma(I)$ are considered. Although all 108 independent atoms had positive definite temperature factors, the ratio of parameters to observed reflections is too low to obtain reliable results. Therefore, in the final calculations an anisotropic model was used for the silicon and sodium atoms only, whereas the oxygen atoms were refined isotropically. The final electron density map was featureless. The largest shift in the final cycle was < 0.001. The resulting fractional atomic coordinates, equivalent isotropic and anisotropic displacement parameters, as well as selected interatomic distances (up to 3.1 Å) and angles are given in Tables 2 - 4. Drawings of structural details were prepared using the program ATOMS [21].

Table 2. Fractional atomic coordinates and equivalent isotropic displacement parameters for the *RT*-phase. *U(eq)* is defined as one third of the trace of the orthogonalized U_{ij} tensor. The oxygen atoms have been refined only isotropically. All atoms occupy general positions.

Atom	*x*	*y*	*z*	*U(eq) / U(iso)*
Si1	0.24777(4)	0.56048(9)	0.05128(5)	0.0170(4)
Si2	0.23917(4)	0.04692(9)	0.04124(5)	0.0166(4)
Si3	0.07150(4)	0.53556(9)	0.37853(5)	0.0162(4)
Si4	0.24780(4)	0.43140(9)	0.14632(5)	0.0185(4)
Si5	0.17091(4)	0.70864(9)	0.23336(5)	0.0170(4)
Si6	0.16914(4)	0.18442(9)	0.02201(5)	0.0174(4)
Si7	0.16435(4)	0.22737(9)	0.22905(5)	0.0180(4)
Si8	0.07911(4)	0.47278(9)	0.27006(5)	0.0170(4)
Si9	0.24469(4)	0.91043(9)	0.12706(5)	0.0197(4)
Si10	0.00738(4)	0.69156(10)	0.36196(6)	0.0225(4)
Si11	0.17984(4)	0.76733(9)	0.12627(5)	0.0164(4)
Si12	0.16169(4)	0.65965(9)	0.02286(5)	0.0163(4)
Si13	0.07436(4)	-0.02108(9)	-0.12902(5)	0.0175(4)
Si14	0.08888(4)	0.07746(9)	-0.02328(5)	0.0161(4)
Si15	0.08338(4)	0.61034(9)	0.18289(5)	0.0182(4)
Si16	0.00459(4)	0.18019(9)	-0.04400(5)	0.0193(4)
Si17	0.01227(4)	0.70959(9)	-0.04857(5)	0.0202(4)
Si18	0.09018(4)	0.10609(9)	0.18195(5)	0.0177(4)
Si19	0.07775(4)	0.56405(9)	-0.02043(5)	0.0172(4)
Si20	0.15842(4)	0.36175(9)	0.31528(5)	0.0179(4)
Si21	0.00494(4)	-0.15504(9)	-0.13644(6)	0.0244(4)
Si22	0.17291(4)	0.29030(9)	0.12221(5)	0.0187(4)
Si23	0.08644(4)	0.03457(9)	-0.23576(5)	0.0186(4)
Si24	0.33690(4)	0.35073(9)	0.18699(5)	0.0174(4)
Na1	0.15292(6)	0.00276(13)	0.10117(7)	0.0257(6)
Na2	0.02182(6)	0.51892(14)	0.06640(8)	0.0298(6)
Na3	0.31350(6)	0.48568(15)	0.27335(8)	0.0326(7)

Na4	0.05263(7)	0.02161(15)	0.06776(8)	0.0371(7)
Na5	0.25072(6)	0.13201(14)	0.31891(9)	0.0333(7)
Na6	0.09274(6)	0.83013(14)	0.02644(8)	0.0287(6)
Na7	0.20937(7)	0.47767(14)	0.25668(8)	0.0343(7)
Na8	0.33940(6)	0.11134(14)	0.15610(8)	0.0270(6)
Na9	0.15811(6)	0.11820(14)	0.34238(8)	0.0275(6)
Na10	0.08488(6)	0.36469(14)	0.15765(7)	0.0265(6)
Na11	0.13473(8)	0.51063(15)	0.09958(9)	0.0408(8)
Na12	0.05292(8)	0.22990(15)	0.26089(10)	0.0475(9)
Na13	0.24329(6)	0.14076(13)	0.15869(8)	0.0270(6)
Na14	0.07455(7)	0.33259(15)	0.02753(10)	0.0431(8)
Na15	0.19990(7)	0.27736(15)	0.43489(9)	0.0403(8)
Na16	0.00464(6)	0.38259(14)	0.33139(8)	0.0319(7)
Na17	0.09830(6)	0.25918(13)	0.39748(7)	0.0268(6)
Na18	0.39546(7)	0.26494(14)	0.10464(8)	0.0355(7)
Na19	0.15839(6)	0.09011(14)	0.47332(8)	0.0296(6)
Na20	0.32768(6)	0.08791(15)	0.02942(9)	0.0391(7)
Na21	0.00326(6)	0.89549(15)	0.32468(10)	0.0409(7)
Na22	0.09217(6)	0.85097(14)	0.15377(7)	0.0287(6)
Na23	0.05973(8)	0.73985(15)	0.26285(9)	0.0451(8)
Na24	0.27082(8)	0.27988(15)	0.06204(9)	0.0466(8)
O1	0.05842(10)	0.3867(2)	0.23307(13)	0.0237(10)
O2	0.11777(10)	0.1749(2)	-0.00724(13)	0.0258(11)
O3	-0.03998(10)	0.1344(3)	-0.06831(14)	0.0321(11)
O4	0.04230(10)	0.1020(2)	-0.01834(13)	0.0272(11)
O5	0.18940(10)	0.0798(2)	0.01840(14)	0.0292(11)
O6	0.10745(10)	-0.0111(2)	0.01325(12)	0.0234(10)
O7	0.11239(10)	0.5974(2)	0.39688(13)	0.0267(11)
O8	0.16520(11)	0.3310(2)	0.25800(13)	0.0260(11)
O9	0.06494(10)	0.0304(2)	-0.18793(13)	0.0253(11)
O10	0.17484(10)	0.1962(2)	0.08616(12)	0.0243(10)
O11	0.23704(12)	0.5201(3)	0.10379(13)	0.0342(11)
O12	0.14484(10)	0.7471(2)	-0.01466(13)	0.0264(11)

O13	0.21362(12)	0.3504(3)	0.11953(15)	0.0500(16)
O14	0.12053(10)	0.6901(2)	0.20168(13)	0.0266(11)
O15	0.14415(10)	0.8425(2)	0.11324(13)	0.0257(11)
O16	0.22637(10)	0.8030(2)	0.12396(13)	0.0238(10)
O17	0.07554(10)	0.5752(2)	0.23898(12)	0.0232(10)
O18	0.11350(9)	0.2090(2)	0.19672(12)	0.0212(10)
O19	0.12934(10)	0.5674(2)	0.01042(13)	0.0239(10)
O20	0.19344(10)	0.6305(2)	0.27566(12)	0.0229(11)
O21	0.05855(10)	0.6675(2)	-0.01152(13)	0.0250(11)
O22	0.08513(10)	0.0680(2)	-0.08689(12)	0.0229(10)
O23	0.20598(10)	0.6219(3)	0.01587(13)	0.0287(11)
O24	0.02767(10)	0.5879(2)	0.38004(13)	0.0265(11)
O25	0.05773(10)	0.4915(2)	0.31752(12)	0.0245(11)
O26	0.05622(11)	0.4818(2)	0.00144(13)	0.0288(11)
O27	0.19312(10)	0.7185(2)	0.18637(12)	0.0230(10)
O28	0.13041(10)	0.4592(2)	0.30123(12)	0.0222(10)
O29	0.26987(10)	0.1158(2)	0.08248(12)	0.0229(10)
O30	0.01161(14)	-0.2199(3)	-0.1810(2)	0.0526(16)
O31	0.18725(10)	0.2455(2)	0.18335(12)	0.0258(11)
O32	0.23494(11)	-0.0594(2)	0.06350(13)	0.0273(11)
O33	0.08878(13)	0.5302(2)	0.14507(14)	0.0370(14)
O34	0.07268(9)	0.5605(2)	-0.08525(12)	0.0190(10)
O35	0.29166(10)	0.3823(3)	0.14320(13)	0.0311(11)
O36	0.02570(10)	-0.0492(2)	-0.13249(13)	0.0235(10)
O37	0.17301(10)	0.8159(2)	0.25843(12)	0.0230(11)
O38	0.02293(16)	0.7427(3)	0.3191(2)	0.071(2)
O39	0.18984(12)	0.2629(3)	-0.00362(14)	0.0355(12)
O40	0.06511(10)	0.1143(2)	-0.27732(13)	0.0230(10)
O41	0.08196(10)	-0.0726(2)	-0.26180(12)	0.0232(11)
O42	0.01013(13)	0.2519(3)	0.00583(18)	0.0588(16)
O43	0.04303(10)	0.6799(3)	0.15386(15)	0.0380(11)
O44	0.14149(13)	0.2839(3)	0.34527(16)	0.0429(14)
O45	-0.01771(10)	0.6392(2)	-0.08889(14)	0.0293(11)

O46	0.16886(10)	0.6745(2)	0.08692(12)	0.0229(10)
O47	0.20417(11)	0.4020(3)	0.35112(17)	0.0498(16)
O48	0.11333(11)	0.0311(2)	0.15704(13)	0.0275(11)
O49	0.24647(10)	0.4677(2)	0.01283(12)	0.0236(10)
O50	0.04392(10)	0.1333(3)	0.13911(13)	0.0275(11)
O51	0.02145(12)	0.2416(3)	-0.0848(2)	0.0671(16)
O52	0.28946(11)	0.6202(3)	0.06697(14)	0.0322(11)
O53	0.18478(10)	0.1445(2)	0.26832(13)	0.0252(11)
O54	0.24867(11)	0.4713(2)	0.20225(13)	0.0267(11)
O55	0.10764(10)	-0.1015(2)	-0.11560(13)	0.0267(11)
O56	0.22577(11)	0.9816(2)	0.15952(13)	0.0285(11)
O57	0.13789(10)	0.0487(2)	-0.20550(13)	0.0229(10)
O58	0.36050(12)	0.2745(2)	0.16372(14)	0.0320(11)
O59	0.13051(11)	0.3468(3)	0.10405(14)	0.0333(12)
O60	0.02729(12)	0.8002(3)	-0.07615(19)	0.0598(16)

Table 3. Anisotropic displacement parameters (Å^2) for the silicon and sodium atoms of the *RT*-phase. The anisotropic displacement factor exponent takes the form: $-2\pi^2 [h^2 a^{*2} U_{11} + ... + 2 h k a^* b^* U_{12}]$

Atom	U_{11}	U_{22}	U_{33}	U_{23}	U_{13}	U_{12}
Si1	0.0167(7)	0.0214(7)	0.0135(6)	-0.0005(5)	0.0055(5)	0.0021(6)
Si2	0.0183(7)	0.0174(7)	0.0159(6)	-0.0013(5)	0.0082(5)	-0.0011(6)
Si3	0.0175(7)	0.0173(7)	0.0157(6)	0.0020(5)	0.0079(5)	0.0007(5)
Si4	0.0180(7)	0.0228(7)	0.0148(6)	0.0015(6)	0.0055(5)	-0.0021(6)
Si5	0.0172(7)	0.0199(7)	0.0154(6)	0.0004(6)	0.0075(5)	-0.0007(6)
Si6	0.0190(7)	0.0196(7)	0.0136(6)	-0.0024(5)	0.0052(5)	-0.0016(6)
Si7	0.0182(7)	0.0188(7)	0.0177(7)	0.0006(6)	0.0068(5)	0.0004(6)
Si8	0.0188(7)	0.0174(7)	0.0163(6)	-0.0010(5)	0.0077(5)	-0.0007(6)
Si9	0.0176(7)	0.0207(7)	0.0204(7)	0.0036(6)	0.0053(6)	-0.0036(6)
Si10	0.0197(7)	0.0211(7)	0.0289(7)	-0.0013(6)	0.0108(6)	0.0026(6)
Si11	0.0168(6)	0.0179(7)	0.0165(7)	-0.0010(5)	0.0083(5)	-0.0019(5)
Si12	0.0160(6)	0.0185(7)	0.0140(6)	-0.0017(5)	0.0041(5)	0.0006(5)
Si13	0.0183(7)	0.0180(7)	0.0184(7)	-0.0016(6)	0.0089(6)	-0.0004(6)

Si14	0.0153(6)	0.0174(7)	0.0149(6)	-0.0015(5)	0.0040(5)	-0.0002(5)
Si15	0.0180(7)	0.0201(7)	0.0165(7)	-0.0015(6)	0.0055(5)	-0.0022(6)
Si16	0.0154(7)	0.0211(7)	0.0213(7)	-0.0013(6)	0.0059(6)	0.0016(6)
Si17	0.0188(7)	0.0183(7)	0.0227(7)	-0.0005(6)	0.0055(6)	0.0016(6)
Si18	0.0174(7)	0.0183(7)	0.0173(7)	-0.0015(5)	0.0054(5)	-0.0001(5)
Si19	0.0186(7)	0.0188(7)	0.0133(6)	-0.0017(5)	0.0037(5)	0.0006(6)
Si20	0.0187(7)	0.0189(7)	0.0162(7)	0.0006(6)	0.0058(5)	0.0001(6)
Si21	0.0166(7)	0.0178(7)	0.0376(8)	0.0064(6)	0.0071(6)	-0.0006(6)
Si22	0.0176(7)	0.0227(7)	0.0171(7)	-0.0028(6)	0.0073(5)	-0.0020(6)
Si23	0.0202(7)	0.0179(7)	0.0192(7)	0.0005(6)	0.0086(6)	0.0002(6)
Si24	0.0201(7)	0.0169(7)	0.0159(7)	0.0006(5)	0.0066(5)	0.0021(6)
Na1	0.0262(10)	0.0284(11)	0.0214(10)	0.0012(9)	0.0061(8)	0.0015(9)
Na2	0.0353(11)	0.0287(11)	0.0288(11)	-0.0019(9)	0.0148(9)	-0.0026(9)
Na3	0.0335(11)	0.0362(12)	0.0285(11)	-0.0044(9)	0.0106(9)	0.0019(10)
Na4	0.0522(14)	0.0297(12)	0.0296(11)	0.0023(9)	0.0134(10)	-0.0063(10)
Na5	0.0227(10)	0.0299(12)	0.0450(13)	0.0061(10)	0.0075(9)	-0.0020(9)
Na6	0.0261(11)	0.0300(11)	0.0312(11)	-0.0032(9)	0.0110(9)	-0.0024(9)
Na7	0.0470(13)	0.0296(12)	0.0350(12)	0.0008(9)	0.0253(10)	-0.0031(10)
Na8	0.0293(11)	0.0271(11)	0.0281(11)	-0.0014(9)	0.0142(9)	0.0020(9)
Na9	0.0285(11)	0.0290(11)	0.0295(11)	0.0018(9)	0.0156(9)	0.0001(9)
Na10	0.0285(11)	0.0260(11)	0.0277(11)	0.0011(9)	0.0128(9)	0.0033(9)
Na11	0.0613(15)	0.0344(12)	0.0382(12)	0.0093(10)	0.0319(12)	0.0059(11)
Na12	0.0710(17)	0.0279(12)	0.0608(15)	0.0046(11)	0.0452(14)	0.0081(12)
Na13	0.0242(10)	0.0262(11)	0.0278(11)	-0.0014(9)	0.0044(8)	0.0018(9)
Na14	0.0302(12)	0.0328(13)	0.0576(15)	0.0062(11)	0.0016(11)	-0.0054(10)
Na15	0.0582(15)	0.0307(12)	0.0346(12)	0.0014(10)	0.0185(11)	0.0062(11)
Na16	0.0251(11)	0.0279(11)	0.0401(12)	0.0073(9)	0.0067(9)	-0.0019(9)
Na17	0.0316(11)	0.0263(11)	0.0237(10)	-0.0013(9)	0.0104(9)	0.0016(9)
Na18	0.0520(13)	0.0246(11)	0.0421(13)	0.0086(10)	0.0320(11)	0.0069(10)
Na19	0.0271(11)	0.0316(11)	0.0335(11)	0.0038(9)	0.0146(9)	0.0012(9)
Na20	0.0286(11)	0.0377(13)	0.0438(13)	0.0051(11)	0.0015(10)	-0.0067(10)
Na21	0.0274(11)	0.0243(11)	0.0631(15)	0.0010(11)	0.0032(11)	-0.0028(9)
Na22	0.0257(11)	0.0392(12)	0.0241(10)	0.0014(9)	0.0120(9)	0.0062(9)

Na23	0.0802(17)	0.0245(11)	0.0441(13)	0.0024(10)	0.0388(13)	0.0082(12)
Na24	0.0834(18)	0.0299(12)	0.0393(13)	-0.0095(10)	0.0377(13)	-0.0144(12)

Table 4. Selected bond distances (Å) up to 3.1 Å and angles (deg.) for the RT - phase.

Si1	-O11	1.631(4)	Si2	-O5	1.641(4)
	-O23	1.653(4)		-O29	1.568(3)
	-O49	1.647(3)		-O32	1.635(3)
	-O52	1.565(4)		-O49	1.647(3)
Si3	-O7	1.561(4)	Si4	-O11	1.640(4)
	-O24	1.649(4)		-O13	1.610(4)
	-O25	1.639(3)		-O35	1.644(4)
	-O34	1.651(3)		-O54	1.562(4)
Si5	-O14	1.639(4)	Si6	-O2	1.643(4)
	-O20	1.576(3)		-O5	1.642(3)
	-O27	1.633(4)		-O10	1.639(3)
	-O37	1.646(3)		-O39	1.567(4)
Si7	-O8	1.647(3)	Si8	-O1	1.572(3)
	-O18	1.656(3)		-O17	1.648(3)
	-O31	1.633(4)		-O25	1.640(4)
	-O53	1.565(3)		-O28	1.654(4
Si9	-O16	1.630(3)	Si10	-O24	1.621(3)
	-O56	1.574(4)		-O38	1.557(5)
	-O32	1.649(3)		-O43	1.605(4)
	-O47	1.620(4)		-O51	1.626(5)
Si11	-O15	1.550(3)	Si12	-O12	1.569(3)
	-O16	1.650(4)		-O19	1.658(3)
	-O27	1.646(3)		-O23	1.634(4)
	-O46	1.637(3)		-O46	1.632(3)
Si13	-O9	1.644(3)	Si14	-O2	1.657(3)
	-O22	1.638(3)		-O4	1.636(4)
	-O36	1.644(4)		-O6	1.578(3)
	-O55	1.549(3)		-O22	1.637(3)

Si15	-O14	1.631(3)	Si16	-O3	1.558(4)
	-O17	1.650(3)		-O4	1.648(3)
	-O33	1.554(4)		-O42	1.617(5)
	-O43	1.644(4)		-O51	1.611(5)
Si17	-O21	1.649(4)	Si18	-O18	1.637(3)
	-O45	1.560(4)		-O48	1.571(4)
	-O60	1.627(5)		-O50	1.637(4)
	-O42	1.626(5)		-O41	1.652(3)
Si19	-O19	1.651(4)	Si20	-O8	1.646(4)
	-O21	1.643(3)		-O28	1.640(3)
	-O26	1.568(4)		-O44	1.559(5)
	-O34	1.653(3)		-O47	1.618(4)
Si21	-O30	1.556(5)	Si22	-O10	1.645(3)
	-O36	1.639(3)		-O13	1.621(4)
	-O60	1.644(5)		-O31	1.646(3)
	-O50	1.637(4)		-O59	1.560(4)
Si23	-O9	1.631(4)	Si24	-O35	1.639(4)
	-O40	1.572(3)		-O58	1.568(4)
	-O41	1.650(3)		-O37	1.643(3)
	-O57	1.656(4)		-O57	1.645(3)
Na1	-O48	2.297(4)	Na2	-O45	2.328(4)
	-O15	2.321(4)		-O26	2.394(4)
	-O6	2.327(4)		-O33	2.514(5)
	-O56	2.440(4)		-O26	2.641(4)
	-O10	2.891(4)		-O24	2.668(4)
	-O5	3.009(4)			
Na3	-O54	2.369(4)	Na4	-O3	2.248(4)
	-O56	2.506(4)		-O4	2.451(4)
	-O53	2.506(4)		-O50	2.534(4)
	-O48	2.617(4)		-O48	2.562(4)
	-O37	2.627(4)		-O6	2.694(4)
	-O57	2.804(4)			

Na5	-O53	2.182(4)	Na6	-O6	2.348(4)
	-O27	2.277(4)		-O15	2.378(4)
	-O54	2.341(4)		-O3	2.404(4)
	-O11	2.500(4)		-O12	2.598(4)
	-O16	2.819(4)		-O21	2.618(4)
				-O60	2.902(5)
Na7	-O54	2.225(4)	Na8	-O20	2.391(4)
	-O20	2.318(4)		-O58	2.403(4)
	-O56	2.544(4)		-O7	2.444(4)
	-O8	2.551(4)		-O28	2.485(4)
	-O47	2.752(5)		-O29	2.499(4)
Na9	-O55	2.297(4)	Na10	-O33	2.373(4)
	-O53	2.407(4)		-O45	2.385(4)
	-O44	2.415(4)		-O59	2.390(4)
	-O52	2.460(4)		-O1	2.428(4)
	-O57	2.658(4)		-O18	2.487(4)
Na11	-O33	2.237(4)	Na12	-O30	2.361(5)
	-O59	2.328(4)		-O1	2.361(4)
	-O19	2.423(4)		-O30	2.481(6)
	-O46	2.649(4)		-O41	2.571(4)
	-O26	3.055(4)		-O18	3.026(3)
Na13	-O20	2.261(4)	Na14	-O26	2.243(4)
	-O56	2.328(4)		-O59	2.270(4)
	-O29	2.455(4)		-O42	2.336(5)
	-O10	2.581(4)		-O45	2.877(4)
	-O31	2.621(4)		-O2	2.953(4)
Na15	-O52	2.255(4)	Na16	-O1	2.238(4)
	-O23	2.510(4)		-O30	2.346(4)
	-O44	2.529(5)		-O45	2.451(4)
	-O12	2.604(4)		-O25	2.458(4)
	-O47	2.854(5)		-O34	2.720(4)

Na17	-O55	2.293(4)	Na18	-O58	2.219(4)
	-O44	2.307(4)		-O7	2.383(4)
	-O12	2.332(4)		-O22	2.532(4)
	-O34	2.772(4)		-O2	2.592(4)
	-O60	2.798(5)		-O38	2.833(6)
	-O30	3.016(5)		-O51	2.978(5)
Na19	-O52	2.342(4)	Na20	-O39	2.237(4)
	-O12	2.387(4)		-O7	2.297(4)
	-O55	2.409(4)		-O49	2.491(4)
	-O6	2.522(4)		-O29	2.740(4)
	-O5	2.732(4)		-O19	2.987(4)
	-O32	2.905(4)			
Na21	-O40	2.224(4)	Na22	-O15	2.306(4)
	-O38	2.277(5)		-O40	2.314(4)
	-O9	2.422(4)		-O3	2.366(4)
	-O36	2.452(4)		-O14	2.625(4)
	-O51	2.973(5)		-O48	2.638(4)
	-O52	3.008(3)		-O43	2.922(4)
Na23	-O38	2.197(5)	Na24	-O29	2.384(4)
	-O40	2.349(4)		-O39	2.389(4)
	-O17	2.511(4)		-O35	2.482(4)
	-O58	2.784(5)		-O39	2.709(5)
	-O43	2.859(5)		-O49	2.952(4)
	-O38	2.903(5)		-O13	2.955(5)
	-O14	3.040(3)			

O - Si - O angles

O11	-Si1	-O23	106.6(2)	O8	-Si7	-O18	103.9(2)
O11	-Si1	-O49	105.5(2)	O8	-Si7	-O31	104.8(2)
O11	-Si1	-O52	112.5(2)	O8	-Si7	-O53	115.1(2)
O23	-Si1	-O49	102.9(2)	O18	-Si7	-O31	106.9(2)
O23	-Si1	-O52	112.5(2)	O18	-Si7	-O53	112.2(2)
O49	-Si1	-O52	116.0(2)	O31	-Si7	-O53	113.1(2)

O5	-Si2	-O29	115.8(2)	O1	-Si8	-O17	115.3(2)
O5	-Si2	-O32	101.5(2)	O1	-Si8	-O25	112.4(2)
O5	-Si2	-O49	105.0(2)	O1	-Si8	-O28	113.3(2)
O29	-Si2	-O32	115.9(2)	O17	-Si8	-O25	104.6(2)
O29	-Si2	-O49	111.5(2)	O17	-Si8	-O28	104.3(2)
O32	-Si2	-O49	105.9(2)	O25	-Si8	-O28	106.0(2)
O7	-Si3	-O24	115.7(2)	O16	-Si9	-O56	114.5(2)
O7	-Si3	-O25	117.3(2)	O16	-Si9	-O32	104.0(2)
O7	-Si3	-O34	115.2(2)	O16	-Si9	-O47	106.5(2)
O24	-Si3	-O25	102.7(2)	O32	-Si9	-O56	113.3(2)
O24	-Si3	-O34	102.4(2)	O47	-Si9	-O56	114.5(2)
O25	-Si3	-O34	101.3(2)	O32	-Si9	-O47	102.8(2)
O11	-Si4	-O13	106.1(2)	O24	-Si10	-O38	115.3(2)
O11	-Si4	-O35	107.1(2)	O24	-Si10	-O43	106.7(2)
O11	-Si4	-O54	107.2(2)	O24	-Si10	-O51	107.2(2)
O13	-Si4	-O35	101.2(2)	O38	-Si10	-O43	115.0(3)
O13	-Si4	-O54	117.7(2)	O38	-Si10	-O51	106.1(2)
O35	-Si4	-O54	116.7(2)	O43	-Si10	-O51	105.8(2)
O14	-Si5	-O20	115.2(2)	O15	-Si11	-O16	116.5(2)
O14	-Si5	-O27	105.6(2)	O15	-Si11	-O27	116.9(2)
O14	-Si5	-O37	104.8(2)	O15	-Si11	-O46	114.2(2)
O20	-Si5	-O27	111.2(2)	O16	-Si11	-O27	101.2(2)
O20	-Si5	-O37	114.6(2)	O16	-Si11	-O46	104.2(2)
O27	-Si5	-O37	104.5(2)	O27	-Si11	-O46	101.8(2)
O2	-Si6	-O5	106.6(2)	O12	-Si12	-O19	114.7(2)
O2	-Si6	-O10	104.5(2)	O12	-Si12	-O23	110.1(2)
O2	-Si6	-O39	113.2(2)	O12	-Si12	-O46	116.7(2)
O5	-Si6	-O10	103.6(2)	O19	-Si12	-O23	105.9(2)
O5	-Si6	-O39	111.6(2)	O19	-Si12	-O46	100.2(2)
O10	-Si6	-O39	116.4(2)	O23	-Si12	-O46	108.4(2)

O9	-Si13	-O22	103.1(2)	O19	-Si19	-O21	107.3(2)
O9	-Si13	-O36	99.5(2)	O19	-Si19	-O26	111.6(2)
O9	-Si13	-O55	116.6(2)	O19	-Si19	-O34	104.7(2)
O22	-Si13	-O36	102.9(2)	O21	-Si19	-O26	111.4(2)
O22	-Si13	-O55	115.1(2)	O21	-Si19	-O34	104.8(2)
O36	-Si13	-O55	117.2(2)	O26	-Si19	-O34	116.4(2)
O2	-Si14	-O4	107.0(2)	O8	-Si20	-O28	104.6(2)
O2	-Si14	-O6	115.0(2)	O8	-Si20	-O44	116.7(2)
O2	-Si14	-O22	100.1(2)	O8	-Si20	-O47	104.1(2)
O4	-Si14	-O6	108.6(2)	O28	-Si20	-O44	115.8(2)
O4	-Si14	-O22	109.4(2)	O28	-Si20	-O47	101.4(2)
O6	-Si14	-O22	116.1(2)	O44	-Si20	-O47	112.4(2)
O14	-Si15	-O17	105.1(2)	O30	-Si21	-O36	115.3(2)
O14	-Si15	-O33	117.8(2)	O30	-Si21	-O60	111.4(2)
O14	-Si15	-O43	99.0(2)	O30	-Si21	-O50	117.2(2)
O17	-Si15	-O33	115.6(2)	O36	-Si21	-O60	103.8(2)
O17	-Si15	-O43	104.7(2)	O36	-Si21	-O50	103.0(2)
O33	-Si15	-O43	112.7(2)	O50	-Si21	-O60	104.7(2)
O3	-Si16	-O4	113.0(2)	O10	-Si22	-O13	102.3(2)
O3	-Si16	-O42	116.1(2)	O10	-Si22	-O31	101.3(2)
O3	-Si16	-O51	116.2(2)	O10	-Si22	-O59	115.9(2)
O4	-Si16	-O42	102.5(2)	O13	-Si22	-O31	104.9(2)
O4	-Si16	-O51	104.5(2)	O13	-Si22	-O59	114.0(2)
O42	-Si16	-O51	102.9(2)	O31	-Si22	-O59	116.6(2)
O21	-Si17	-O45	116.4(2)	O9	-Si23	-O40	110.2(2)
O21	-Si17	-O60	100.6(2)	O9	-Si23	-O41	106.3(2)
O21	-Si17	-O42	105.3(2)	O9	-Si23	-O57	106.1(2)
O45	-Si17	-O60	115.0(2)	O40	-Si23	-O41	114.3(2)
O42	-Si17	-O45	110.2(2)	O40	-Si23	-O57	114.6(2)
O42	-Si17	-O60	108.4(2)	O41	-Si23	-O57	104.6(2)

O18	-Si18	-O48	116.1(2)	O35	-Si24	-O58	112.2(2)
O18	-Si18	-O50	103.0(2)	O35	-Si24	-O37	107.2(2)
O18	-Si18	-O41	104.2(2)	O35	-Si24	-O57	103.9(2)
O48	-Si18	-O50	110.7(2)	O37	-Si24	-O58	113.4(2)
O41	-Si18	-O48	114.9(2)	O57	-Si24	-O58	115.9(2)
O41	-Si18	-O50	106.9(2)	O37	-Si24	-O57	103.2(2)

Si - O - Si angles

Si6	-O2	-Si14	128.4(2)	Si5	-O27	-Si11	135.2(2)
Si14	-O4	-Si16	136.9(2)	Si8	-O28	-Si20	129.3(2)
Si2	-O5	-Si6	128.4(2)	Si7	-O31	-Si22	135.7(2)
Si7	-O8	-Si20	131.9(2)	Si2	-O32	-Si9	125.9(2)
Si13	-O9	-Si23	137.6(2)	Si3	-O34	-Si19	126.3(2)
Si6	-O10	-Si22	131.2(2)	Si4	-O35	-Si24	135.6(2)
Si1	-O11	-Si4	141.4(3)	Si13	-O36	-Si21	127.9(2)
Si4	-O13	-Si22	147.1(3)	Si5	-O37	-Si24	129.0(2)
Si5	-O14	-Si15	145.1(2)	Si18	-O41	-Si23	127.9(2)
Si9	-O16	-Si11	128.7(2)	Si16	-O42	-Si17	143.9(3)
Si8	-O17	-Si15	134.3(2)	Si10	-O43	-Si15	144.6(3)
Si7	-O18	-Si18	126.3(2)	Si11	-O46	-Si12	132.9(2)
Si12	-O19	-Si19	129.0(2)	Si9	-O47	-Si20	157.1(3)
Si17	-O21	-Si19	124.8(2)	Si1	-O49	-Si2	131.9(2)
Si13	-O22	-Si14	132.7(2)	Si18	-O50	-Si21	141.2(2)
Si1	-O23	-Si12	137.6(2)	Si10	-O51	-Si16	144.8(3)
Si3	-O24	-Si10	133.6(2)	Si23	-O57	-Si24	126.8(2)
Si3	-O25	-Si8	138.3(2)	Si17	-O60	-Si21	128.4(3)

Results and discussion

Description of the structure at room temperature

The crystal structure of γ-$Na_2Si_2O_5$ at room temperature is shown in Figure 1. Silicate tetrahedra form a three-dimensional framework with the composition $[Si_2O_5]^{2-}$ and a Si:O ratio of 1:2.5. Apart from γ-$Na_2Si_2O_5$, this ratio has been observed only for two other framework silicates, although it is known for many single layer, double chain and a few double ring silicates [22]. Basic building units of the structure are spiral *achter* single chains running parallel [010] (see Figure 2a).

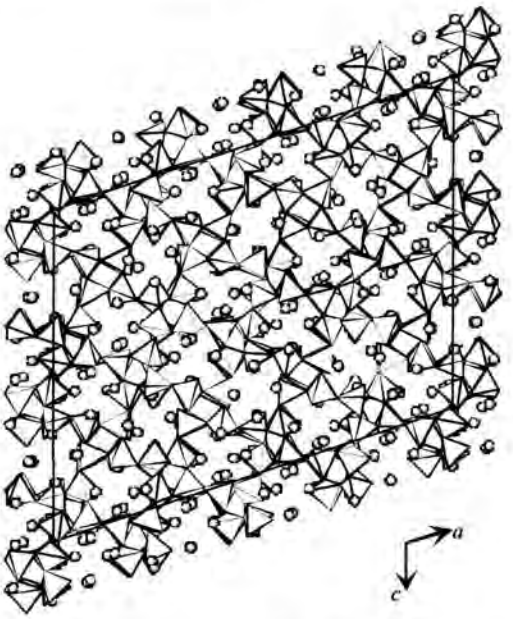

Figure 1. Projection of the whole structure of the RT-phase of γ-$Na_2Si_2O_5$ parallel

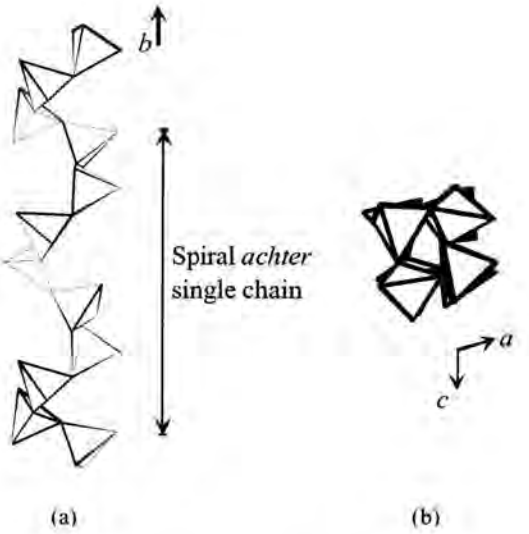

Figure 2. Single tetrahedral *achter* single chain within the framework of the *RT*-phase. (a) side view and (b) projection parallel [010].

Since the space group symmetry implies the existence of 2_1-screw axis running parallel to the chains, two revolutions of the spiral account for the *b* lattice constant. In a projection parallel [010] the chains appear as four-membered rings (Figure 2b). Linkage between neighboring chains is provided by tetrahedra sharing common oxygen atoms.

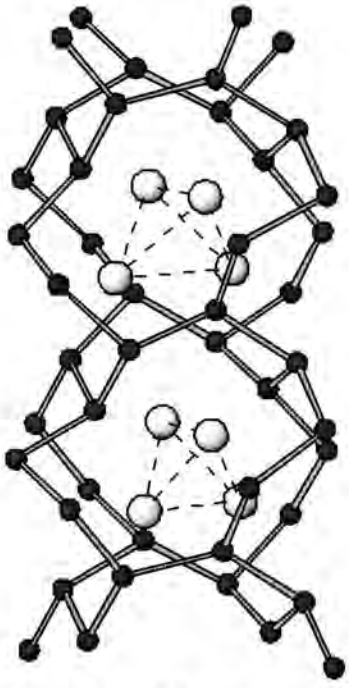

Figure 3. Organization of the silicate framework surrounding a single tunnel. Small and big circles correspond to the Si and Na atoms, respectively. Each of the $[8^2 10^2 10^2]$ composite building units enclose four Na atoms.

Groups of four spirals are connected in such way that they enclose central tunnels (see Figure 3). In a projection parallel [010] the tunnels appear as eight-membered rings. Alternatively, the tunnels can be considered as being built from $[8^2 10^2 10^2]$ composite building units. Each of these units or cavities contains four sodium atoms for charge compensation. They are located at the corners of distorted $[Na_4]$ - tetrahedra (cf. Figure 3).

There are 24 symmetrically independent Si atoms, each of which is tetrahedrally coordinated. All SiO_4-tetrahedra have three bridging (br.) and one non-bridging (nbr.) vertex. This connectivity implies, that the $\gamma(RT)$-phase of disodium disilicate belongs structurally to the rare group of interrupted silicate frameworks. Concerning the individual Si-O bond distances two groups can be distinguished:

The $Si\text{-}O_{nbr.}$ bond lengths are significantly shorter (1.549 - 1.578 Å) than the $Si\text{-}O_{br.}$ bond distances (1.605 - 1.658 Å) . This shortening results from the stronger attraction between O and Si than between O and Na in the structure, and is a typical result for silicates containing Q^3 units. Whereas the average values of the O-Si-O angles for all 24 tetrahedra are very close to the ideal value of 109.47°, the individual O-Si-O angles range from 99° to 117°. This indicates that the tetrahedra deviate considerably from regularity. However, the scatter is similar to the values reported in the literature for other interrupted frameworks. The Si-O-Si angles show a spread between 124.8° and 157.1° with an average of 134.4°. This mean value is about 6° lower than the value 140° corresponding to an unstrained Si-O-Si angle [22].

The calculation of the bond-valence sums (BVS) for the tetrahedral sites using the parameters for the Si-O bond given in [23] differed less than 10% from the expected value of 4.00 valence units (v.u.) for silicon (BVS = 4.16 - 4.37 v.u.).Charge balance in the structure is achieved by an incorporation of sodium ions in the channels of the tetrahedral network running parallel *b*.

Within the channels, the Na ions are irregularly coordinated by five to seven oxygen ligands. Na-O distances cover a wide range, as can be seen in Table 4. However, the values are consistent with Na-O distances reported in the literature.

The framework density [24] of the porous crystal structure of γ-$Na_2Si_2O_5$ at room conditions is 16.4 T-atoms/1000Å^3. This value is comparable with those observed in natural zeolitic materials like cancrinite or edingtonite, for example [25].

High temperature studies

In the DSC run only one broad endothermic effect was observed in the range up to 620°C, with a temperature of 563°C representing the maximum of the reaction. On cooling, an exothermic effect appeared at almost the same temperature (561°C). In order to study this effect in more detail the single crystal used for the structure determination at room conditions was heated to 575°C. The data collection was performed with the same instrumental settings used for the room temperature measurement. It revealed that the thermal effect is related to a structural phase transformation. Only the strong main reflections (already conspicuous at room conditions) remained above the transition: they correspond to a tetragonal body centered unit cell with lattice constants of a = 11.869(2)Å and c = 7.176(2)Å. The weak superstructure reflections disappeared. An analysis of the systematic absences resulted in the space group $I4_1/a$ for the high temperature phase. Unfortunately, the crystal was not stable throughout the whole data collection. In the course of the measurement powder rings with increasing intensity appeared on the images. The evaluation of the powder rings pointed to a gradually transformation of the metastable single crystal of γ(*HT*)-$Na_2Si_2O_5$ to a polycrystalline aggregate of the β-modification of disodium disilicate. Therefore, the structure solution by direct methods and the refinement of the high temperature phase was based on the 3418 reflections collected on the first 70 frames, where no powder rings could be observed. The internal R-value for merging these data in Laue group $4/m$ was 0.095. The refinement using anisotropic displacement parameters converged to $R1$ = 0.071. We are aware of the fact, that the quality of this data set and of the derived structural data (see Table 5) is definitely lower compared with the results obtained at room conditions. However, the principle features of the *HT*-phase and of the transition can be derived without any doubt.

Table 5. Fractional atomic coordinates and isotropic displacement parameters for the *HT*-phase at 575°C. O3 resides on Wyckoff-site 8(*c*); all other atoms occupy general positions.

Atom	*x*	*y*	*z*	*U(iso)*
Si	0.3869(3)	0.0422(3)	0.5798(5)	0.039(2)
Na	0.3665(7)	0.3308(6)	0.7115(9)	0.051(3)
O1	0.3240(11)	-0.0760(10)	0.6358(16)	0.092(9)
O2	0.3706(21)	0.1470(12)	0.7288(16)	0.084(8)
O3	0.5	0.0	0.5	0.1102(11)

Concerning the relationships between the space group symmetries, the *RT*-modification of γ-$Na_2Si_2O_5$ can be considered as a subgroup of index 24 of the *HT*-phase. The transformation is induced by cooperative rotations of the tetrahedra without any breaking of primary bonds. As a consequence of these rotations the symmetry of the basic spiral chains in the *HT*-structure is increased (they are located around the 4_1- screw axis of the tetragonal structure) and the translation period along the chain direction is decreased by a factor two, resulting in *vierer* single chains. Neighboring chains are linked by an oxygen atom (O3) residing on a center of inversion. The high temperature factor of this bridging oxygen atom may point to the existence of a split position, avoiding an energetically unfavorable straight T-O-T angle. However, the introduction of a split atom model did not significantly improve the refinement and therefore, this question can not be settled with certainty. A projection of the whole structure parallel [001] is given in Figure 4a.

Topological aspects

The high- and the room-temperature modification of γ-$Na_2Si_2O_5$ belong to the group of interrupted tetrahedral framework structures. The connectivity of the T-atoms can be characterized by their coordination sequences which are identical for all Si atoms in the asymmetric units of both phases : 3-6-12-22-35-50-69-92-116-142. Furthermore, the vertex symbols [26] of all tetrahedral centers are $8_1 \cdot 8_1 \cdot 10_3$. Since both structures are exclusively build from Q^3 units they can be classified as three-dimensional 3-connected nets. Detailed theoretical studies on these net types have been performed by Wells [27], for example. Actually, the net observed in γ-$Na_2Si_2O_5$ has been already mentioned in his comprehensive listing and is denoted $8^2$10-a. The maximal topological symmetry of this framework type is $I4_1/amd$.

It belongs to the class of the so-called archimedean 3-**connected nets, indicating that at least** two of the shortest rings meeting at each vertex are of different kinds concerning the number of points belonging to the circuits.

It is interesting to note, that the same kind of net has been already observed for a group of compounds with a completely different chemical composition. Within the crystal structures of the so-called five electron compounds LiGe and LiSi, the Ge and Si atoms occupy the corners of the same net type [28]. Furthermore, the same topology of the tetrahedral framework as in γ(*RT*) - and γ(*HT*) - $Na_2Si_2O_5$ can be found in the chemically closely related mineral grumantite ($NaHSi_2O_5 \times H_2O$) [29].

Many of the known interrupted tetrahedral framework structures can be derived from unbroken parent frameworks [27]. For the derivation of the parent framework for the topologically equivalent two γ-phases we focussed on the less complex *HT*-modification. The theoretical parent framework structure was derived from the *HT*-phase by inserting one additional tetrahedral atom at the position (0, 1/4, 5/8), corresponding to the Wyckoff-site 4*b* of space group $I4_1/a$ (see Figure 4b). The resulting three-dimensional 4-connected net is the same that can be found in the diamond structure or in cristobalite (see Figure 4c). Therefore, the tetrahedral nets observed in γ-$Na_2Si_2O_5$ can be considered as a *defect* cristobalite net where 20% of the tetrahedral centers have been removed.

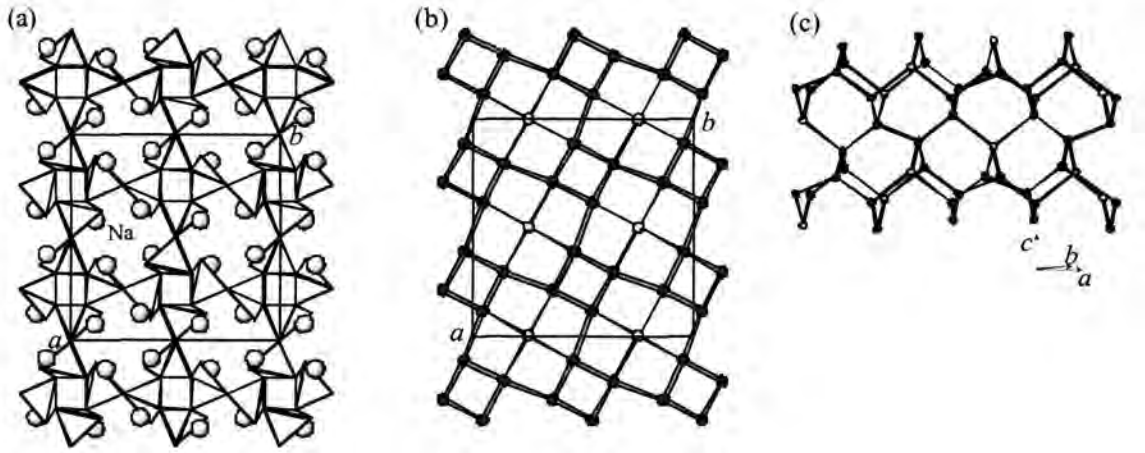

Figure 4. (a) Projection of the *HT*-phase parallel [001]; (b) Topology of the corresponding theoretical parent framework structure. Dark gray circles indicate the Si-atoms. The light gray circles represent the additional T-atoms at (0, 1/4, 5/8) inserted to construct the 4-connected net. The resulting new bonds (thin black lines) have been added as a guide for the eyes; (c) Side view of a 5.4 Å wide slab parallel (2 -1 0) cut from the derived parent fra-mework structure showing the characteristic six-membered rings of the diamond / cristobalite net.

To our best knowledge three-dimensional three connected nets for oxides and fluorides containing tetrahedral building units have been observed only for the mineral grumantite [29], $K_2Si_2O_5$ [30], o - P_2O_5 [31], $La_2Be_2O_5$ [32], $CsBe_2F_5$ [33] and $K_2CeSi_6O_{15}$ [34]. The characteristic topological parameters of these compounds derived from the published structural data are given in Table 6.

Table 6. Summary of the basic topological data for the T-atoms in the oxide framework compounds crystallizing in three-dimensional 3-connected networks.

Compound	Loop configurations	Coordination sequences	Reference
γ - $Na_2Si_2O_5$ (RT,HT) ;	$8_1 \cdot 8_1 \cdot 10_3$	3-6-12-22-35-50-69-92-116-142	This work
$NaHSi_2O_5 \times H_2O$			[29]
$K_2Si_2O_5$	$10_2 \cdot 10_2 \cdot 6_1$	3-6-11-20-32-46-60-80-102-122	[30]
o - P_2O_5, $La_2Be_2O_5$	$10_4 \cdot 10_4 \cdot 10_2$	3-6-12-24-38-56-77-102-129-160	[31,32]
$CsBe_2F_5$	$10_5 \cdot 10_5 \cdot 10_5$	3-6-12-24-35-48-69-86-108-138	[33]
$K_2CeSi_6O_{15}$	$8_1 \cdot 8_1 \cdot 6_1$	3-6-11-18-30-44-57-74-95-116	[34]
	$6_1 \cdot 8_1 \cdot 10_1$	3-6-11-19-30-44-57-73-95-117	

Concluding remarks

Three different X-ray powder diffraction patterns of the γ-phase are listed in the Powder Diffraction File (PDF-2 entries 18-1242, 19-1235, 22-1395). Whereas a high degree of coincidence can be found concerning the strong reflections of the three entries, the number and the positions of the weak reflections differ considerably. However, one has to keep in mind that the polycrystalline material used in previous powder diffraction studies frequently contained impurity phases which can easily account for the differences observed for the class of low intensity lines (see Introduction). The comparison between a simulated powder diffraction pattern based on the structural data of the present investigation obtained at room temperature and the experimentally determined data mentioned above reveals that all pronounced reflections are reproduced nicely. Nevertheless, our results differ from the only other diffraction study on γ-$Na_2Si_2O_5$ using single crystals [14]. Although we did not observe any indication for the existence of an incommensurately modulated structure with satellite reflections parallel to b^* as described in [14], there exists a striking relationship between our unit cell parameters and those reported by Hoffmann and Scheel for the average structure (AS) defined from the main reflections (see Introduction).

$$(\mathbf{a}_{AS} \quad \mathbf{b}_{AS} \quad \mathbf{c}_{AS}) = (\mathbf{a} \quad \mathbf{b} \quad \mathbf{c}) \times \begin{pmatrix} -1/3 & 0 & -1/2 \\ 0 & 1/2 & 0 \\ 2/3 & 0 & -1 \end{pmatrix}$$

Furthermore, focussing on the very strong reflections Hoffmann and Scheel reported the same pseudo-tetragonal sub-cell that was observed for the *RT*-phase in our diffraction experiments. In summary one can say that there are sufficient arguments to postulate the existence of two sub-modifications of γ-$Na_2Si_2O_5$ which can be preserved at room conditions: (a) the modulated phase described by Hoffmann and Scheel and (b) the so-called *RT*-phase of the present investigation. However, it cannot be excluded that the modulated phase may have been stabilized by the incorporation of small amounts of cations from the oxides plates used as substrates.

Acknowledgement

Financial support for this work has been received from the Deutsche Forschungsgemeinschaft (DFG) under the grant Ka1342/1. The manuscript benefited from the helpful comments of two anonymous reviewers.

References

[1] Kracek, F.C.: The system sodium oxide - silica. J. Phys. Chem. **34** (1930) 1583-1598.

[2] Willgallis, A.; Range, K.J: Zur Polymorphie des $Na_2Si_2O_5$. Glastechn. Ber. **37** (1963) 194 - 200.

[3] Williamson, J.; Glasser, F.P.: The crystallisation of $Na_2O.2SiO_2$ - SiO_2 glasses. Phys. Chem. Glasses **7** (1966) 127 - 138.

[4] Neilson, G; Weinberg, J.: Crystallization of Na_2O-SiO_2 gel and glass. J. Non-Cryst. Solids **63** (1984) 365.

[5] Mogensen, G; Christensen, N.H.: Crystallization in SiO_2-Na_2O glasses. Phys. Chem. Glasses **2** (1981) 17.

[6] Vogel, W. Glaschemie, Springer Verlag (1992).

[7] Wolf, F.; Schwieger, W.: Zum Ionenaustausch einwertiger Kationen an synthetischen Natriumpolysilicaten mit Schichtstruktur. Z. Anorg. Allg. Chem. **457** (1979) 224-228.

[8] Rieck, H.P.: Natriumschichtsilicate und Schichtkieselsäuren. Nachr. Chem. Techn. Lab. **44** (1996) 699 - 705.

[9] Heinemann, I., Frischat, G. H.: The sodium transport mechanism in Na_2O * $2SiO_2$ glass determined by the Chemla experiment. Physics Chem. Glasses **34** (1993) 255 - 260.

[10] Kanzaki, M.; Xue, X.; Stebbins, J.F.: Phase relations in Na_2O-SiO_2 and $K_2Si_4O_9$ systems up to 14 GPa and ^{29}Si NMR study of the new high-pressure phases: implications to the structure of high-pressure silicate glasses. Phys. Earth Planet. Int. **107** (1998) 9-21.

[11] Maekawa, H.; Yokokawa, T.: Effects of temperature on silicate melt structure: a high temperature ^{29}Si NMR study of $Na_2Si_2O_5$. Geochim. Cosmochim. Acta **61** (1997) 2569-2575.

[12] Kahlenberg, V.; Dörsam, G.; Wendschuh-Josties, M.; Fischer, R.X.: The crystal structure of δ-$Na_2Si_2O_5$. J. Solid State Chem. **146** (1999) 380 - 386.

[13] Rakic, S.; Kahlenberg, V.; Weidenthaler, C.; Zibrowius, B.: Structural characterization of high pressure C-$Na_2Si_2O_5$ by single crystal diffraction and ^{29}Si MAS NMR. Phys. Chem. Mineral. **29** (2002) 477 - 484.

[14] Hoffmann, W.; Scheel, H.J.: Über die γ - und δ - Modifikationen des Natriumdisilikates, $Na_2Si_2O_5$. Z. Kristallogr. **129** (1969) 396 - 404.

[15] Tuinstra, F.; Storm, G.M.: A universal high-temperature device for single-crystal diffraction. J. Appl. Crystallogr. **11** (1978) 257 - 259.

[16] Scheufler, C.; Engel, K.V.; Kirfel, A.: An improved gas-stream heating device for a single-crystal diffractometer. J. Appl. Crystallogr. **30** (1997) 411-412.

[17] Altomare A.; Burla M.C.; Camalli M.; Cascarano G.L.; Giacovazzo C.; Guagliardi A.; Moliterni A.G.G.; Polidori G.; Spagna R.: SIR97: a new tool for crystal structure determination and refinement. J. Appl. Crystallogr. **32** (1999) 115-119.

[18] Sheldrick, G.M.: SHELX97 - Programs for Crystal Structure Analysis (Release 97-2). Universität Göttingen, Germany (1998).

[19] Spek, A.L.: PLATON, A Multipurpose Crystallographic Tool, University of Utrecht, The Netherlands, (1998).

[20] Ibers, J.A.; Hamilton, W.C., Eds.: International tables for X - ray crystallography, Volume IV, The Kynoch Press, Birmingham, U.K. (1974).

[21] Dowty, E.: ATOMS Version5.1 - Shape Software (2000).

[22] Liebau, F.: Structural chemistry of silicates. Springer-Verlag, Berlin 1985.

[23] Brown, I.D.; Altermatt, D.: Bond - valence parameters obtained from a systematic analysis of the inorganic crystal structure database. Acta Crystallogr. **B41** (1985) 244 - 247.

[24] Brunner, G.O.; Meier, W.M.: Framework density distributions of zeolite type tetrahedral nets. Nature **337** (1989) 146.

[25] Baerlocher, Ch.; Meier, W.M.; Olson, D.H.: Atlas of zeolite framework types. 5th revised edition. Elsevier, 2001.

[26] O'Keefe, M.; Hyde, S.T.: Vertex symbols for zeolite nets. Zeolites **19** (1997) 370-374.

[27] Wells, A.F.: Further Studies of Three-dimensional Nets. American Crystallographic Association Monographs No. 8, 1979.

[28] Evers, J.; Oehlinger, G.; Sextl, G.: Hochdruck-Synthese von LiSi: Raumnetzstruktur aus dreibindigen (Si) - Ionen. Angew. Chem. **105** (1993) 1532 - 1534.

[29] Yamnova, N.Ya.; Pushcharovskii, D.Yu.; Andrianov, V.I.; Rastsvetaeva, R.K.; Khomyakov, A.P.; Mikheeva, M.G.: A new type of silicate radical in the structure of grumantite $Na(Si_2O_4(OH))*H_2O$. Dokl. Akad. Nauk SSSR **305** (1989) 868 - 871.

[30] DeJong, B.H.W.S.; Supèr, H.T.J.; Spek, A.L.; Veldman, N.; Nachtegaal, G.; Fischer, J.C.: Mixed alkali systems: Structure and ^{29}Si MASNMR of $Li_2Si_2O_5$ and $K_2Si_2O_5$. Acta Crystallogr. **B54** (1998) 568-577.

[31] Arbib, E.H.; Elouadi, B.; Chaminade, J.P.; Darriet, J.: New refinement of the crystal structure of o-P_2O_5. J. Sol. State Chem. **127** (1996) 350 - 353.

[32] Harris, L.A.; Yakel, H.L.: The crystal structure of $La_2Be_2O_5$. Acta Crystallogr., **24** (1968) 672 - 682.

[33] LeFur, Y.; Aleonard, S.: Structure du pentafluorodiberyllate $CsBe_2F_5$. Acta Crystallogr., **B28** (1972) 2115 - 2118.

[34] Karpov; O.G.; Pobedimskaya, E.A.; Belov, N.V.: Crystal structure of a K, Ce silicate with a three-dimensional anion framewok: $K_2CeSi_6O_{15}$. Sov. Phys. Crystallogr. 22 (1977) 215 - 217.

13. Zusammenfassung

Im Rahmen dieses Projektes wurden die Kristallchemie und die polymorphen Formen im System $Me_2Si_2O_5$ (Me: Na, K) untersucht. Die folgenden Teilaspekte wurden bearbeitet :

1. Synthesen zum α-$Na_2Si_2O_5$, Vorcharakterisierung der Proben mittels thermischer Analysen und *HT*-Pulverdiffraktometrie, Sammlung von Einkristalldatensätzen bei hohen Temperaturen.

   Kristalle der zur Gruppe der Einfach-Schichtsilikate gehörenden Phase des α-$Na_2Si_2O_5$ konnten relativ leicht und schnell aus Gläsern entsprechender Zusammensetzung gewonnen werden. Eigene thermische Analysen zeigten zwei reversible Effekte bei 682°C und 710°C und bestätigten somit zunächst die Resultate älterer Arbeiten. Nicht verifiziert werden konnte dagegen die bisherige Vorstellung einer Symmetrieabfolge orthorhombisch ? monoklin ? orthorhombisch für die drei Sub-Modifikationen des α-$Na_2Si_2O_5$. Die postulierten klaren Aufspaltungen von Reflexen konnten weder in Neutronenbeugungs-, noch in Röntgenbeugungsmessungen an Pulvern nachvollzogen werden. Entsprechend der Einkristalldiffraktometrie kann nur ein Phasenübergang als gesichert gelten. Er führt von der bei Raumtemperatur stabilen *Pcnb* - Phase zu einer Hochtemperaturphase mit der Raumgruppensymmetrie *Aba*2. Neben einer spontanen Verzerrung der Tetraeder wird die Umwandlung primär durch Rotationen der Tetraeder induziert.

2. Synthesen zum γ- $Na_2Si_2O_5$, Strukturanalysen an der γ-Phase, Untersuchung der strukturellen Phasenübergänge.

   Die Synthese der metastabilen γ- $Na_2Si_2O_5$ wurde ebenfalls durch die Kristallisation von Gläsern erreicht. Die thermischen Analysen mittels DSC zeigten lediglich ein breites Ereignis bei etwa 560°C. Aufgrund der Einkristallmessungen bei Raumtemperatur wurde nachgewiesen, daß es sich bei der γ-Phase um ein neuartiges unterbrochenes Tetraedergerüst handelt. Das Beugungsbild zeigte zwar die typischen Merkmale einer Überstruktur, allerdings konnten die Ergebnisse früherer Arbeiten zur Existenz einer inkommensurabel modulierten Phase nicht nachvollzogen werden. Der in der DSC Aufnahme beobachtete Effekt ist mit einem Phasenübergang verknüpft, der von der monoklinen *RT*-Phase zu einer tetragonalen *HT*-Phase führt, deren Struktur ebenfalls ermittelt werden konnte.

3. Synthesen zum $K_2Si_2O_5$, Untersuchung temperaturinduzierter Phasenübergänge, Strukturanalyse der gemittelten Struktur des $K_2Si_2O_5$.

Die Herstellung der Kristalle des $K_2Si_2O_5$ erfolgte ebenfalls durch die Leuterung eines stöchiometrisch zusammengesetzten Glases. Typisch für die Phase ist eine ausgeprägte Verzwilligung. Es wurden praktisch keine unverzwillingten Kristalle gefunden. Die Luftempfindlichkeit der Proben erforderte besondere Maßnahmen bei der Präparation. Neben der Zwillingsbildung wurde die Strukturlösung auch durch das Vorhandensein von Überstruktureffekten erschwert. Der Versuch einer Bestimmung der Gesamtstruktur scheiterte zwar, jedoch konnte zumindest für die gemittelte Struktur ein kristallchemisch plausibles Modell gefunden und verfeinert werden. Danach zählt das Kaliumdisilikat ebenfalls zur Gruppe der Einfach-Schichtsilikate, enthält im Gegensatz zu den natriumhaltigen Phasen allerdings ausschließlich Vierer- und Achterringe und keinerlei Secherringe aus Tetraedern. DTA-Aufnahmen zeigten, daß es bei etwa 218°C und 580°C zu zwei Effekten kommt, die auf die Existenz von *HT*-Modifikationen hindeuten.

4. Synthese, Datensammlung und Strukturanalyse des C-$Na_2Si_2O_5$, ^{29}Si-MAS-NMR-spektroskopische Messungen

Eine aus der Literatur bekannte Hochdruckmodifikation des $Na_2Si_2O_5$, die sog. C-Phase, wurde bei einem Druck von ca. 1 kbar und bei einer Temperatur von 700°C erfolgreich synthetisiert. Die Einkristalle zeigten erneut eine intensive polysynthetische Verzwillingung. Dennoch konnte die bislang unbekannte Struktur der C-Phase aus Einkristallbeugungsdaten gelöst werden. Die Tetreaderschichten innerhalb des Kristalls sind bezüglich der Geometrie identisch mit denen des β-$Na_2Si_2O_5$. Unterschiede zwischen den beiden polymorphen Formen resultieren aus Stapelvarianten der jeweiligen Schichtpackete. Zusätzlich wurden ^{29}Si-MAS-NMR Messungen durchgeführt. Sie bestätigten das röntgenographisch gefundene Strukturmodell mit insgesamt vier symmetrisch unabhängigen T-Positionen.

5. Synthese und Charakterisierung von Mischkristallen im System $Na_2Si_2O_5$-$K_2Si_2O_5$ bei Raumdruck

In Rahmen dieses Projektes wurden Synthesen zu den Mischverbindungen $Na_{2-x}K_xSi_2O_5$ im Bereich $0 \leq x \leq 1$ vorgenommen und die Produkte mittels Einkristall- und Pulverdiffraktometrie charakterisiert. Diese waren meist mehrphasig; mitunter auch mit einem hohen glasigen Anteil. Über einen weiten Bereich tauchte allerdings insbesondere eine Phase auf, deren Kristallstruktur an einer Probe der Zusammensetzung $Na_{1.55}K_{0.45}Si_2O_5$. bestimmt werden konnte. Die bislang unbekannte Struktur zeigt eine Verwandtschaft mit der δ- Modifikation des $Na_2Si_2O_5$. Ferner wurde für x = 1 ein weiteres neues Einfachschichtsilikat gefunden ($NaKSi_2O_5$-I) und strukturell charakterisiert. Die Schichten enthalten dabei Achter-, Sechser- und Viererringe aus Tetraedern.

6. Hydrothermalsynthesen und Charakterisierung von Mischkristallen im System $Na_2Si_2O_5$-$K_2Si_2O_5$

Gläser der Zusammensetzung $Na_{2-x}K_xSi_2O_5$ (x = 0.0 ; 0.5; 1.0; 1.5; 2) wurden mittels Hydrothermalsynthesen bei Temperaturen zwischen 500°C und 700°C, sowie Drucken von 1kbar - 3kbar rekristallisiert und die Produkte röntgenographisch untersucht. Für x = 0 trat bei einem Druck von 3 kbar und einer Temperatur von 700°C neben der schon erwähnten C-Phase eine neue Disilikatvariante auf, die mit κ-$Na_2Si_2O_5$ bezeichnet wurde. Diese Phase stellt ebenfalls eine Einfach-Schichtstruktur dar und zeigt viele Ähnlichkeiten mit β-$Na_2Si_2O_5$. Dieser Strukturtyp wurde auch bei der Kristallisation eines kaliumhaltigen Glases der Zusammensetzung $Na_{1.5}K_{0.5}Si_2O_5$ gefunden. Die chemische Zusammensetzung der kristallinen Na-K-Mischphase war jedoch mit $Na_{1.84}K_{0.16}Si_2O_5$ deutlich natriumreicher als das Eduktglas. Dies deutet auf eine begrenzte Substitutionsmöglichkeit Na ? K hin. Für x = 1 ergaben die Synthesen bei 1kbar und 500°C als Ergebnis eine neue $NaKSi_2O_5$ Modifikation ($NaKSi_2O_5$-II), die isotyp mit $NaRbSi_2O_5$ ist. Strukturell gesehen handelt es sich um ein Doppelkettensilikat. Für die gleichen p-T Bedingungen konnte schließlich aus einem Glas mit x = 1.5 eine weitere neue Schichtstrukturvariante der Zusammensetzung $Na_{0.67}K_{1.33}Si_2O_5$ erhalten werden. Auch diese Phase enthält Achter-, Sechser- und Viererringe in den Tetraederlagen und ist somit eng mit dem bei Raumdruck hergestellten $NaKSi_2O_5$-I verwandt.